ADVANCES IN PID, SMITH AND DEADBEAT CONTROL

BY

LU XIANG (B.ENG., M.ENG.)

DEPARTMENT OF ELECTRICAL AND
COMPUTER ENGINEERING

A THESIS SUBMITTED
FOR THE DEGREE OF PHILOSOPHY DOCTOR

NATIONAL UNIVERSITY OF SINGAPORE
2006

Acknowledgments

I would like to express my sincere appreciation to my supervisors, Prof. Wang, Qing-Guo and Prof. Lee, Tong-Heng for their excellent guidance and gracious encouragement through my study. Their uncompromising research attitude and stimulating advice helped me in overcoming obstacles in my research. Their wealth of knowledge and accurate foresight benefited me in finding the new ideas. Without them, I would not able to finish the work here. Especially, I am indebted to Prof Wang Qing-Guo for his care and advice not only in my academic research but also in my daily life. I wish to extend special thanks to A/Prof. Xiang Chen for his constructive suggestions which benefit my research a lot. It is also my great pleasure to thank A/Prof. Xu Jianxin, Prof. Chen Ben Mei, Prof. Ge Shuzhi Sam, A/Prof. Ho Wenkung who have in one way or another give me their kind help.

Also I would like to express my thanks to Dr. Zheng Feng and Dr. Lin Chong, Dr. Yang Yongsheng, and Dr. Bi Qiang. for their comments, advice, and inspiration. Special gratitude goes to my friends and colleagues. I would like to express my thanks to Mr. Zhou Hanqin, Mr. Li Heng, Mr. Liu Min, Mr. Ye Zhen, Mr. Zhang Zhiping, Ms. Fu Jun, and many others working in the Advanced Control Technology Lab. I enjoyed very much the time spent with them. I also appreciate the National University of Singapore for the research facilities and scholarship.

Finally, I wish to express my deepest gratitude to my wife Wu Liping. Without her love, patience, encouragement and sacrifice, I could not have accomplished this. I also want to thank my parents for their love and support, It is not possible to thank them adequately. Instead I devote this thesis to them and hope they will find joy in this humble achievement.

Contents

Acknowledgements **i**

List of Figures **vi**

List of Tables **vii**

Summary **viii**

1 Introduction **1**

1.1 Motivation 1

1.2 Contributions 9

1.3 Organization of the Thesis 11

2 PID Control for Stabilization **12**

2.1 Introduction 12

2.2 Problem Formulation 13

2.3 Preliminary 16

2.4 First-order Non-integral Unstable Process 20

2.4.1 P/PI controller 20

2.4.2 PD/PID controller 26

2.5 Second-order Integral Processes with An Unstable Pole 30

2.5.1 P/PI controller 31

2.5.2 PD/PID controller 33

2.6 Second-order Non-integral Unstable Process with A Stable Pole . . 36

2.6.1 P/PI controller 37

2.6.2 PD/PID controller 42
2.7 Conclusion 51
2.8 Appendix 52

3 PID Control for Regional Pole Placement 55
3.1 Introduction 55
3.2 Regional Pole Placement by Static Output Feedback 57
3.3 Regional Pole Placement by PID Controller 62
3.4 Conclusion 64

4 A Two-degree-of-freedom Smith Control for Stable Delay Processes 65
4.1 Introduction 65
4.2 The Proposed Method 66
4.3 Stability Analysis 71
4.4 Typical design cases 73
4.5 Examples 75
4.6 Rejection of periodic disturbance 82
4.7 Conclusion 87

5 A Double Two-degree-of-freedom Smith Scheme for Unstable Delay Processes 88
5.1 Introduction 88
5.2 The Proposed Scheme 90
5.3 Internal Stability 92
5.4 Controller Design 93
5.5 Examples 100
5.6 Conclusion 108

6 A Smith-Like Control Design for Processes with RHP Zeros 109
6.1 Introduction 109
6.2 The Control Scheme 110

6.3 Stability Analysis . . . 115
6.3.1 Design procedure . . . 119
6.3.2 Model reduction . . . 120
6.4 Simulation Examples . . . 121
6.5 Conclusion . . . 129

7 Deadbeat Tracking Control with Hard Input Constraints 132
7.1 Introduction . . . 132
7.2 Preliminaries . . . 133
7.3 Bounded Input Constraints Case . . . 135
7.4 Hard Input Constraints Case . . . 138
7.4.1 Design procedure and computational aspects . . . 145
7.4.2 Numerical example . . . 147
7.5 Conclusion . . . 149

8 Conclusions 150
8.1 Main Findings . . . 150
8.2 Suggestions for Further Work . . . 152

Bibliography 154

Author's Publications 163

List of Figures

2.1 Unity output feedback system 14
2.2 Nyquist Contour 17
2.3 Nyquist plots of G_3 with P controller 25
2.4 Nyquist plots of G_3 with PI controller 26
2.5 Nyquist plots of G_3 with PD controller 30
2.6 Nyquist plots of G_3 with PID controller 31
2.7 Nyquist plots of G_4 with PD controller 36
2.8 Nyquist plots of G_4 with PID controllers 37
2.9 Nyquist plots of G_5 with P controller 43
2.10 Nyquist plots of G_5 with PI controller 44
2.11 Nyquist plots of G_5 with PD controller 50
2.12 Nyquist plots of G_5 with PID controller 52

4.1 Two-degree-of-freedom Smith control structure 67
4.2 Illustration of desired disturbance rejection 70
4.3 System structure with multiplicative uncertainty 73
4.4 Responses of Example 1 for step disturbance 77
4.5 Left-hand-sides of (4.16) for Example 1 78
4.6 Responses of Example 1 against model change 79
4.7 Responses of Example 1 against disturbance change 80
4.8 Responses of Example 1 with C_2 redesigned 81
4.9 Responses of Example 2 for step disturbance 83
4.10 Responses of Example 3 for sinusoidal disturbance 85

4.11 Responses comparison for C_2 with different τ 86
4.12 Disturbance response with modified design of C_2, $\tau = 0.8$ 87

5.1 Majhi's Smith predictor control scheme 90
5.2 Proposed double two-degree-of-freedom control structure 91
5.3 Step responses for IPDT process 102
5.4 Step responses for unstable FOPDT process 103
5.5 Step responses for unstable SOPDT process (gain=2) 104
5.6 Step responses for unstable SOPDT process (gain=2.2) 105
5.7 Step responses for unstable SOPDT process (gain=1.8) 106

6.1 Smith control structure 111
6.2 Step response specifications against tuning parameter τ 114
6.3 Performance comparison of processes with 2 RHP zeros 116
6.4 Illustration of robust stability condition for uncertain time delay . . 119
6.5 Time and frequency responses of G_0 and its model in Example 1 . . 122
6.6 Modelling error for the process in Example 1 123
6.7 Closed-loop step response of Example 1 123
6.8 System robustness of Example 1 124
6.9 Robust stability check against uncertain RHP zero of Example 1 . . 125
6.10 Step responses against uncertain RHP zero of Example 1 126
6.11 Robust stability check against uncertain time delay of Example 1 . 126
6.12 Step responses against uncertain time delay of Example 1 127
6.13 Robust stability check against combined uncertainties of Example 1 127
6.14 Step responses against combined uncertainties of Example 1 128
6.15 Closed-loop step response of Example 2 129
6.16 System robustness of Example 2 130

7.1 Single loop feedback system 135
7.2 Minimum-time deadbeat control for Example 1 139
7.3 Minimum ISE deadbeat control for Example 2 with hard constraints 148

List of Tables

2.1 Stabilizability Results of Low-order Unstable Delay Processes . . . 14

5.1 Performance Specifications of Disturbance Responses 107

6.1 Performance Specification Comparison for Systems with RHP Zero(s) 131

Summary

In the field of Industrial process control, the performance, robustness and real constraints of control systems become more important to ensure strong competitiveness. All these requirements demand new approaches to improve the performance for industrial process control. In this thesis, it is motivated to explore new control techniques for the development of (i) PID stabilization and design for single variable process; (ii) Smith predictor design for improved disturbance performance and for processes with RHP zeros; and (iii) deadbeat controller design with hard constraints.

PID controllers are the dominant choice in process control and many results have been reported in literature. In this thesis, based on the Nyquist stability theorem, the stabilization of five typical unstable time delay processes is investigated. For each process, the maximum stabilizable time delay for different controllers is derived, and the computational method is also provided to determine the stabilization gain. The analysis provides theoretical understanding of the stabilization issue as well as guidelines for actual controller design. Recently, with the advance of linear matrix inequality (LMI) theory, it is possible to combine different objectives as one optimization problem. For the PID design part, an LMI approach is presented for the regional pole placement problem by PID controllers. It is shown that the problem of regional pole placement by PID controller design may be converted into that of static output feedback (SOF) controller design after appropriate formulation. The difficulty of SOF synthesis is that the problem inherently is a bilinear problem which is hard to be solved via an optimization with LMI constraints. In the thesis, an iterative LMI optimization method is developed to solve

the problem.

For industrial process control, when time delay dominant plants are considered, the conventional PID methods need to make trade-off between performance and stability, and could not meet more stringent requirements. The Smith predictor is a good way to control the processes with time delay. Currently, most modified Smith designs have not paid enough efforts to disturbance rejection, which is known to be much more important than set-point performance in industrial control practice. In the thesis, two modified Smith predictor control schemes are proposed for both stable and unstable processes. For stable time delay processes, a two-degree-of-freedom Smith scheme is investigated. The disturbance controller is designed to mimic the behavior of completely rejecting the disturbance after the transfer delay. This novel tuning rule enables convenient design of disturbance controller with superior disturbance rejection, as well as easy trade-off between system robustness and performance. For unstable time delay processes, a double two-degree-of-freedom control scheme is proposed, where the four controllers in the scheme are well placed to separately tune the denominators and numerators of closed-loop transfer functions from the set-point and disturbance. The disturbance controller is tuned to minimize the integral squared error, and two options are provided to meet practical situations for the trade-off between control performance and control action limits. In both designs, explicit controller formulas for several typical industrial processes are provided to facilitate the application. The internal stability of both schemes are analyzed, and the simulations demonstrate greatly improved disturbance over existing approaches. In addition to the modified Smith predictor design for improved disturbance rejection, a Smith like controller design is also given for processes with RHP zeros. It is shown that RHP zeros and possible dead time can be removed from the characteristic equation of the scheme so that the control design is greatly simplified, and enhanced performance is achievable. The relationships between the time domain specifications and the tuning parameter are developed to meet the design requirements on performance and robustness. Compared with the single-loop design, the proposed scheme provides

robust, improved, and predictable performance than the popular PI control.

Deadbeat control is an important issue in the discrete control area, In the thesis, a polynomial approach is employed to solve the deadbeat tracking problem with hard input constraints. The general formula for controllers with bounded input is derived first. Based on this general formula and with extensive analysis, the deadbeat requirement and hard constraints combine to constitute a finite number of linear inequalities constraints. The deadbeat nature of the error enables easy evaluation of various time-domain performance indices, and the controller design could be efficiently solved with linear programming or quadratic programming to optimize such benchmarks.

The schemes and results presented in this thesis have both practical values and theoretical contributions. The results of the simulations show that the proposed methods are helpful in improving the performance or the robustness of industrial control systems.

Chapter 1

Introduction

1.1 Motivation

Over the past fifty years, in parallel with the development of computer and communication technologies, control technology has made numerous significant successes in many areas. Its broad applications include guidance and control systems for aerospace vehicles, supervision control systems in the manufacturing industries, industrial process control systems, and real-time communication control systems. These applications have had an enormous impact on the development of modern society. In the meanwhile, control theorists and engineers have developed reliable techniques for modelling, analysis, design, and testing that enable development and implementation of the wide variety of very complex engineering systems in use today.

In the field of Industrial process control, improved productivity, efficiency, and product goals generate a demand for more effective control strategies to be implemented in the production line. For example, the hydrocarbon and chemical processing industries maintain high product quality by monitoring thousands of sensor signals and making corresponding adjustments to hundreds of valves, heaters, pumps, and other actuators. In accordance to the challenges, many advanced control techniques have been implemented in industry in recent years (Roffel and Betlem, 2004). From the industrial perspective, the performance, robustness and

real constraints of control systems become more important to ensure strong competitiveness. All these requirements call for a strong need for new approaches to improve the performance for industrial process control. Therefore, this thesis is motivated to explore new control techniques for improved performance of industrial process control systems.

Among most unity feedback control structures, the proportional-integral-derivative (PID) controllers have been widely used in many industrial control systems since Ziegler and Nichols proposed their first PID tuning method. Industries have been using the conventional PID controller in spite of the development of more advanced control techniques. The importance of PID control comes from its simple structure, convenient applicability and clear effects of each proportional, integral and derivative control. On the other hand, the general performance of PID controller is satisfactory in many applications. For these reasons, in industrial process control applications, more than 90% of the controllers are of PID type (Åström and Hagglünd, 1995; Åström and Hagglünd, 2001).

Through the past decades, numerous tuning methods have been proposed to improve the performance of PID controllers (Åström *et al.*, 1993; Åström and Hagglünd, 1995; Tan *et al.*, 1999). Some tuning rules aim to minimize an appropriate performance criterion. The well known integral absolute error (IAE) and time weighted IAE criteria were employed to design PID controllers in Rovira *et al.* (1969). The integral squared error (ISE), the time weighted ISE and the exponential time weighted ISE were chosen as performance indices in Zhuang and Atherton (1993). Some Tuning rules are designed to give a specified closed loop response. Such rules may be defined by specifying the desired poles of the closed-loop response, or the achievement of a specified gain margin and/or phase margin. With some approximation, Ho *et al.* (1995) presented an analytical formula to design the PID controller for the first-order and second-order plus dead time processes to meet gain and phase margin specifications. Fung *et al.* (1998) proposed a graphic method to devise PI controllers based on exact gain and phase margin specifications. Recently, using the ideas from iterative feedback tuning, Ho *et al.* (2003)

presented relay autotuning of the PID controllers to yield specified phase margin and bandwidth. Some PID tuning rules are based on recording appropriate parameters at the ultimate frequency (Hang *et al.*, 2002; Ho *et al.*, 1996). There are also some robust tuning rules, with an explicit robust stability and robust performance criterion built in to the design process, say those internal-model-based PID tuning method for example (Morari and Zafiriou, 1989; Chien and Fruehauf, 1990). All these tuning methods have greatly enriched the study of PID controller design, however, there still lacks a clear scenario on what kind of process could be stabilized by PID controllers.

Stabilization is one of the key issues in control engineering, and it is essential for successful operations of control schemes. As we know, time delay is commonly encountered in industrial process systems, and the stabilization problem is even more complicated when the time delay processes are open-loop unstable. In industrial and chemical practice, there are some open-loop unstable processes in industry such as chemical reactors, polymerization furnaces and continuous stirred tank reactors. Such unstable processes coupled with time delay make control system design a difficult task, which has attracted increased attention from the control community (Chidambaram, 1997). Typically, unstable delay processes in industrial process systems are of low order. Thus, the stabilization of low-order unstable delay processes becomes an interesting topic. Silva *et al.* (2004) investigated the complete set of stabilizing PID controllers based on the Hermite-Biehler theorem for quasi-polynomials, which involves finding the zeros of a transcendental equation to determine the range of stabilizing gains. However, this approach is mathematically involved. It does not provide an explicit characterization of the boundary of the stabilizing PID parameter region, and the maximal stabilizable time delay for some typical yet simple processes still remains obscure. Polynomial calculation is another branch for stabilizing PID analysis (Söylemez *et al.*, 2003). Hwang and Hwang (2004) applied the D-partition method to characterize the stability domain in the space of system and controller parameters. The stability boundary is reduced to a transcendental equation, and the whole stability domain is drawn in

a two-dimensional plane by sweeping the remaining parameter(s). However, this result only provides sufficient condition regarding the size of the time delay for stabilization of first-order unstable processes. There is thus a high demand to investigate the stabilization problem of first or second-order unstable delay processes by PID controllers.

One of the fundamental problems in control theory and practice is the design of feedback laws that place the closed-loop poles at desired locations. Although many literatures have been devoted to the problem of exact pole placement (Kimura, 1975; Wang and Rosenthal, 1992; Wang, 1996), in practice, it is often the case that pointwise closed-loop pole placement is not required. In specific, when PID controller design is considered, exact pole placement in general is not applicable due to the limited manipulatable controller parameters. Another pole placement technique is dominant pole placement design, where the controller is calculated such that the dominant poles are placed to ensure desired dynamic performance. The applications could be found in Prashanti and Chidambaram (2000) and Zhang *et al.* (2002). However, a common challenge for dominant pole placement is the difficulty to guarantee that the placed poles are indeed dominant. In contrast to exact or dominant pole placement schemes, where all or part of the closed-loop poles are fixed, regional pole placement (RPP) aims to constrain the closed-loop poles within some suitable region in the left-half complex plane. In Shafieia and Shentona (1994), based on the method of D-partition, a PID tuning method was proposed to shift all the poles to a certain desirable region, but this method is graphical in nature. Recent years, owing to the contribution of Boyd *et al.* (1994), many control problems have been synthesized with linear matrix inequalities (LMI). In Chilali and Gahinet (1996), the conception of LMI regions is proposed to formulate the regional pole placement problem as an LMI one and then solve it together with H_∞ design. However, the result confines to state feedback or full-order dynamic output feedback controllers, which have the limitations in case that full access to the state vector is not available or the full-order dynamic output controllers are difficult to implement due to cost, reliability or hardware implementation constraints. As we

know, PID controllers are reducible to static output feedback (SOF) controllers through state augmentations. Hence, it is an interesting topic to find a SOF or PID controller to meet the regional pole placement specifications. It is well known that SOF is one of the open problem in control theory (Bernstein, 1992; Syrmos *et al.*, 1997), since SOF problem is inherently bilinear which is hard to be formulated into an optimization problem with LMI constraints. In specific, the regional pole placement problem by SOF controllers remains open despite its simple form. It is thus useful in this respect to find a design scheme to cope with the regional pole placement problem through PID controllers.

Nowadays, many control designs focus on set-point response, but overlook disturbance rejection performance. However, in industrial control practice, there is no doubt that disturbance rejection is much more important than set-point tracking (Åström and Hagglünd, 1995; Shinskey, 1996), since the set-point reference signal may be kept unchanged for years, and the system performance is mainly affected by varying disturbances (Luyben, 1990). In fact, countermeasure of disturbance is one of the key factors for successful and failed applications (Takatsu and Itoh, 1999). In view of the great importance of disturbance rejection in process control, good solutions have been sought for a long time. To cope with the disturbance, one possible way is to design the single controller in the feedback system, where trade-off has to be made between the set-point response and disturbance rejection performance. As for conventional PI or PID methods within the framework of a unity feedback control structure, many improved tuning rules have been provided (Ogata, 1990; Ho and Xu, 1998; Park *et al.*, 1998; Silva *et al.*, 2004; Chen and Seborg, 2002). However, owing to the water-bed effect between the set-point response and the load disturbance response, the improvement of the disturbance response is not significant, and the set-point response is usually accompanied with excessive overshoot and large settling time when the time delay is significant. A better approach is to introduce an additional controller to manipulate the disturbance rejection. Recently, a compensator called disturbance observer is introduced in the area of motion control (Ohnishi, 1987). The equivalent disturbance is es-

timated as the difference between the outputs of the actual process and that of the nominal model, and then it is fed to the process inverse model to cancel the disturbance effect on the output. However, one crucial obstacle for the application of disturbance observer to industrial process control is the process time delay, which exists in most industrial processes. Since the inverse model would contain a pure predictor which is physically unrealizable. Therefore, it is appealing to find a design for disturbance rejection control for time delay processes.

As is well known, the Smith predictor controller (Smith, 1959) is an effective dead-time compensator for time delay processes. With Smith predictor, the time delay can be removed from the characteristic equation of the closed-loop system, and the control design is greatly simplified into the delay-free case. However, the one degree-of-freedom nature of the original Smith predictor still requires a trade-off to be made between set-point tracking and disturbance rejection. Moreover, the original Smith predictor scheme will be unstable when applied to an unstable process. In order to improve the performance as well as extend the applicability of Smith predictor, many approaches have been proposed. A two degree-of-freedom scheme was investigated for improved disturbance rejection in Huang *et al.* (1990) and Palmor (1996). Their scheme features delay-free nominal stabilization, and the disturbance compensator controller is composed of a first order lag and a time delay to approximate the inverse of time delay in low frequency range. However, their proposed design of disturbance compensator is not as effective as expected due to the inaccurate approximation of inverse delay, and the corresponding disturbance performance improvement is insignificant. Aiming to enhance the disturbance response and robustness as well, another double-controller scheme was proposed for stable first order processes with time delay (Tian and Gao, 1998). However, its disturbance response is not tuned with special care. Moreover, this scheme is effective only for process with dominant delay, when the process time delay is relatively small, even its nominal performance deteriorates. Thus, there is a high demand for a new control scheme to provide substantial improvement on disturbance rejection and keep nominal delay-free stabilization like that in the

original Smith predictor.

In recent years, advanced control systems concerning unstable processes have been strongly appealed in industry, which therefore have attracted much attention in the process control community (Chidambaram, 1997). To overcome the obstacle of the original Smith predictor for unstable processes, Åström *et al.* (1994) presented a modified Smith predictor (MSP) for an integrator plus time delay process with decoupling design, which leads to faster set-point response and better disturbance rejection. Matausek and Micic (1996) and Kwak *et al.* (1999) considered the same problem with similar results by providing easier tuning schemes. In 1999, Majhi and Atherton (1999) proposed a modified Smith predictor control scheme which has high performance particularly for unstable and integrating process. This method achieves optimal integral squared time error for set-point response and employs an optimum stability approach with a proportional controller for an unstable process. Later, the same control structure is revisited in Majhi and Atherton (2000*a*), Majhi and Atherton (2000*b*) and Kaya (2003) to achieve better performance with easier tuning methods. However, the disturbance controller in these schemes mainly contributes to enhancing the stability of disturbance response, and still could not improve the performance significantly. Furthermore, it should be noted that many MSP control methods restricted focus on unstable processes modelled in the form of a first order rational part plus time delay, which in fact, cannot represent a variety of industrial and chemical unstable processes well enough. Besides, there usually exist the process unmodelled dynamics that inevitably tend to deteriorate the control system performance, especially for the load disturbance rejection. It is therefore motivated to devise a new control scheme for unstable time delay processes, which could enable manipulation of disturbance transient response without causing any loss of the existing benefits of the previous schemes and is robust against modelling errors.

Another control problem frequently encountered in industrial process but less addressed by researchers is the right-half-plane (RHP) zeros. RHP zeros have been identified in many chemical engineering systems, such as the boilers, sim-

ple distillation columns, and coupled distillation column (Holt and Morari, 1985). Compared with its minimum phase counter-part, a system with RHP zeros has similar inherent performance limitations to those of the time delay process, such as the closed-loop gain, bandwidth, and the integrals of sensitivity and complementary sensitivity functions (Middleton, 1991; Qiu and Davison, 1993; Seron *et al.*, 1997). Although it is well accepted that system with RHP zeros is difficult to control (Middleton, 1991), there are relatively few literatures focusing on specific controller design for RHP zeros. Noting that RHP zeros share the same non-minimum phase property as time delay, and that the time delay has a common bridge with RHP zeros in its first order Padé approximation, it is natural to consider extending the Smith predictor for time delay process to a Smith-like controller for process with RHP zeros. Therefore, it is desirable to have a new control scheme for systems with RHP zeros by developing a Smith-like controller.

In the area of discrete systems control, deadbeat control is a fundamental issue. Different from the commonly mentioned asymptotically tracking where the output follows the reference signal asymptomatically, deadbeat control aims to drive the tracking error to zero in finite time and keep it zero for all discrete times thereafter. The problem of deadbeat control received attention since 1950s, and has been extensively studied in the 1980s (Kimura and Tanaka, 1981; Emami-Naeini and Franklin, 1982; Schlegel, 1982). However, the minimum time deadbeat control usually suffers from the problem of large control magnitude, which prevents the practical implementation. On the other hand, saturation nonlinearities are ubiquitous in engineering systems (Hu and Lin, 2001; Hu *et al.*, 2002), and the analysis and controller design for system with saturation nonlinearities is an important problem in practical situations. Consequently, it is of practically imperative to incorporate hard constraints into the deadbeat controller. The challenges are the formulation and solving of controller with hard constraints, which motivates the last topic in this thesis: deadbeat tracking control with hard input constraints.

1.2 Contributions

This present thesis mainly covers three topics: PID stabilization and control problem, modified Smith predictor design for industrial processes, and constrained deadbeat control problem. Several new control schemes are addressed for single variable linear processes in industrial process control, aiming to improve the performance, disturbance response and system robustness. In particular, the thesis has investigated the following areas:

A. PID Control for Stabilization

Based on the Nyquist stability theorem, the stabilization problem for unstable (including integral) time delay processes is investigated. Especially, for P, PI, PD or PID controllers, the explicit maximal stabilizable time delays are given in terms of the parameters from first-order unstable process, second-order integral process with an unstable pole, and second-order non-integral unstable process are established. In parallel with the stabilization analysis, the computational methods are also provided to find the stabilization controllers.

B. PID Control for Regional Pole Placement

An iterative LMI algorithm is presented for the regional pole placement problem by PID controllers. The regional pole placement problem by SOF controllers is addressed first and formulated as a bilinear linear problem, which is proven equivalent to a quadratic matrix problem and solved via an iterative LMI approach. Then it is shown that PID regional pole placement problem is easily converted to a SOF one, and thus could be solved within the same framework. The result is applicable to general reduced order feedback controller design.

C. A Two-degree-of-freedom Smith Control for Stable Delay Processes

A two-degree-of-freedom Smith control scheme is investigated for improved disturbance rejection of stable delay processes. This scheme enables delay-free stabilization and separate tuning of set-point and disturbance responses. In specific,

a novel disturbance controller design is presented to mimic the behavior of completely rejecting the disturbance after the transfer delay. Through the analysis and examples, the rejection of different kinds of disturbances is addressed, such as step type and periodic one. It is shown that the disturbance performance is greatly improved.

D. A Double Two-degree-of-freedom Smith Scheme for Unstable Delay Processes

A double two-degree-of-freedom control scheme is proposed for enhanced control of unstable delay processes. The scheme is motivated by the modified Smith predictor control in Majhi and Atherton (1999) and devised to improve in the following ways: (i) one more freedom of control is introduced to enable manipulation of disturbance transient response, and is tuned based on minimization of the integral squared error; (ii) four controllers are well placed to separately tune the denominators and numerators of closed-loop transfer functions from the set-point and disturbance, which allows easy design of each controller and good control performance for both set-point and disturbance responses. Controller formulas for several typical process models are provided, with two options provided to meet practical situations for the trade-off between control performance and control action limits. Especially, improvement of disturbance response is extremely great.

E. A Smith-Like Control Design for Processes with RHP Zeros

Motivated by the common non-minimum phase property of dead time and right-half-plane (RHP) zero, a Smith-like scheme is presented for systems with RHP zeros. It is shown that RHP zeros and possible dead time can be removed from the characteristic equation of the scheme so that the control design is greatly simplified, and enhanced performance is achievable. By model reduction, a unified design with a single tuning parameter is presented for processes of different orders. The relationships between the time domain specifications and the tuning parameter are developed to facilitate the design trade-off. It is also shown that the design ensures the gain margin of 2 and phase margin of $\pi/3$, as well as allows 100%

perturbation of the RHP zero or uncertain time delay of $|\Delta L| \leq \tau/0.42$.

F. Deadbeat Tracking Control with Hard Input Constraints

In this thesis, a polynomial approach is employed to solve the deadbeat tracking problem with hard input constraints. The general formula for controllers with bounded input is derived first. Based on this general formula, hard constraints are imposed and the problem is formulated as a specific linear infinite programming problem. Then it is proven that the hard input constraints can be ensured approximately with arbitrary accuracy by choosing a suitable finite subset of the inequalities. The reduction from infinite inequality constraints to finite ones leads to easy controller calculation by employing linear programming or quadratic programming algorithms.

1.3 Organization of the Thesis

The thesis is organized as follows. Chapter 2 focuses on the PID stabilization analysis for low-order unstable delay processes, where explicit and complete stabilizability results in terms of the upper limit of time delay size are provided. Chapter 3 is devoted to regional pole placement by PID controllers through iterative LMI algorithms. Chapter 4 is concerned with a two-degree-of-freedom Smith control for stable time delay processes, where the novel design of the disturbance controller enables significantly improved disturbance rejection. Chapter 5 investigates a double two-degree-of-freedom control scheme for unstable delay processes. Chapter 6 presents a Smith-like control design for systems with RHP zeros. Chapter 7 addresses the deadbeat tracking control with hard input constraints taken into consideration. Finally in Chapter 8, general conclusions are given and suggestions for further works are presented.

Chapter 2

PID Control for Stabilization

2.1 Introduction

Time delay is commonly encountered in chemical, biological, mechanical and electronic systems. There are some unstable processes in industry such as chemical reactors and their stabilization is essential for successful operations. Especially, unstable processes coupled with time delay makes control system design a difficult task, which has attracted increased attention from control community (Chidambaram, 1997). Recently, many techniques have been reported to improve PID tuning for unstable delay processes. Shafiei and Shenton (Shafiei and Shenton, 1994) proposed a graphical technique for PID controller tuning based on the D-partition method. Poulin and Pomerleau (Poulin and Pomerleau, 1996) utilized the Nichols chart to design PI/PID controller for integral and unstable processes with maximum peak-resonance specification. Wang et al. (Wang *et al.*, 1999*a*) investigated PID controllers based on gain and phase margin specifications. Sree et al. (Sree *et al.*, 2004) designed PI/PID controllers for first-order delay systems by matching the coefficients of the numerator and the denominator of the closed loop transfer function. However, these works do not provide a clear scenario on what kind of process could be stabilized by PID controllers.

Typically, most unstable delay processes in practical systems are of low order (1st or 2nd-order). Thus, stabilization of low-order unstable delay processes

becomes an interesting topic. Silva et al. (Silva *et al.*, 2004) investigated the complete set of stabilizing PID controllers based on the Hermite-Biehler theorem for quasi-polynomials. However, this approach is mathematically involved, it does not provide an explicit characterization of the boundary of the stabilizing PID parameter region, and the maximal stabilizable time delay for some typical yet simple processes still remains obscure. Hwang and Hwang (2004) applied D-partition method to characterize the stability domain in the space of system and controller parameters. The stability boundary is reduced to a transcendental equation, and the whole stability domain is drawn in two-dimensional plane by sweeping the remaining parameter(s). However, this result only provides sufficient condition regarding the size of the time delay for stabilization of first-order unstable processes.

In this chapter, we aim to provide a thorough yet simple approach solving the stabilization problem of first or second-order unstable delay processes by PID controller or its special cases. The tool used for stability analysis is the well-known Nyquist criterion and hence easy to follow. For each case, the necessary and sufficient condition concerning the maximal delay for stabilizability is established and the range of the stabilizing control parameters is also derived. The stabilizability results for five typical processes are summarized in Table 2.1. It is believed that the results could serve as a guideline for the design of stabilizing controllers in practical industrial process control.

The rest of the chapter is organized as follows. After the problem statement in Section 2.2, some preliminaries are presented in Section 2.3. The stabilization for first-order non-integral unstable process, second-order integral process with an unstable pole, and second-order non-integral unstable process with a stable pole are addressed in Sections 2.4-2.6, respectively. Finally, Section 2.7 concludes the chapter.

2.2 Problem Formulation

In this chapter, the processes of interest are those unstable/integral processes with time delay which are most popular in industry. Suppose that such a process is

Table 2.1. Stabilizability Results of Low-order Unstable Delay Processes

Process	P	PI	PD	PID
$\frac{1}{s}e^{-Ls}$	$\forall L > 0$	$\forall L > 0$	$\forall L > 0$	$\forall L > 0$
$\frac{1}{s(s+1)}e^{-Ls}$	$\forall L > 0$	$\forall L > 0$	$\forall L > 0$	$\forall L > 0$
$\frac{1}{s-1}e^{-Ls}$	$L < 1$	$L < 1$	$L < 2$	$L < 2$
$\frac{1}{s(s-1)}e^{-Ls}$	none	none	$L < 1$	$L < 1$
$\frac{1}{(s-1)(Ts+1)}e^{-Ls}$	$L < 1 - T$	$L < 1 - T$	$L < \sqrt{1+T^2} - T + 1$	$L < \sqrt{1+T^2} - T + 1$

controlled in the unity feedback system (Figure 2.1) by a simple controller. By simple controllers, we mean the PID type and its special cases, namely, P, PI, PD, and PID.

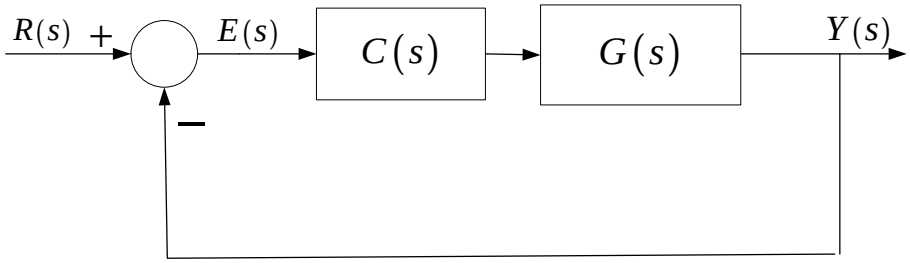

Figure 2.1. Unity output feedback system

To formulate the stabilization problem with fewest possible parameters, some normalization is adopted throughout the chapter. This is best illustrated by an example. Let the actual process and controller be $\bar{G}(s) = \frac{\bar{K}}{(\bar{T}_1 s-1)(\bar{T}s+1)}e^{-\bar{L}s}$ and $\bar{C}(s) = \bar{K_P}(1 + \bar{K_D}s + \frac{\bar{K_I}}{s})$ respectively. One can scale down the time delay and all time constants by T_1, and absorb the process gain $\bar{K}$ into the controller so that $L = \bar{L}/T_1$, $T = \bar{T}/T_1$, $K_D = \bar{K_D}/T_1$, $K_I = \bar{K_I}T_1$, $K_P = \bar{K_P}\bar{K}$.

It follows that the open-loop transfer function is expressed as

$$\bar{G}(s)\bar{C}(s) = \frac{\bar{K}\bar{K_P}(1 + \bar{K_D}s + \frac{\bar{K_I}}{s})}{(\bar{T}_1 s - 1)(\bar{T}s + 1)}e^{-\bar{L}s} \overset{s=T_1 s}{\Longrightarrow} \frac{K_P(1 + K_D s + \frac{K_I}{s})}{(s-1)(Ts+1)}e^{-Ls} = G(s)C(s) \tag{2.1}$$

where

$$G(s) = \frac{1}{(s-1)(Ts+1)}e^{-Ls} \text{ and } C(s) = K_P(1 + K_D s + \frac{K_I}{s})$$

are the normalized process and controller, respectively.

The five normalized processes of interest are

- integral process,

$$G_1(s) = \frac{1}{s}e^{-Ls}, \tag{2.2}$$

- second-order integral process with a stable pole,

$$G_2(s) = \frac{1}{s(s+1)}e^{-Ls}, \tag{2.3}$$

- first-order non-integral unstable process,

$$G_3(s) = \frac{e^{-Ls}}{s-1}, \tag{2.4}$$

- second-order integral process with an unstable pole,

$$G_4(s) = \frac{1}{s(s-1)}e^{-Ls}, \tag{2.5}$$

- second-order non-integral unstable process with a stable pole,

$$G_5(s) = \frac{1}{(s-1)(Ts+1)}e^{-Ls}, \tag{2.6}$$

where $L > 0$ is assumed throughout this chapter. These processes are to be stabilized by one of the following four controllers:

$$C_1(s) = K_P, \tag{2.7}$$

$$C_2(s) = K_P(1 + \frac{K_I}{s}), \tag{2.8}$$

$$C_3(s) = K_P(1 + K_D s), \tag{2.9}$$

$$C_4(s) = K_P(1 + K_D s + \frac{K_I}{s}). \tag{2.10}$$

The corresponding open-loop transfer function, $Q_{il}(s) = G_i(s)C_l(s)$, $i \in \{1,\ 2,\ 3,\ 4,\ 5\}$ and $l \in \{1,\ 2,\ 3,\ 4\}$, is re-written as

$$Q_{il}(s) = G_i(s)C_l(s) = K\frac{N(s)}{s^v D(s)}e^{-Ls},\ L > 0, \tag{2.11}$$

where K is the gain, v a non-negative integer representing type of the loop, $N(s)$ and $D(s)$ both rational polynomials of s with $N(0) = D(0) = 1$.

Recall that the Nyquist contour consists of the imaginary axis plus the right semi-circle with infinity radius if the open-loop transfer function $Q_{il}(s)$ has no pole on such a contour, that is $v = 0$ in our case of $i \in \{3,\ 5\}$ and $l \in \{1,\ 3\}$. If the open-loop has a pole at the origin ($v \neq 0$ in our case of $i \in \{1,\ 2,\ 4\}$ or $l \in \{2,\ 4\}$), then the contour needs to be modified by replacing the origin with a infinitesimal semicircle of $s = re^{j\phi}$ with $r \to 0$ and $-\pi/2 \leq \phi \leq \pi/2$, as depicted in Figure 2.2. This modification implies that (i) the pole at the origin is outside of the modified contour (not counted as an unstable pole); and (ii) the part of the Nyquist curve corresponding to the above infinitesimal semicircle around the origin, is the plot of $Ke^{-jv\phi}/r^v$, and incurs the total clockwise phase change of $-v\pi$. The Nyquist stability theorem is now applied to the open loop $Q_{il}(s)$ in (2.11), which leads to the following Theorem.

Theorem 2.1. *Given the open-loop transfer function $Q_{il}(s)$ in (2.11) with P^+ unstable poles inside the Nyquist contour, the closed-loop system in Figure 2.1 is stable if and only if the Nyquist plot of $Q_{il}(s)$ encircles the critical point, $(-1,\ 0)$, P^+ times anticlockwise.*

It can be readily seen that $P^+ = 0$ for the loop with G_1 or G_2 and $P^+ = 1$ otherwise for G_3 through G_5.

2.3 Preliminary

Due to the delay element in the open-loop transfer function $Q_{il}(s)$ defined in (2.11), the phase of $Q_{il}(j\omega)$, denoted by $\Phi_{Q_{il}}(\omega)$, will approach $-\infty$ when frequency $\omega \to \infty$. Consequently, if $\lim_{\omega\to\infty} |Q_{il}(j\omega)| \geq 1$, the Nyquist curve of $Q_{il}(s)$ will encircle/pass the critical point infinite times clockwise, which violates Theorem 2.1 and the closed-loop is unstable. Hence, the following lemma follows.

Lemma 2.1. *For the open-loop $Q_{il}(s)$ in (2.11),*

$$\lim_{\omega\to\infty} |Q_{il}(j\omega)| < 1 \tag{2.12}$$

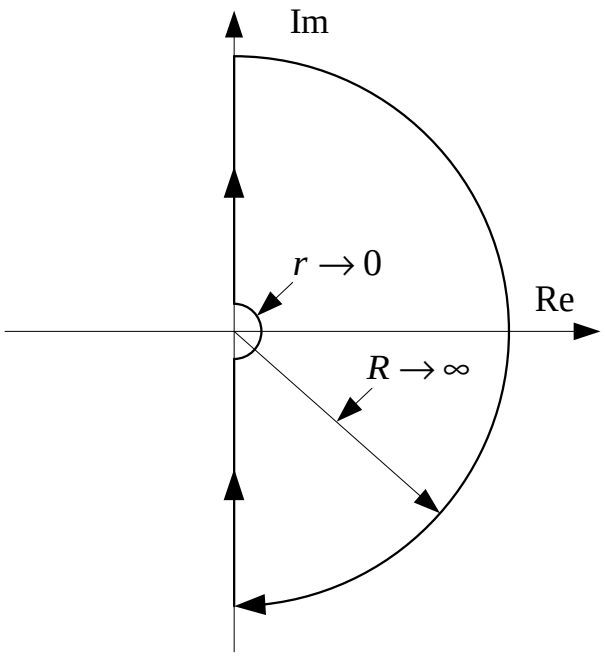

Figure 2.2. Nyquist Contour

is necessary for the closed-loop stability.

Suppose first that the loop has no integrator ($v = 0$). Then $Q_{il}(0) = K$ is finite. The Nyquist curve starts at $Q_{il}(0) = K$ and, $|Q_{il}(j\infty)| < 1$ due to (2.12), should end right to the critical point, $(-1,\ 0)$, to meet Theorem 2.1 for stability.

- If $K > -1$, $Q_{il}(0)$ is also right to the critical point, then the net number of the encirclements around $(-1,\ 0)$ has to be even. Therefore, $K < -1$ is necessary for stability if $P^+ = 1$.

- In contrast, if $K < -1$, $Q_{il}(0)$ is now left to the critical point, then the net number of the encirclements around $(-1,\ 0)$ is odd. Therefore, $K > -1$ is necessary for stability if $P^+ = 0$.

Suppose next that the loop has one integrator ($v = 1$).

- If $K > 0$, the part of Nyquist curve corresponding to the infinitesimal semicircle rotates $-\pi$ clockwise from phase angle $\pi/2$ to $-\pi/2$ with infinite radius. Thus the whole Nyquist curve is composed of two symmetrical parts,

one starting from $(+\infty,\ 0)$ and ending at $Q_{il}(j\infty)$, while the other from $Q_{il}(-j\infty)$ to $(+\infty,\ 0)$. Since the Nyquist curve should end at $|Q_{il}(j\infty)| < 1$ for stability, it follows that the Nyquist curve encircles the critical point an even number of times for the entire frequency range. Therefore, $K > 0$ is necessary for stability if $P^+ = 0$.

- In contrast, if $K < 0$, the part of Nyquist curve corresponding to the infinitesimal semicircle rotates $-\pi$ clockwise from $-\pi/2$ to $-3\pi/2$ with infinite radius. Then the whole Nyquist curve is composed of two symmetrical parts, one starting from $(-\infty,\ 0)$ and ending at $Q_{il}(j\infty)$, while the other from $Q_{il}(-j\infty)$ to $(-\infty,\ 0)$. Consequently, the Nyquist curve should encircle the critical point an odd number of times for the entire frequency range. Therefore, $K < 0$ is necessary for stability if $P^+ = 1$.

Following a similar argument, one can conclude that in case of $v = 2$, $K > 0$ is necessary for stability if $P^+ = 0$ while $K < 0$ is necessary for stability if $P^+ = 1$.

Lemma 2.2. *Consider the open-loop $Q_{il}(s)$ in (2.11), the necessary condition for closed-loop stability is that*

(i). For $v = 0$: $K > -1$ if $P^+ = 0$; and $K < -1$ if $P^+ = 1$.

(ii). For $v = 1, 2$: $K > 0$ if $P^+ = 0$; and $K < 0$ if $P^+ = 1$.

Consider the stabilization of process G_1 or G_2 by the proportional controller $C_1 = K_P$, with $P^+ = 0$ and $v = 1$, it follows from Lemma 2.2 that $K = K_P > 0$ must be met, and from Theorem 1 that no encirclement of the critical point should be made. Since the magnitude of the open-loop, $M_{Q_{i1}}(\omega)$ with $i = \{1,\ 2\}$, monotonically decreases with ω, the Nyquist curve will not encircle the critical point if its first intersection with the real axis lies between -1 and 0, which is always possible by setting a small enough positive K_P. This means that G_1 or G_2 with arbitrary delay $L > 0$ is stabilizable by the proportional controller. Since P controller is a special case of PD, PI and PID ones, it is concluded that processes G_1 and G_2 with arbitrary delay $L > 0$ are also stabilizable by PI, PD, or PID controllers, which is summarized in the following Theorem 2.2.

Theorem 2.2. *The process, G_1 in (2.2) or G_2 in (2.3) is stabilizable for any delay $L > 0$ by P, PD, PI, or PID controller. In the case of P controller, the stabilizing range of K_P is given by*

$$0 < K_P < \frac{\pi}{2L}, \tag{2.13}$$

for process G_1; and

$$0 < K_P < \omega_{c1}\sqrt{1+\omega_{c1}^2} \tag{2.14}$$

where ω_{c1} is the positive phase crossover frequency meeting

$$\frac{\pi}{2} - L\omega_{c1} - \arctan(\omega_{c1}) = 0$$

for process G_2.

In the following, two more technical lemmas are presented, which will be used frequently for stability analysis throughout the chapter.

Lemma 2.3. *Given the open-loop transfer function $Q_{il}(s)$ defined in (2.11), a necessary condition for the closed-loop stability is that the polynomial,*

$$H(s) = \frac{\frac{d^{m+1}}{ds^{m+1}}[s^v D(s)e^{Ls}]}{e^{Ls}}, \tag{2.15}$$

has all its zeros lie in the open left half plane, where m is the degree of $N(s)$.

Proof: The closed-loop stability requires the stability of closed-loop characteristic function $F_0(s) = s^v D(s) + KN(s)e^{-Ls}$, or $F_1(s) = s^v D(s)e^{Ls} + KN(s)$. It follows from (Kharitonov *et al.*, 2005) that the derivative of such a stable quasi-polynomial is also stable, thus the $(m+1)$-th order derivative of $F_1(s)$, $H(s)e^{Ls}$, is also stable. Then $H(s)$ has all its zeros lie in the open left half plane.

Lemma 2.4. *Let the open-loop transfer function $Q_{il}(s)$ in (2.11) have $P^+ > 0$. If, for some integer k and for $\forall\omega \geq 0$, there hold*

(i). $\Phi_{Q_{il}}(\omega) < -2k\pi + 3\pi$, *and*

(ii). $\frac{d\Phi_{Q_{il}}(\omega)}{d\omega} < 0$ *for* $\Phi_{Q_{il}}(\omega) \leq -2k\pi - \pi$,

then the closed-loop system is stable only if

$$\max\left(\Phi_{Q_{il}}(\omega)|_{\omega>0}\right) > -2k\pi + \pi. \tag{2.16}$$

Proof: Anti-clockwise encirclement around the critical point is required for stability. This is not obtainable for the portion of the Nyquist curve corresponding either to $s = re^{j\phi}$ with $r \to 0$ since possible poles of $Q_{il}(s)$ would cause the curve to rotate clockwise only, or to $s = jw$ which meets (ii) as its phase keeps decreasing. Taking into account (i), anti-clockwise encirclement can occur only if the curve has the phase increase in the phase range of $-2k\pi - \pi < \Phi_{Q_{il}}(\omega) < -2k\pi + 3\pi$, and traverses the negative real axis from the second quadrant to the third quadrant therein, that is, there holds (2.16). The proof is complete.

In the following three sections, the stabilization analysis is presented for processes G_3, G_4 and G_5 respectively. Due to the symmetry property of the Nyquist curve, subsequent analysis focuses on the positive frequency band and $\omega > 0$ is always assumed unless otherwise indicated.

2.4 First-order Non-integral Unstable Process

In this section, stabilization of

$$G_3(s) = \frac{1}{s-1}e^{-Ls}$$

is under consideration.

2.4.1 P/PI controller

For P controller, $C_1(s) = K_P$, the open-loop frequency response is given by

$$Q_{31}(j\omega) = \frac{K_P}{-1+j\omega}e^{-jL\omega},$$

with $P^+ = 1$ and $v = 0$. It follows from Lemma 2.2 that $K = Q_{31}(0) = -K_P < -1$, or $K_P > 1$ is necessary for stabilization. The loop has the magnitude as

$$M_{Q_{31}}(\omega) = K_P\sqrt{\frac{1}{1+\omega^2}},$$

which always decreases from K_P to zero. The phase is

$$\Phi_{Q_{31}}(\omega) = -L\omega + \arctan(\omega) - \pi, \tag{2.17}$$

with $\Phi_{Q_{31}}(0) = -\pi$. Its derivative is

$$\frac{d}{d\omega}\Phi_{Q_{31}}(\omega) = -L + \frac{1}{\omega^2 + 1}.$$

If $L \geq 1$, then $\frac{d}{d\omega}\Phi_{Q_{31}}(\omega) < 0$ for $\omega > 0$, $\Phi_{Q_{31}}(\omega)$ is always less than $-\pi$, and there could be no anticlockwise encirclement. Assuming that both $K_P > 1$ and $L < 1$ are true, the phase will initially increase from $-\pi$ for small frequencies and then decrease infinitely due to the delay, while the magnitude decreases monotonically from $M_{Q_{31}}(0) = K_P$ to zero. Moreover, there is exactly one positive solution, say ω_{c1}, for $\Phi_{Q_{31}}(\omega) = -\pi$. In order for the possible anticlockwise encirclement around the critical point to occur, this intersection of Nyquist curve against the negative real axis must lie between -1 and 0, that is

$$M_{Q_{31}}(\omega_{c1}) = K_P\sqrt{\frac{1}{1 + \omega_{c1}^2}} < 1. \tag{2.18}$$

As long as (2.18) is true, $M_{Q_{31}}(\omega)$ will always be less than 1 for $\omega > \omega_{c1}$ and $Q_{31}(s)$ will have no encirclement (either clockwise or anticlockwise) around the critical point thereafter. Consequently, there is one and only one anticlockwise encirclement for the whole frequency span when $K_P > 1$, $L < 1$ and (2.18) are all true.

As for the PI controller, $C_2(s) = K_P(1 + K_I/s)$, the open-loop frequency response is

$$Q_{32}(j\omega) = K_P\frac{1 - jK_I/\omega}{-1 + j\omega}e^{-jL\omega}, \tag{2.19}$$

with $P^+ = 1$ and $v = 1$. It follows from Lemma 2.2 that $K = -K_PK_I < 0$, or $K_PK_I > 0$. Assume that $K_P > 0$ and $K_I > 0$ first, then the loop has its magnitude as

$$M_{Q_{32}}(\omega) = K_P\sqrt{\frac{1 + \left(\frac{K_I}{\omega}\right)^2}{1 + \omega^2}},$$

which always decreases from ∞ to 0. The phase is

$$\Phi_{Q_{32}}(\omega) = -L\omega - \arctan\left(\frac{K_I}{\omega}\right) + \arctan(\omega) - \pi, \tag{2.20}$$

with its derivative as

$$\frac{d}{d\omega}\Phi_{Q_{32}}(\omega) = -L + \frac{1}{1+\omega^2} + \frac{K_I}{K_I^2+\omega^2}.$$

It is noted that for $\Phi_{Q_{32}}(\omega) \leq -3\pi$, or $-L\omega \leq -2\pi + \arctan\left(\frac{K_I}{\omega}\right) - \arctan(\omega)$, the derivative of phase is always negative since

$$\begin{aligned}
\frac{d}{d\omega}\Phi_{Q_{32}}(\omega) &= \frac{1}{\omega}\left(-L\omega + \frac{\omega}{1+\omega^2} + \frac{K_I\omega}{K_I^2+\omega^2}\right) \\
&\leq \frac{1}{\omega}\left(-2\pi + \arctan\left(\frac{K_I}{\omega}\right) - \arctan(\omega) + \frac{\omega}{1+\omega^2} + \frac{K_I\omega}{K_I^2+\omega^2}\right) \\
&< \frac{1}{\omega}\left(-2\pi + \frac{\pi}{2} + 0 + \frac{1}{2} + \frac{1}{2}\right) \\
&< 0.
\end{aligned}$$

Since $\Phi_{Q_{32}}(\omega) < -\pi/2$, it follows from Lemma 2.4 that $\Phi_{32}(\omega) > -\pi$ for some $\omega > 0$ is necessary for closed-loop stability.

In case of $L \geq 1$, it can be readily seen from the previous P-control discussion that $\Phi_{Q_{32}}(\omega) = \Phi_{Q_{31}}(\omega) - \arctan(K_I/\omega) \leq \Phi_{Q_{31}}(\omega)$, $\Phi_{Q_{31}}(\omega)$ and then $\Phi_{Q_{32}}(\omega)$ are always less than $-\pi$. In consequence, the Nyquist curve has no anticlockwise encirclement around the critical point and the closed-loop is unstable when $K_P > 0$, $K_I > 0$ and $L \geq 1$.

In case of $L < 1$, it is seen from previous analysis for the case of P-control that, $\Phi_{Q_{31}}(\omega) > -\pi$ holds when ω is small. It follows by continuity argument that it is always possible to make $\Phi_{Q_{32}}(\omega) > -\pi$ at some frequency by choosing sufficiently small K_I. Thus K_I should be chosen to ensure

$$\max(\Phi_{Q_{32}}(\omega)) > -\pi \tag{2.21}$$

for possible anticlockwise encirclement.

It is noted that the second-order derivative of phase is

$$\frac{d^2}{d\omega^2}\Phi_{Q_{32}}(\omega) = -\frac{2\omega}{(1+\omega^2)^2} - \frac{2K_I\omega}{(\omega^2+K_I^2)^2},$$

which is always negative for $\omega > 0$, thus the Nyquist curve will have exactly two crossings with the negative real axis with phase angle $-\pi$ as long as (2.21) is true.

In order to have anticlockwise encirclement around the critical point, K_P should be chosen such that

$$M_{Q_{32}}(\omega_{c2}) < 1 < M_{Q_{32}}(\omega_{c1}), \tag{2.22}$$

where $\omega_{c1} < \omega_{c2}$ are the two phase crossover frequencies satisfying $\Phi_{Q_{32}}(\omega) = -\pi$. Inequality (2.22) is always feasible since $M_{Q_{32}}$ is monotonically decreasing. Moreover, when (2.22) is true, $M_{Q_{32}}(\omega)$ will always be less than 1 for $\omega > \omega_{c2}$ and $Q_{32}(s)$ will have no encirclement around the critical point thereafter. Consequently, there is exactly one anticlockwise encirclement when (2.21), (2.22), $L < 1$, $K_P > 0$ and $K_I > 0$ are all true.

Now assume that $K_P < 0$ and $K_I < 0$. The phase turns out to be

$$\Phi_{Q_{32}}(\omega) = -L\omega - \arctan\left(\frac{K_I}{\omega}\right) + \arctan(\omega),$$

which is always less than π. It is also noted that, for $\Phi_{Q_{32}}(\omega) \leq -\pi$, the derivative of phase is negative since

$$\begin{aligned}
\frac{d}{d\omega}\Phi_{Q_{32}}(\omega) &= \frac{1}{\omega}\left(-L\omega + \frac{\omega}{1+\omega^2} + \frac{K_I\omega}{K_I^2+\omega^2}\right) \\
&\leq \frac{1}{\omega}\left(-\pi + \arctan\left(\frac{K_I}{\omega}\right) - \arctan(\omega) + \frac{1}{2} + \frac{1}{2}\right) \\
&< \frac{1}{\omega}\left(-\pi + 0 + 0 + \frac{1}{2} + \frac{1}{2}\right) \\
&< 0.
\end{aligned}$$

It is thus concluded from Lemma 2.4 that $Q_{32}(s)$ does not have anticlockwise encirclement around the critical point, and that the closed-loop is unstable when both K_P and K_I are negative.

The above stability analysis for P/PI controller may be summarized in the following Theorem 2.3.

Theorem 2.3. *The process, $G_3(s) = \frac{1}{s-1}e^{-Ls}$, is stabilizable by P controller ($C_1(s) = K_P$) or PI controller ($C_2(s) = K_P(1 + K_I/s)$, if and only if $L < 1$. If $L < 1$, the stabilizing gain for P controller is bounded by*

$$1 < K_P < \sqrt{1+\omega_{c1}^2}, \tag{2.23}$$

with the positive phase crossover frequency ω_{c1} solved from

$$-L\omega_{c1} + \arctan(\omega_{c1}) = 0. \tag{2.24}$$

The stabilizing parameters for PI controller satisfy

$$K_P > 0,\ K_I > 0. \tag{2.25}$$

Choose K_I such that

$$\max(\Phi_{Q_{32}}(\omega)) > -\pi. \tag{2.26}$$

The range of K_P is given by

$$\sqrt{\frac{(1+\omega_{c1}^2)}{(K_I/\omega_{c1})^2+1}} < K_P < \sqrt{\frac{(1+\omega_{c2}^2)}{(K_I/\omega_{c2})^2+1}}, \tag{2.27}$$

with $\omega_{c1} < \omega_{c2}$ the two positive phase crossover frequencies solved from

$$-L\omega - \arctan\left(\frac{K_I}{\omega}\right) + \arctan(\omega) = 0. \tag{2.28}$$

In the following, a specific example will be given to illustrate the procedure to design stabilizing gains for P and PI controllers.

Example 1. Given the process $G_3 = \frac{1}{s-1}e^{-0.5s}$, design stabilizing P/PI controllers.

Since the time delay $L = 0.5 < 1$, it follows from Theorem 2.3 that the process is stabilizable by P/PI controller. When P controller is considered, The phase cross over frequency $\omega_{c1} = 2.331$ is solved from (2.24), and K_P is bounded by $(1,\ 2.536)$ from (2.23). Choose $K_P = 1.5$, then the open-loop transfer function turns to be $Q_{31}(s) = \frac{1.5}{s-1}e^{-0.5s}$. The Nyquist plot of $Q_{31}(s)$ is given in Figure 2.3(a), which indicates a stable closed-loop. For comparison, let the process delay increase to 1.5 with other settings unchanged, the Nyquist plot of $Q_{31}(s) = \frac{1.5}{s-1}e^{-1.5s}$ is given in Figure 2.3(b), which indicates an unstable closed-loop.

As for stabilizing PI controller, it is noted that due to the continuity argument, a sufficiently small positive K_I always ensures (2.26). In this example, choose $K_I = 0.2$ to make $\max(\Phi_{Q_{32}}(\omega)) > -\pi$. Then the crossover frequencies $\omega_{c1} = 0.734$ and $\omega_{c2} = 2.029$ are solved from (2.28), and K_P is in turn bounded by $(1.197,\ 2.251)$.

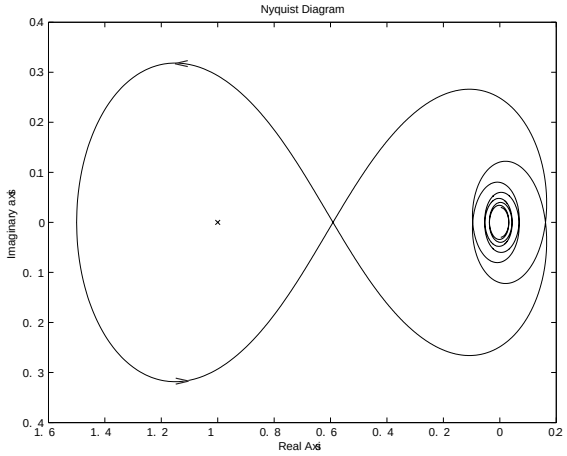

(a) $G_3 = \frac{e^{-0.5s}}{s-1}$ and $C_1 = 1.5$

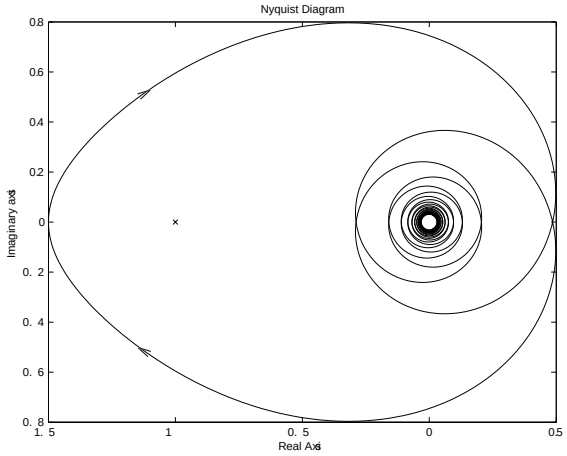

(b) $G_3 = \frac{e^{-1.5s}}{s-1}$ and $C_1 = 1.5$

Figure 2.3. Nyquist plots of G_3 with P controller

Let $K_P = 1.5$, then the PI controller is given by $C_2 = 1.5 + 0.3/s$, and the open-loop transfer function is $Q_{32}(s) = \frac{1.5+0.3/s}{s-1}e^{-0.5s}$. The Nyquist plot is illustrated in Figure 2.4(a), which indicates a stable closed-loop. For comparison, let the process delay increase to 1.5 with other settings unchanged again, the Nyquist plot of $Q_{32}(s) = \frac{1.5+0.3/s}{s-1}e^{-1.5s}$ is given in Figure 2.4(b), which indicates an unstable closed-loop.

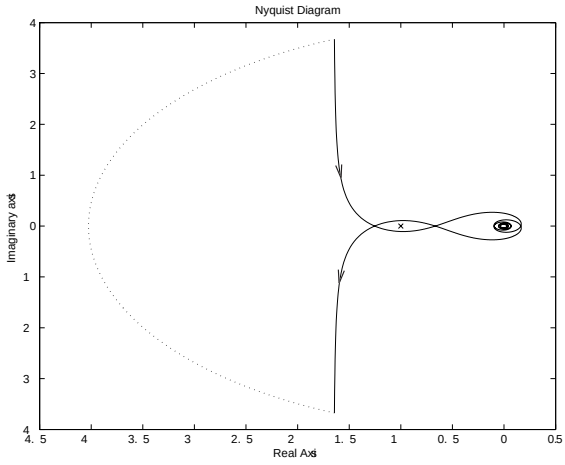

(a) $G_3 = \frac{e^{-0.5s}}{s-1}$ and $C_2 = 1.5 + 0.3/s$

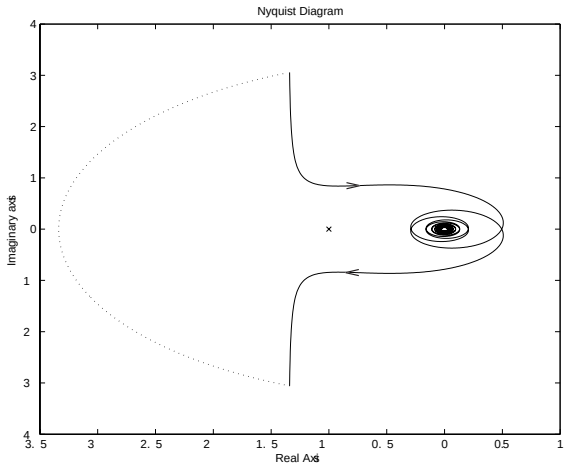

(b) $G_3 = \frac{e^{-1.5s}}{s-1}$ and $C_2 = 1.5 + 0.3/s$

Figure 2.4. Nyquist plots of G_3 with PI controller

2.4.2 PD/PID controller

For PD controller, $C_3(s) = K_P(1 + K_D s)$, the open-loop frequency response is

$$Q_{33}(j\omega) = K_P \frac{1 + jK_D\omega}{j\omega - 1} e^{-jL\omega},$$

with $P^+ = 1$ and $v = 0$. It follows from Lemma 2.1 and Lemma 2.2 that

$$|Q_{33}(\infty)| = |K_P K_D| < 1, \text{ and } K = K_P > 1, \tag{2.29}$$

are necessary, which lead to

$$|K_D| < 1. \tag{2.30}$$

The loop has its magnitude as

$$M_{Q_{33}}(\omega) = K_P \sqrt{\frac{1 + K_D^2 \omega^2}{1 + \omega^2}},$$

which decreases with the frequency ω. The phase

$$\Phi_{Q_{33}}(\omega) = -L\omega + \arctan(K_D\omega) + \arctan(\omega) - \pi \tag{2.31}$$

begins from $\Phi_{Q_{33}}(0) = -\pi$ and is always less than 0 for $\omega > 0$, with its derivative being

$$\frac{d}{d\omega}\Phi_{Q_{33}}(\omega) = -L + \frac{K_D}{(K_D\omega)^2 + 1} + \frac{1}{\omega^2 + 1}.$$

When $\Phi_{Q_{33}}(\omega) \leq -3\pi$, the derivative of phase is always negative since

$$\begin{aligned}
\frac{d}{d\omega}\Phi_{Q_{33}}(\omega) &= \frac{1}{\omega}\left(-L\omega + \frac{K_D\omega}{(K_D\omega)^2 + 1} + \frac{\omega}{\omega^2 + 1}\right) \\
&\leq \frac{1}{\omega}\left(-2\pi - \arctan(K_D\omega) - \arctan(\omega) + \frac{K_D\omega}{(K_D\omega)^2 + 1} + \frac{\omega}{\omega^2 + 1}\right) \\
&< \frac{1}{\omega}\left(-2\pi + 0 + 0 + \frac{1}{2} + \frac{1}{2}\right) \\
&< 0.
\end{aligned}$$

It follows from Lemma 2.4 that $\Phi_{Q_{33}}(\omega) > -\pi$ for some $\omega > 0$ is necessary for any possible anticlockwise encirclement to occur. Thus the derivative of phase must be positive for some ω and this is possible only when

$$\max\left(\frac{d}{d\omega}\Phi_{Q_{33}}(\omega)\right) = \left.\frac{d}{d\omega}\Phi_{Q_{33}}(\omega)\right|_{\omega=0} = 1 + K_D - L > 0. \tag{2.32}$$

Combining (2.30) and (2.32) yields

$$L - 1 < K_D < 1. \tag{2.33}$$

Given arbitrary L that satisfies $L < 2$, there always exists derivative gain K_D satisfying (2.33) such that the phase, $\Phi_{Q_{33}}(\omega)$, increases from $-\pi$ first and then decreases infinitely. Since

$$\frac{d^2}{d\omega^2}\Phi_{Q_{33}}(\omega) = -\frac{2K_D^2\omega}{(1 + K_D^2\omega^2)^2} - \frac{2\omega}{(1 + \omega^2)^2} < 0,$$

the Nyquist curve will cross the negative real axis with the phase $-\pi$ only once at the positive phase crossover frequency, ω_{c1}, with $\Phi_{Q_{33}}(\omega_{c1}) = -\pi$. For anticlockwise encirclement to occur, this intersection should lie between -1 and 0 such that

$$M_{Q_{33}}(\omega_{c1}) < 1. \tag{2.34}$$

Moreover, when (2.34) is true, $Q_{33}(s)$ will have no encirclement around the critical point for $\omega > \omega_{c1}$. Since the magnitude is always decreasing, there is exactly one anticlockwise encirclement when (2.29), (2.33), and $L < 2$ are all true.

As for PID controller, $C_4(s) = K_P(1 + K_D s + K_I/s)$, the open-loop transfer function is

$$Q_{34}(s) = K_P \frac{K_D s + 1 + K_I/s}{s(s-1)} e^{-Ls}.$$

According to Lemma 2.3, the closed-loop stability requires $H(s) = L^3 s^2 + (6L^2 - L^3)s + 6L - 3L^2$ be stable. It follows that $6L - 3L^2 > 0$, or $L < 2$, is necessary. Since PD controller, which could stabilize G_3 if $L < 2$, is a special case of PID controller, it can be thus concluded that PID controller could stabilize G_3 if and only if $L < 2$.

Now we are ready to state Theorem 2.4, concerning stabilization of G_3 using PD or PID controller.

Theorem 2.4. *The process, $G_3(s) = \frac{1}{s-1}e^{-Ls}$, is stabilizable by PD controller ($C_3(s) = K_P(1 + K_D s)$) or PID controller ($C_4(s) = K_P(1 + K_D s + K_I/s)$) if and only if $L < 2$. If $L < 2$, the stabilizing parameters for PD controller are found from*

$$L - 1 < K_D < 1, \tag{2.35}$$

and

$$1 < K_P < \sqrt{\frac{1 + \omega_{c1}^2}{1 + (K_D \omega_{c1})^2}}. \tag{2.36}$$

with phase crossover frequency ω_{c1} satisfying

$$-L\omega_{c1} + \arctan(K_D \omega_{c1}) + \arctan(\omega_{c1}) = 0. \tag{2.37}$$

The following example illustrates the procedure to design stabilizing controllers for G_3.

Example 2. Given the process $G_3 = \frac{1}{s-1}e^{-1.5s}$, design stabilizing PD/PID controllers.

Since the time delay $L = 1.5 < 2$, it follows from Theorem 2.4 that the process is stabilizable by PD controller. The derivative gain K_D is bounded by $(0.5,\ 1)$ from (2.35). Choose $K_D = 0.7$, then the phase cross over frequency $\omega_{c1} = 0.756$ is solved from (2.37), and then K_P is bounded by $(1,\ 1.108)$ from (2.36). Choose $K_P = 1.05$, then PD controller is $C_3 = 0.735s + 1.05$ and the open-loop transfer function turns to be $Q_{33}(s) = \frac{0.735s+1.05}{s-1}e^{-1.5s}$. The Nyquist plot of $Q_{33}(s)$ is given in Figure 2.5(a), which indicates a stable closed-loop. In comparison, let the process delay increase to 2.5 with other settings unchanged, the Nyquist plot of $Q_{33}(s) = \frac{0.735s+1.05}{s-1}e^{-2.5s}$ is given in Figure 2.5(b), which indicates an unstable closed-loop.

When PID controller is used, let K_D in the same range of PD, then there exists a sufficiently small positive K_I such that $\max(\Phi_{Q_{34}}) > -\pi$. It can be readily shown that if K_I is in the range of $0 < K_I < 1 - K_D$, the magnitude will decrease monotonically. Then K_P given by

$$\sqrt{\frac{1+\omega_{c1}^2}{1+(K_D\omega_{c1}-\frac{K_I}{\omega_{c1}})^2}} < K_P < \sqrt{\frac{1+\omega_{c2}^2}{1+(K_D\omega_{c2}-\frac{K_I}{\omega_{c2}})^2}},$$

is stabilizing and not empty, where the two positive phase crossover frequencies $\omega_{c1} < \omega_{c2}$ are solved from

$$-L\omega + \arctan\left(K_D\omega - \frac{K_I}{\omega}\right) + \arctan(\omega) = 0.$$

For this example, choose $K_D = 0.9$ and $K_I = 0.05$ so that $\max(\Phi_{Q_{34}}) > -\pi$ is met, and $\omega_{c1} = 0.379$ and $\omega_{c2} = 0.977$ are solved. Then K_P is in the interval $(1.047,\ 1.077)$. Let $K_P = 1.06$, the PID controller is $C_4 = 0.954s + 1.06 + 0.053/s$, and the open-loop transfer function turns to be $Q_{34}(s) = \frac{0.954s+1.06+0.053/s}{s-1}e^{-1.5s}$. The Nyquist plot is given in Figure 2.6(a), which indicates a stable closed-loop. In comparison, let the process delay increase to 2.5 with other settings unchanged, the corresponding Nyquist plot of is given in Figure 2.6(b), which indicates an unstable closed-loop.

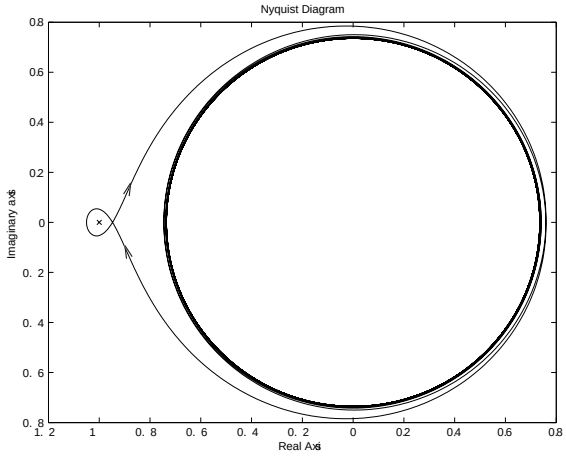

(a) $G_3 = \frac{e^{-1.5s}}{s-1}$ and $C_3 = 0.735s + 1.05$

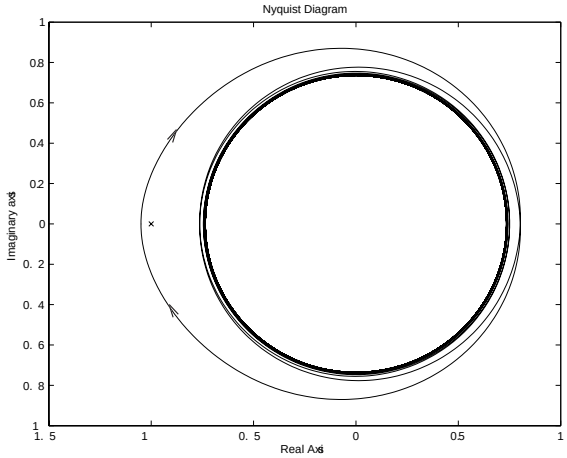

(b) $G_3 = \frac{e^{-2.5s}}{s-1}$ and $C_3 = 0.735s + 1.05$

Figure 2.5. Nyquist plots of G_3 with PD controller

2.5 Second-order Integral Processes with An Unstable Pole

In this section, stabilization of

$$G_4(s) = \frac{1}{s(s-1)}e^{-Ls}$$

is under consideration.

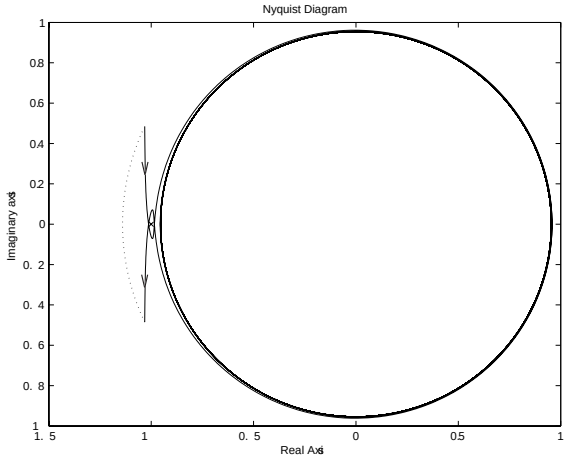

(a) $G_3 = \frac{e^{-1.5s}}{s-1}$ and $C_4 = 0.954s + 1.06 + 0.053/s$

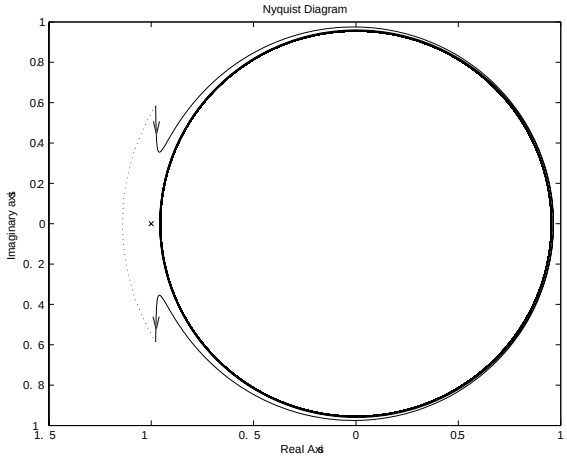

(b) $G_3 = \frac{e^{-2.5s}}{s-1}$ and $C_4 = 0.954s + 1.06 + 0.053/s$

Figure 2.6. Nyquist plots of G_3 with PID controller

2.5.1 P/PI controller

For P controller, $C_1(s) = K_P$, the open-loop frequency response is

$$Q_{41}(j\omega) = \frac{K_P}{j\omega(-1 + j\omega)} e^{-jL\omega},$$

with $P^+ = 1$ and $v = 1$. It follows from Lemma 2.2 that $K = K_P > 0$ is necessary. Then the phase is

$$\Phi_{Q_{41}}(\omega) = -L\omega + \arctan\omega - \frac{3\pi}{2},$$

which is always less than $-\pi$, with its derivative as

$$\frac{d}{d\omega}\Phi_{Q_{41}}(\omega) = -L + \frac{1}{1+\omega^2}.$$

It follows that for $\Phi_{Q_{41}}(\omega) \leq -3\pi$, its derivative is always negative since

$$\begin{aligned}\frac{d}{d\omega}\Phi_{Q_{41}}(\omega) &= \frac{1}{\omega}\left(-L\omega + \frac{\omega}{1+\omega^2}\right)\\ &\leq \frac{1}{\omega}\left(-\frac{3}{2}\pi - \arctan\omega + \frac{1}{2}\right)\\ &< 0.\end{aligned}$$

It is concluded from Lemma 2.4 that $Q_{41}(s)$ has no anticlockwise encirclement, and the closed-loop is always unstable.

As for PI controller, $C_2(s) = K_P(1 + K_I/s)$, the analysis proceeds similarly. The open-loop frequency response is

$$Q_{42}(j\omega) = K_P\frac{1 - jK_I/\omega}{j\omega(-1+j\omega)}e^{-jL\omega},$$

with $P^+ = 1$ and $v = 2$. It follows from Lemma 2.2 that $K = K_P K_I > 0$.

Assume $K_P > 0$ and $K_I > 0$ first, then the phase is

$$\Phi_{Q_{42}}(\omega) = -L\omega + \arctan\omega - \arctan\left(\frac{K_I}{\omega}\right) - \frac{3}{2}\pi,$$

with $\Phi_{Q_{42}}(\omega) < -\pi$ and its derivative being

$$\frac{d}{d\omega}\Phi_{Q_{42}}(\omega) = -L + \frac{1}{1+\omega^2} + \frac{\frac{K_I}{\omega^2}}{1+\frac{K_I}{\omega}^2}.$$

It follows that for $\Phi_{Q_{42}}(\omega) \leq -3\pi$, its derivative is always negative since

$$\begin{aligned}\frac{d}{d\omega}\Phi_{Q_{42}}(\omega) &= \frac{1}{\omega}\left(-L\omega + \frac{\omega}{1+\omega^2} + \frac{\frac{K_I}{\omega}}{1+\frac{K_I}{\omega}^2}\right)\\ &\leq \frac{1}{\omega}\left(-\frac{3}{2}\pi - \arctan\omega + \arctan\left(\frac{K_I}{\omega}\right) + \frac{1}{2} + \frac{1}{2}\right)\\ &< \frac{1}{\omega}\left(-\frac{3}{2}\pi + 0 + \frac{1}{2}\pi + \frac{1}{2} + \frac{1}{2}\right)\\ &< 0.\end{aligned}$$

By invoking Lemma 2.4, $Q_{42}(s)$ has no anticlockwise encirclement around the critical point and the stabilization of G_4 is not achievable with PI controller in the case of $K_P > 0$ and $K_I > 0$.

Assume $K_P < 0$ and $K_I < 0$ then, and the phase is

$$\Phi_{Q_{42}}(\omega) = -L\omega + \arctan\omega - \arctan\left(\frac{K_I}{\omega}\right) - \frac{1}{2}\pi,$$

with $\Phi_{Q_{42}}(\omega) < 0$. It is also noted that, for $\Phi_{Q_{42}}(\omega) \leq -\pi$, the derivative is negative

$$\begin{aligned}
\frac{d}{d\omega}\Phi_{Q_{42}}(\omega) &= -L + \frac{1}{1+\omega^2} + \frac{\frac{K_I}{\omega^2}}{1+\frac{K_I}{\omega}^2} \\
&\leq \frac{1}{\omega}\left(-\frac{1}{2}\pi - \arctan\omega + \arctan\left(\frac{K_I}{\omega}\right) + \frac{1}{2} + \frac{1}{2}\right) \\
&< \frac{1}{\omega}\left(-\frac{1}{2}\pi + 0 + 0 + \frac{1}{2} + \frac{1}{2}\right) \\
&< 0.
\end{aligned}$$

In consequence, $Q_{42}(s)$ also has no anticlockwise encirclement around the critical point by Lemma 2.4, and the stabilization of G_4 is not achievable with PI controller in the case of $K_P < 0$ and $K_I < 0$.

In summary, both P and PI controller could not stabilize G_4.

2.5.2 PD/PID controller

For PD controller, $C_3(s) = K_P(1 + K_D s)$, the open-loop frequency response is

$$Q_{43}(j\omega) = K_P \frac{1 + jK_D\omega}{j\omega(-1 + j\omega)} e^{-jL\omega}, \tag{2.38}$$

with $P^+ = 1$ and $v = 1$. It is noted that (2.38) is reducible to $Q_{32}(j\omega)$ in (2.19) by

$$\begin{aligned}
Q_{43}(j\omega) &= K_P \frac{1 + jK_D\omega}{j\omega(-1 + j\omega)} e^{-jL\omega} \\
&= K_{Pnew} \frac{1 - jK_{Inew}/\omega}{-1 + j\omega} e^{-jL\omega},
\end{aligned}$$

if we define $K_{Pnew} = K_P K_D$ and $K_{Inew} = 1/K_D$. Then the results for PD stabilization of G_4 can be derived directly from Theorem 2.3.

As for PID controller, $C_4(s) = K_P(1 + K_D s + K_I/s)$, the open-loop transfer function is given by

$$Q_{44}(s) = K_P \frac{K_D s + 1 + K_I/s}{s(s-1)} e^{-Ls}.$$

It follows from Lemma 2.3 that the closed-loop stability requires $H(s) = L^3 s^3 + (9L^2 - L^3)s^2 + (18L - 6L^2)s + 6 - 6L$ be stable, which in turn leads to $6 - 6L > 0$ or $L < 1$. Since PD controller is a special case of PID controller, PID controller could always stabilize G_4 if $L < 1$. It is thus concluded that PID controller could stabilize G_4 if and only if $L < 1$.

The above analysis leads to the following Theorem 5.

Theorem 2.5. *The process, $G_4(s) = \frac{1}{s(s-1)} e^{-Ls}$, is stabilizable by PD controller ($C_3(s) = K_P(1 + K_D s)$) or PID controller ($C_4(s) = K_P(1 + K_D s + K_I/s)$) if and only if $L < 1$. If $L < 1$, the stabilizing parameters for PD controller satisfy*

$$K_P > 0, \ K_D > 0. \tag{2.39}$$

Choose sufficiently large K_D such that

$$\max(\Phi_{Q_{43}}(\omega)) > -\pi. \tag{2.40}$$

The range of K_P is given by

$$\sqrt{\frac{\omega_{c1}^2(1+\omega_{c1}^2)}{1+K_D^2\omega_{c1}^2}} < K_P < \sqrt{\frac{\omega_{c2}^2(1+\omega_{c2}^2)}{1+K_D^2\omega_{c2}^2}}, \tag{2.41}$$

with $\omega_{c1} < \omega_{c2}$ the two phase crossover frequencies solved from

$$-L\omega + \arctan(K_D\omega) + \arctan(\omega) - \frac{\pi}{2} = 0. \tag{2.42}$$

The procedure to design stabilizing PD/PID controllers for G_4 is illustrated by the example below.

Example 3. Given the process $G_4 = \frac{1}{s(s-1)} e^{-0.5s}$, design stabilizing PD/PID controller.

Since the time delay $L = 0.5 < 1$, it follows from Theorem 2.5 that the process is stabilizable by PD controller. Then a sufficiently large K_D, which corresponds to

a sufficiently small K_I for the stabilization of G_3 by PI controller, always ensures (2.40). Choose $K_D = 5$ here, the crossover frequencies $\omega_{c1} = 0.734$ and $\omega_{c2} = 2.029$ are determined from (2.42), and K_P is bounded by $(0.239,\ 0.450)$. Let $K_P = 0.3$, the PD controller is then given by $C_3 = 1.5s + 0.3$, and the open-loop transfer function is $Q_{43}(s) = \frac{1.5s+0.3}{s(s-1)}e^{-0.5s}$. The Nyquist plot is illustrated in Figure 2.7(a), which indicates a stable closed-loop. In comparison, let the process delay increase to 1.5 with other settings unchanged, the Nyquist plot of $Q_{43}(s) = \frac{1.5s+0.3}{s(s-1)}e^{-1.5s}$ is given in Figure 2.7(b), which indicates an unstable closed-loop.

When PID controller is employed, let K_D in the same range of PD, then there exists a sufficiently small positive K_I such that $\max(\Phi_{Q_{44}}) > -\pi$. It can be readily shown that if K_I is in the range of $0 < K_I < 1/2K_D$, the magnitude will decrease monotonically. Then K_P given by

$$\sqrt{\frac{\omega_{c1}^2(1+\omega_{c1}^2)}{1+(K_D\omega_{c1}-\frac{K_I}{\omega_{c1}})^2}} < K_P < \sqrt{\frac{\omega_{c2}^2(1+\omega_{c2}^2)}{1+(K_D\omega_{c2}-\frac{K_I}{\omega_{c2}})^2}},$$

is stabilizing and not empty, where the two positive phase crossover frequencies $\omega_{c1} < \omega_{c2}$ are solved from

$$-L\omega + \arctan\left(K_D\omega - \frac{K_I}{\omega}\right) + \arctan(\omega) + \frac{\pi}{2} = 0,$$

In this example, choose $K_D = 6$ and $K_I = 0.08$, and then K_P is within the interval $(0.200,\ 0.386)$. Let $K_P = 0.3$, the PID controller is $C_4 = 1.8s + 0.3 + 0.024/s$ and the open-loop transfer function turns to be $Q_{44}(s) = \frac{1.8s+0.3+0.03/s}{s(s-1)}e^{-0.5s}$. The Nyquist plot is given in Figure 2.8(a), which indicates a stable closed-loop. In comparison, let the process delay increase to 1.5 with other settings unchanged, the corresponding Nyquist plot of is given in Figure 2.8(b), which indicates an unstable closed-loop.

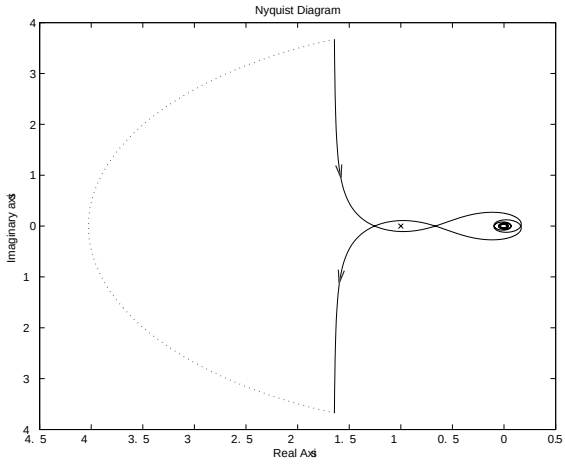

(a) $G_4 = \frac{e^{-0.5s}}{s(s-1)}$ and $C_3 = 1.5s + 0.3$

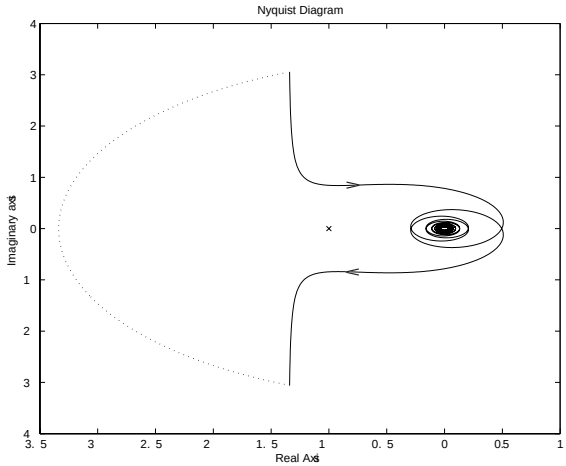

(b) $G_4 = \frac{e^{-1.5s}}{s(s-1)}$ and $C_3 = 1.5s + 0.3$

Figure 2.7. Nyquist plots of G_4 with PD controller

2.6 Second-order Non-integral Unstable Process with A Stable Pole

In this section, stabilization of

$$G_4(s) = \frac{1}{(s-1)(Ts+1)}e^{-Ls}$$

is considered.

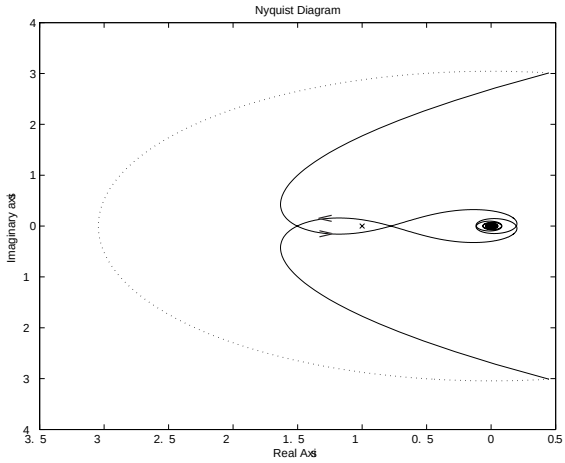

(a) $G_4 = \frac{e^{-0.5s}}{s(s-1)}$ and $C_4 = 1.8s+0.3+0.024/s$

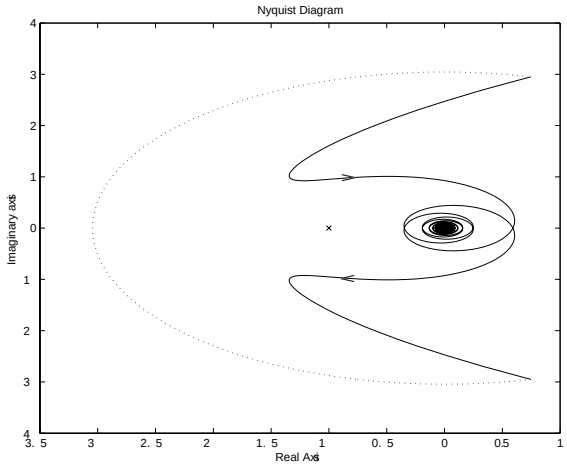

(b) $G_4 = \frac{e^{-1.5s}}{s(s-1)}$ and $C_4 = 1.8s+0.3+0.024/s$

Figure 2.8. Nyquist plots of G_4 with PID controllers

2.6.1 P/PI controller

For P controller, $C_1(s) = K_P$, the open-loop frequency response is

$$Q_{51}(j\omega) = \frac{K_P}{(j\omega - 1)(jT\omega + 1)} e^{-jL\omega},$$

with $P^+ = 1$ and $v = 0$. It follows from Lemma 2.2 that $K = K_P > 1$ is necessary. Then the loop has magnitude as

$$M_{Q_{51}}(\omega) = \sqrt{\frac{K_P^2}{(1+\omega^2)(1+T^2\omega^2)}},$$

which always decreases from K_P to 0. The phase is

$$\Phi_{Q_{51}}(\omega) = -L\omega + \arctan(\omega) - \arctan(T\omega) - \pi, \tag{2.43}$$

with its first and second order derivatives as

$$\frac{d}{d\omega}\Phi_{Q_{51}}(\omega) = -L + \frac{1}{1+\omega^2} - \frac{T}{1+T^2\omega^2},$$

and

$$\frac{d^2}{d\omega^2}\Phi_{Q_{51}}(\omega) = -\frac{2\omega}{(1+\omega^2)^2} + \frac{2T^3\omega}{(1+T^2\omega^2)^2}.$$

It is easy to check that $\Phi_{Q_{51}}(0) = -\pi$ and $\Phi_{Q_{51}}(\omega)$ is always less than $-\pi/2$. Moreover, for $\Phi_{Q_{51}}(\omega) \le -3\pi$, the derivative of phase is always negative since

$$\begin{aligned}
\frac{d\Phi_{Q_{51}}}{d\omega} &= \frac{1}{\omega}\left(-L\omega + \frac{\omega}{1+\omega^2} - \frac{T\omega}{1+T^2\omega^2}\right) \\
&\le \frac{1}{\omega}\left(-2\pi - \arctan\omega + \arctan T\omega + \frac{\omega}{1+\omega^2} - \frac{T\omega}{1+T^2\omega^2}\right) \\
&< \frac{1}{\omega}\left(-2\pi + 0 + \frac{1}{2}\pi + \frac{1}{2} + 0\right) \\
&< 0.
\end{aligned}$$

It follows from Lemma 2.4 that $\Phi_{Q_{51}}(\omega) > -\pi$ for some $\omega > 0$ is necessary for closed-loop stability, and this requires $\frac{d}{d\omega}\Phi_{Q_{51}}(\omega)$ to be positive for some ω. Let $d^2\Phi_{Q_{51}}(\omega)/d\omega^2 = 0$ yields

$$\begin{aligned}
\omega_1^2 &= 0, \\
\omega_2^2 &= \frac{T\sqrt{T} + T + \sqrt{T}}{T^2}.
\end{aligned}$$

Then the maximum value for $\frac{d}{d\omega}\Phi_{Q_{51}}(\omega)$ becomes

$$\max\left(\frac{d}{d\omega}\Phi_{Q_{51}}(\omega)\right) = \begin{cases} 1 - L - T, & : \quad \omega = \omega_1,\ 0 < T < 1 \\ \frac{T\sqrt{T}-1}{T\sqrt{T}+T+\sqrt{T}+1} - L & : \quad \omega = \omega_2,\ T \ge 1 \end{cases}$$

If $T \geq 1$, it follows from (2.43) that $\Phi_{Q_{51}}(\omega) < -\pi$, and thus the closed-loop is always unstable. If $0 < T < 1$, the stabilization requirement for $\frac{d}{d\omega}\Phi_{Q_{51}}(\omega)$ turns to be

$$\frac{d}{d\omega}\Phi_{Q_{51}}(\omega)|_{\omega=\omega_1} = 1 - L - T > 0, \text{ or } L < 1 - T. \tag{2.44}$$

In this case, the phase will increase from $-\pi$ first and then decrease, and there is one and only one intersection with the negative real axis with $\Phi_{Q_{51}}(\omega) = -\pi$. In order for the anticlockwise encirclement of critical point to occur, this intersection should lie between -1 and 0, that is

$$M_{Q_{51}}(\omega_{c1}) < 1, \ \Phi_{Q_{51}}(\omega_{c1}) = -\pi,$$

or equivalently

$$1 < K_P < \sqrt{(1+\omega_{c1}^2)(1+T^2\omega_{c1}^2)}. \tag{2.45}$$

As for $\omega > \omega_{c1}$, $M_{Q_{51}}(\omega)$ is always less than 1 so that there is no encirclement around the critical point thereafter. Consequently, there is exactly one anticlockwise encirclement when $L < 1 - T$ and (2.45) are all true.

As for PI controller, $C_2(s) = K_P(1 + \frac{K_I}{s})$, the open-loop frequency response is

$$Q_{52}(j\omega) = K_P \frac{1 - j\frac{K_I}{\omega}}{(j\omega - 1)(jT\omega + 1)} e^{-jL\omega}, \tag{2.46}$$

with $P^+ = 1$ and $v = 1$. It follows from Lemma 2.2 that $K = -K_P K_I < 0$, or $K_P K_I > 0$ is necessary for closed-loop stability.

Assume $K_P > 0$ and $K_I > 0$ first, then the open-loop has its magnitude as

$$M_{Q_{52}}(\omega) = K_P \sqrt{\frac{1 + \left(\frac{K_I}{\omega}\right)^2}{(1+\omega^2)(1+T^2\omega^2)}},$$

which always decreases from ∞ to 0. The phase of (2.46) is

$$\Phi_{Q_{52}}(\omega) = -L\omega + \arctan(\omega) - \arctan\left(\frac{K_I}{\omega}\right) - \arctan(T\omega) - \pi, \tag{2.47}$$

with its derivative being

$$\frac{d}{d\omega}\Phi_{Q_{52}}(\omega) = -L + \frac{1}{1+\omega^2} + \frac{\frac{K_I}{\omega^2}}{1 + \left(\frac{K_I}{\omega}\right)^2} - \frac{T}{1 + (T\omega)^2}.$$

It follows that $\Phi_{Q_{52}}(\omega) < -\pi/2$. Moreover, when $\Phi_{Q_{52}}(\omega) \leq -3\pi$, the derivative of phase is always negative since

$$\begin{aligned}
\frac{d}{d\omega}\Phi_{Q_{52}}(\omega) =& \frac{1}{\omega}\left(-L\omega + \frac{\omega}{1+\omega^2} + \frac{\frac{K_I}{\omega}}{1+\left(\frac{K_I}{\omega}\right)^2} - \frac{T\omega}{1+T^2\omega^2}\right) \\
\leq& \frac{1}{\omega}\left(-2\pi - \arctan\omega + \arctan\left(\frac{K_I}{\omega}\right) + \arctan T\omega \right. \\
& \left. + \frac{\omega}{1+\omega^2} + \frac{\frac{K_I}{\omega}}{1+\left(\frac{K_I}{\omega}\right)^2} - \frac{T\omega}{1+T^2\omega^2}\right) \\
<& \frac{1}{\omega}\left(-2\pi + 0 + \frac{1}{2}\pi + \frac{1}{2}\pi + \frac{1}{2} + \frac{1}{2} + 0\right) \\
<& 0.
\end{aligned}$$

In consequence, anticlockwise encirclement is possible only when there exists some $\omega > 0$ such that $\Phi_{Q_{52}}(\omega) > -\pi$ by invoking Lemma 2.4.

In case of $L \geq 1 - T$, it is readily seen from the previous P-control discussion that $\Phi_{Q_{52}}(\omega) = \Phi_{Q_{51}}(\omega) - \arctan(K_I/\omega) \leq \Phi_{Q_{51}}(\omega)$, $\Phi_{Q_{51}}(\omega)$ and then $\Phi_{Q_{52}}(\omega)$ are always less than $-\pi$. In consequence, the Nyquist curve has no anticlockwise encirclement around the critical point and the closed-loop is unstable when $K_P > 0$, $K_I > 0$ and $L \geq 1 - T$.

In case of $L < 1 - T$, $\Phi_{Q_{51}}(\omega) > -\pi$ holds from some small ω, and it is always possible to find $\Phi_{Q_{52}}(\omega) > -\pi$ by reducing K_I due to the continuity argument. Thus K_I should be chosen to ensure

$$\max(\Phi_{Q_{52}}(\omega)|_{\omega>0}) > -\pi. \tag{2.48}$$

In order to have anticlockwise encirclement around the critical point, K_P should be chosen such that

$$M_{Q_{52}}(\omega_{c2}) < 1 < M_{Q_{52}}(\omega_{c1}), \tag{2.49}$$

where $0 < \omega_{c1} < \omega_{c2}$ are the first two phase crossover frequencies satisfying $\Phi_{Q_{52}}(\omega) = -\pi$. Inequality (2.49) is always feasible since $M_{Q_{52}}(\omega)$ is monotonically decreasing. Moreover, when (2.49) is true, $M_{Q_{52}}(\omega)$ will always be less than 1 for $\omega > \omega_{c2}$ and $Q_{52}(s)$ will have no encirclement around the critical point for $\omega > \omega_{c2}$. Consequently, there is exactly one anticlockwise encirclement when (2.48), (2.49), $L < 1 - T$, $K_P > 0$ and $K_I > 0$ are all true.

Assume $K_P < 0$ and $K_I < 0$ then, the phase is

$$\Phi_{Q_{52}}(\omega) = -L\omega + \arctan(\omega) - \arctan\left(\frac{K_I}{\omega}\right) - \arctan(T\omega),$$

which is always less than $\pi/2$. Moreover, for $\Phi_{Q_{52}}(\omega) \leq -\pi$, its derivative is always negative since

$$\begin{aligned}
\frac{d}{d\omega}\Phi_{Q_{52}}(\omega) &= \frac{1}{\omega}\left(-L\omega + \frac{\omega}{1+\omega^2} + \frac{\frac{K_I}{\omega}}{1+\left(\frac{K_I}{\omega}\right)^2} - \frac{T\omega}{1+(T\omega)^2}\right) \\
&\leq \frac{1}{\omega}\left(-\pi - \arctan(\omega) + \arctan\left(\frac{K_I}{\omega}\right) + \arctan(T\omega) + \frac{1}{2} + \frac{1}{2} + 0\right) \\
&< \frac{1}{\omega}\left(-\pi + 0 + 0 + \frac{1}{2}\pi + \frac{1}{2} + \frac{1}{2} + 0\right) \\
&< 0.
\end{aligned}$$

It follows from Lemma 2.4 that $Q_{52}(j\omega)$ has no anticlockwise encirclement, and that the closed-loop is unstable when $K_P < 0$ and $K_I < 0$. Then we have the following theorem.

Theorem 2.6. *The process, $G_5(s) = \frac{1}{(Ts+1)(s-1)}e^{-Ls}$, is stabilizable by P controller ($C_1(s) = K_P$) or PI controller ($C_2(s) = K_P(1 + \frac{K_I}{s})$) if and only if $L < 1 - T$. If $L < 1 - T$, the stabilizing gain for P controller is bounded by*

$$1 < K_P < \sqrt{(1+\omega_{c1}^2)(1+T^2\omega_{c1}^2)}. \tag{2.50}$$

with the phase crossover frequency ω_{c1} satisfying

$$-L\omega_{c1} + \arctan(\omega_{c1}) - \arctan(T\omega_{c1}) = 0. \tag{2.51}$$

And the stabilizing parameters for PI controller satisfy

$$K_P > 0,\ K_I > 0. \tag{2.52}$$

K_I is chosen such that

$$\max(\Phi_{Q_{52}}(\omega)) > -\pi, \tag{2.53}$$

and the range of K_P is given by

$$\sqrt{\frac{(1+\omega_{c2}^2)(1+T^2\omega_{c2}^2)}{1+\left(\frac{K_I}{\omega_{c2}}\right)^2}} < K_P < \sqrt{\frac{(1+\omega_{c1}^2)(1+T^2\omega_{c1}^2)}{1+\left(\frac{K_I}{\omega_{c1}}\right)^2}}, \tag{2.54}$$

with $\omega_{c1} < \omega_{c2}$ the first two phase crossover frequencies solved from

$$-L\omega + \arctan(\omega) - \arctan\left(\frac{K_I}{\omega}\right) - \arctan(T\omega) = 0. \tag{2.55}$$

The procedure to design stabilizing P/PI controllers for G_5 is illustrated by the example below.

Example 4. Given the process $G_5 = \frac{1}{(0.5s+1)(s-1)}e^{-0.3s}$, design stabilizing P/PI controllers.

Since $L = 0.3 < 1 - T = 0.5$, it follows from Theorem 2.6 that the process is stabilizable by P or PI controller. The phase crossover frequency $\omega_{c1} = 1.100$ is solved from (2.51). Then K_P is bounded by $1 < K_P < 1.697$. Let $C_1 = K_P = 1.5$, the open-loop transfer function is $Q_{51}(s) = \frac{1.5}{(0.5s+1)(s-1)}e^{-0.3s}$. The Nyquist plot is shown in Fig 2.9(a), which indicates a stable closed-loop. In comparison, let the process delay increase to 1.3 with other settings unchanged, the Nyquist plot of $Q_{51}(s) = \frac{1.5}{(0.5s+1)(s-1)}e^{-1.3s}$ is given in Figure 2.9(b), which indicates an unstable closed-loop.

When PI controller is considered, one may choose sufficiently small K_I to ensure (2.53). In this example, by choosing $K_I = 0.02$, (2.53) is met, then K_P is bounded by $(1.072,\ 1.591)$ from (2.54). Let $K_P = 1.3$, the PI controller is $C_2 = 1.3 + 0.026/s$ and the open-loop transfer function turns to be $Q_{52}(s) = \frac{1.3s+0.026/s}{(0.5s+1)(s-1)}e^{-0.3s}$. The Nyquist plot is given in Figure 2.10(a), which indicates a stable closed-loop. In comparison, let the process delay increase to 1.3 with other settings unchanged, the corresponding Nyquist plot of is given in Figure 2.10(b), which indicates an unstable closed-loop.

2.6.2 PD/PID controller

For PD controller, $C_3(s) = K_P(1 + K_D s)$, the open-loop frequency response is

$$Q_{53}(j\omega) = K_P \frac{1 + jK_D\omega}{(j\omega - 1)(jT\omega + 1)}e^{-jL\omega}, \tag{2.56}$$

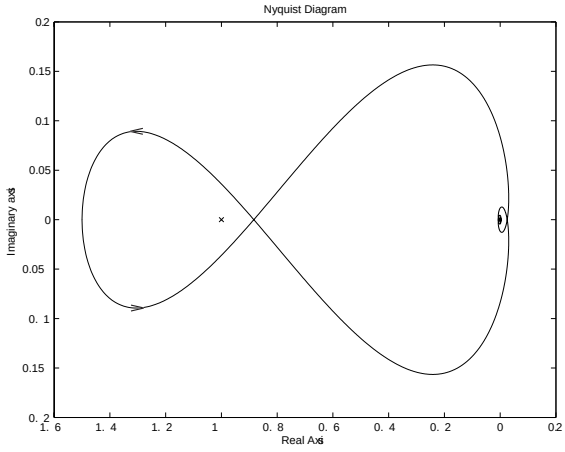

(a) $G_5 = \frac{e^{-0.3s}}{(0.5s+1)(s-1)}$ and $C_1 = 1.5$

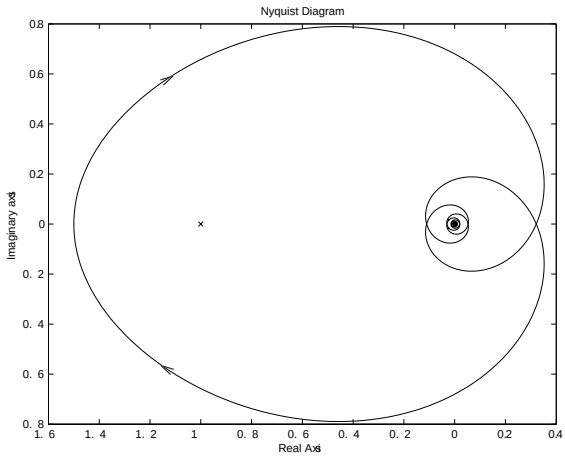

(b) $G_5 = \frac{e^{-1.3s}}{(0.5s+1)(s-1)}$ and $C_1 = 1.5$

Figure 2.9. Nyquist plots of G_5 with P controller

with $P^+ = 1$ and $v = 0$. It follows from Lemma 2.2 that $K = K_P > 1$ is necessary for stabilization. Then the magnitude and phase are

$$M_{Q_{53}}(\omega) = K_P \sqrt{\frac{1 + K_D^2\omega^2}{(1+\omega^2)(1+T^2\omega^2)}}, \tag{2.57}$$

and

$$\Phi_{Q_{53}}(\omega) = -L\omega + \arctan(\omega) + \arctan(K_D\omega) - \arctan(T\omega) - \pi, \tag{2.58}$$

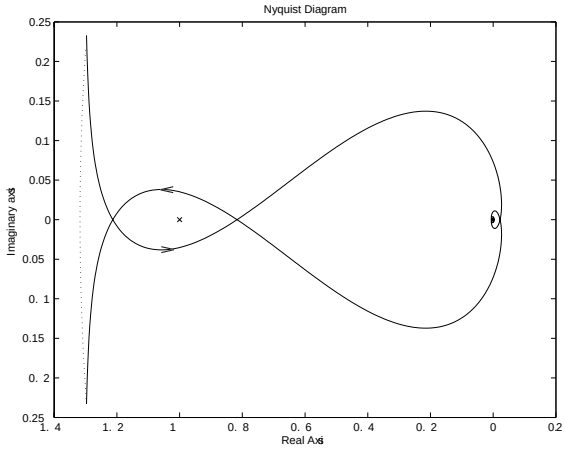

(a) $G_5 = \frac{e^{-0.3s}}{(0.5s+1)(s-1)}$ and $C_2 = 1.3+0.026/s$

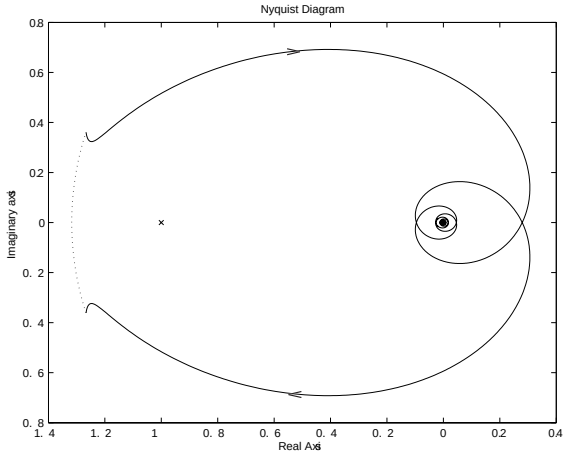

(b) $G_5 = \frac{e^{-1.3s}}{(0.5s+1)(s-1)}$ and $C_2 = 1.3+0.026/s$

Figure 2.10. Nyquist plots of G_5 with PI controller

respectively, with $\Phi_{Q_{53}}(0) = -\pi$ and $\Phi_{Q_{53}}(\omega) < 0$ for $\omega > 0$. Notice that

$$\frac{d}{d\omega}\left(\frac{M_{Q_{53}}^2}{K_P^2}\right) = -\frac{2\omega}{(1+\omega^2)^2(1+T^2\omega^2)^2}(T^2K_D^2\omega^4 + 2T^2\omega^2 + 1 + T^2 - K_D^2), \quad (2.59)$$

it follows that if $(1 + T^2 - K_D^2) > 0$, or equivalently

$$K_D < \sqrt{1+T^2}, \quad (2.60)$$

then $dM_{Q_{53}}/d\omega < 0$ always holds, and $M_{Q_{53}}(\omega)$ decreases monotonically from K_P to 0 when ω increases from 0 to ∞. Otherwise, if

$$K_D > \sqrt{1+T^2}, \tag{2.61}$$

then $dM_{Q_{53}}/d\omega$ is positive when ω is small and turns negative when ω increases, so that $M_{Q_{53}}(\omega)$ increases from K_P first and then decreases to 0 as ω increases. As for the phase, one sees that $\Phi_{Q_{53}}(0) = -\pi$ and

$$\frac{d}{d\omega}\Phi_{Q_{53}}(\omega) = -L + \frac{1}{1+\omega^2} + \frac{K_D}{1+K_D^2\omega^2} - \frac{T}{1+T^2\omega^2} \tag{2.62}$$

with

$$\left.\frac{d\Phi_{Q_{53}}}{d\omega}\right|_{\omega=0} = -L + 1 + K_D - T. \tag{2.63}$$

When $\Phi_{Q_{53}} \leq -3\pi$, the derivative of phase is always negative since

$$\begin{aligned}\frac{d}{d\omega}\Phi_{Q_{53}}(\omega) &= \frac{1}{\omega}\left(-L\omega + \frac{\omega}{1+\omega^2} + \frac{K_D\omega}{1+K_D^2\omega^2} - \frac{T\omega}{1+(T\omega)^2}\right) \\ &\leq \frac{1}{\omega}\left(-3\pi - \arctan(\omega) - \arctan(K_D\omega) + \arctan(T\omega) + \pi + \frac{1}{2} + \frac{1}{2}\right) \\ &< 0.\end{aligned}$$

It follows from Lemma 2.4 the closed-loop is stable only if $\max\left(\Phi_{Q_{53}}(\omega)\right) > -\pi$. The stabilization issue will be discussed for four cases separately, which correspond to four possible combinations of signs of $(1+T^2-K_D^2)$ and $(-L+1+K_D-T)$.

Case A In this case,

$$\begin{cases} K_D < \sqrt{1+T^2} \\ 1 + K_D - T - L > 0 \end{cases}, \tag{2.64}$$

which leads to

$$L < \sqrt{1+T^2} - T + 1. \tag{2.65}$$

Given arbitrary L satisfying (2.65), K_D is chosen within the range

$$L + T - 1 < K_D < \sqrt{1+T^2}, \tag{2.66}$$

which is not empty. Since $\frac{d}{d\omega}\Phi_{Q_{53}}(\omega)\big|_{\omega=0} > 0$, the stabilization is possible. In order for the anti-clockwise encirclement to occur, the first intersection of Nyquist

curve with the real axis for positive frequency should lie between -1 and 0. It follows that $M_{Q_{53}}(\omega_{c1}) < 1$, which leads to

$$1 < K_P < \sqrt{\frac{(1+\omega_{c1}^2)(1+T^2\omega_{c1}^2)}{1+K_D^2\omega_{c1}^2}}, \tag{2.67}$$

combined with the requirement $K_P > 1$. (2.67) is also not empty since $dM_{Q_{53}}/d\omega < 0$. Moreover, when (2.67) is true, $M_{Q_{53}}(\omega)$ is always less than 1 for $\omega > \omega_{c1}$, and Q_{53} does not encircle the critical point for $\omega > \omega_{c1}$. Consequently, PD controller could always stabilize process (2.6) under case A when (2.65), (2.66) and (2.67) are all true. In the rest of this subsection, it is demonstrated that PD controller could not stabilize process (2.6) if $L \geq \sqrt{1+T^2} - T + 1$.

Case B In this case,

$$\begin{cases} K_D > \sqrt{1+T^2} \\ 1 + K_D - T - L > 0 \end{cases}, \tag{2.68}$$

and $L \geq \sqrt{1+T^2} - T + 1$ is assumed. For convenience of analysis, let

$$K_D = \sqrt{1+T^2+\delta^2},\ \delta > 0 \,\text{and}\, \omega_0 = \frac{\delta}{T},$$

and denote by ω_{cp} the smallest positive frequency that $\Phi_{Q_{53}}(\omega_{cp}) = -\pi$. Let $d\Phi_{Q_{53}}/d\omega = 0$, it follows from (2.58) that

$$a_3x^3 + a_2x^2 + a_1x + a_0 = 0, \tag{2.69}$$

where

$$\begin{aligned} x &= \omega^2, \\ a_3 &= -LK_D^2T^2, \\ a_2 &= K_DT^2 + K_D^2T^2 - TK_D^2 - LK_D^2T^2 - LT^2 - LK_D^2, \\ a_1 &= -LT^2 - LK_D^2 - L - TK_D^2 - T + T^2 + K_D^2 + K_DT^2 + K_D, \\ a_0 &= 1 + K_D - L - T. \end{aligned}$$

Since $a_3 < 0$, $a_2 < 0$, and $a_0 > 0$, the roots satisfy

$$x_1 + x_2 + x_3 = -\frac{a_2}{a_3} < 0 \text{ and } x_1x_2x_3 = -\frac{a_0}{a_3} > 0,$$

hence there exists only one positive root. In other words, $d\Phi_{Q_{53}}(\omega)/d\omega = 0$ has only one positive solution. Since $\frac{d}{d\omega}\Phi_{Q_{53}}(\omega)\big|_{\omega=0} > 0$, it follows that $\Phi_{Q_{53}}(\omega)$ increases first at small frequency and then always decreases. Thus $\Phi_{Q_{53}}(\omega) > -\pi$ when $0 < \omega < \omega_{cp}$ and $\Phi_{Q_{53}}(\omega) < -\pi$ when $\omega > \omega_{cp}$. On the other hand, let

$$\Psi(\delta) = \Phi_{Q_{53}}(\omega_0) = -L\frac{\delta}{T} + \arctan\left(\frac{\delta}{T}\right) + \arctan\left(\frac{\delta}{T}\sqrt{1+T^2+\delta^2}\right) - \arctan(\delta) - \pi,$$

It can be proved that

$$\begin{aligned}
\frac{d\Psi(\delta)}{d\delta} &= -\frac{L}{T} + \frac{T}{T^2+\delta^2} + \frac{(1+T^2+2\delta^2)T}{\sqrt{(1+T^2+\delta^2)}(T^2+\delta^2)(1+\delta^2)} - \frac{1}{1+\delta^2} \\
&\leq -\frac{\sqrt{1+T^2}+1-T}{T} + \frac{T}{T^2+\delta^2} + \frac{(1+T^2+2\delta^2)T}{\sqrt{(1+T^2+\delta^2)}(T^2+\delta^2)(1+\delta^2)} - \frac{1}{1+\delta^2} \\
&< 0. \qquad (2.70)
\end{aligned}$$

The proof for inequality (2.70) is given in 2.8. Then we have

$$\Phi_{Q_{53}}(\omega_0) < \Psi(\delta)|_{\delta\to 0} = -\pi,$$

and in turn $\omega_0 > \omega_{cp}$. Thus

$$\begin{aligned}
\left(M_{Q_{53}}(\omega_{cp})\right)^2 &= K_P^2 \frac{1+K_D^2\omega_{cp}^2}{(1+\omega_{cp}^2)(1+T^2\omega_{cp}^2)} \\
&= K_P^2\left(1 + \frac{T^2\omega_{cp}^2(\omega_0^2-\omega_{cp}^2)}{1+(1+T^2)\omega_{cp}^2+T^2\omega_{cp}^4}\right) \\
&> K_P^2 = \left(M_{Q_{53}}(0)\right)^2,
\end{aligned}$$

which prevents anticlockwise encirclement. Consequently, the stabilization fails for case B.

Case C In this case,

$$\begin{cases} K_D < \sqrt{1+T^2} \\ 1 + K_D - T - L < 0 \end{cases}, \qquad (2.71)$$

and assume $L \geq \sqrt{1+T^2} + 1 - T$. Then it follows that

$$\begin{aligned}
\Phi_{Q_{53}}(\omega) &\leq -(\sqrt{1+T^2}+1-T)\omega + \arctan(\omega) + \arctan(\sqrt{1+T^2}\omega) - \arctan(T\omega) - \pi \\
&\triangleq \Theta(\omega).
\end{aligned}$$

Let

$$\frac{d\Theta(\omega)}{d\omega} = 0,$$

which leads to

$$(b_2x^2 + b_1x + b_0)x = 0,$$

where

$$\begin{aligned}
&x = \omega^2,\\
&b_2 = (1+T^2)T^2 > 0,\\
&b_1 = \sqrt{1+T^2}T^4 + 2\sqrt{1+T^2}T^2 + 2T^2 + \sqrt{1+T^2} + 1 - T^5 - 2T^3 > 0,\\
&b_0 = \sqrt{1+T^2}T^2 + \sqrt{1+T^2} + 1 - T^3 > 0.
\end{aligned}$$

It is clear that there is no positive solution for x or ω. Combined with the fact that $d\Theta(\omega)/d\omega|_{\omega=\infty} < 0$, it is clear that $d\Theta(\omega)/d\omega < 0$ for $\omega > 0$ and

$$\Theta(\omega) < \Theta(0) = -\pi.$$

Consequently, $\Phi_{Q_{53}}(\omega) < -\pi$ holds for $\omega > 0$, and there is no anticlockwise encirclement.

Case D In this case,

$$\begin{cases} K_D > \sqrt{1+T^2} \\ 1 + K_D - T - L < 0 \end{cases}, \tag{2.72}$$

and assume $L \geq \sqrt{1+T^2} + 1 - T$. Still let $d\Phi_{Q_{53}}/d\omega = 0$, it follows from (2.69) that $a_i < 0$ for $i = 0, 1, 2, 3$, and there is no positive root for x or ω. Thus $d\Phi_{Q_{53}}/d\omega$ keeps the negative sign when $\omega > 0$. Consequently, $\Phi_{Q_{53}}(\omega) < -\pi$ for $\omega > 0$, and once again there is no anticlockwise encirclement.

As for PID controller, $C_4(s) = K_P(1 + K_Ds + K_I/s)$, the open-loop transfer function is

$$Q_{54}(s) = K_P\frac{K_Ds + 1 + K_I/s}{(s-1)(Ts+1)}e^{-Ls}.$$

It follows from Lemma 2.3 that the closed-loop stability requires $H(s) = TL^3s^3 + (9TL^2 + L^3 - TL^3)s^2 + (18TL + 6L^2 - 6TL^2 - L^3)s + 6T + 6L - 6TL - 3L^2$ be stable. Then the constant term $6T + 6L - 6TL - 3L^2 > 0$ is necessary, which leads to

$L < \sqrt{1+T^2} - T + 1$. Also noting that PD is a special case of PID controller, it is concluded that PID controller could stabilize G_5 if and only if $L < \sqrt{1+T^2} - T + 1$.

Summarizing the previous analysis, the following theorem is obtained.

Theorem 2.7. *The process, $G_5(s) = \frac{1}{(Ts+1)(s-1)}e^{-Ls}$, is stabilizable by PD controller ($C_3(s) = K_P(1+K_Ds)$) or PID controller ($C_4(s) = K_P(1+K_Ds+K_I/s)$)if and only if $L < \sqrt{1+T^2} - T + 1$. If $L < \sqrt{1+T^2} - T + 1$, the stabilizing controller parameters for PD controller can be found from*

$$L + T - 1 < K_D < \sqrt{1+T^2}, \tag{2.73}$$

and

$$1 < K_P < \sqrt{\frac{(1+\omega_{c1}^2)(1+T^2\omega_{c1}^2)}{1+K_D^2\omega_{c1}^2}} \tag{2.74}$$

with the phase crossover frequency ω_{c1} satisfying

$$-L\omega_{c1} + \arctan(\omega_{c1}) + \arctan(K_D\omega_{c1}) - \arctan(T\omega_{c1}) = 0. \tag{2.75}$$

The following example illustrates the procedure to design stabilizing PD/PID controllers for G_5.

Example 5. Given the process $G_5 = \frac{1}{(0.5s+1)(s-1)}e^{-1.2s}$, design stabilizing PD/PID controllers.

Since $L = 1.2 < \sqrt{1+0.5^2} - 0.5 + 1$, it follows from Theorem 2.7 that the process is stabilizable by PD controller. According to (2.73), a stabilizing gain of K_D could be found from the range $(0.7,\ 1.118)$. Let $K_D = 1$, then $\omega_{c1} = 0.821$ is solved numerically from (2.75), and $1 < K_P < 1.081$ is determined from (2.74). Let $K_P = 1.04$, then $C_3 = 1.04 + 1.04s$, and $Q_{53}(s) = \frac{1.04s+1.04}{(0.5s+1)(s-1)}e^{-1.2s}$. The Nyquist plot is shown in Fig 2.11(a), which indicates a stable closed-loop. In comparison, let the process delay increase to 2.2 with other settings unchanged, the Nyquist plot of $Q_{53}(s) = \frac{1.04s+1.04}{(0.5s+1)(s-1)}e^{-2.2s}$ is given in Figure 2.11(b), which indicates an unstable closed-loop.

When PID controller is used, let K_D in the same range of PD, then there exists a sufficiently small positive K_I such that $\max(\Phi_{54}) < -\pi$. It is easily shown that if

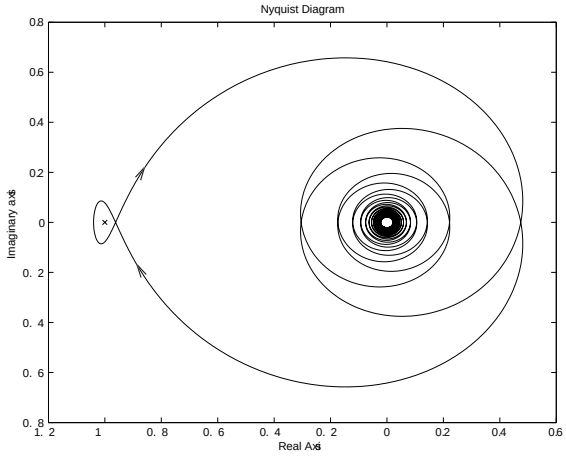

(a) $G_5 = \frac{e^{-1.2s}}{(0.5s+1)(s-1)}$ and $C_3 = 1.04s + 1.04$

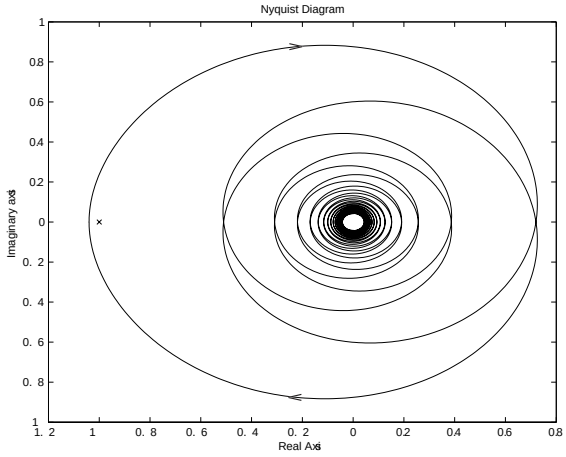

(b) $G_5 = \frac{e^{-2.2s}}{(0.5s+1)(s-1)}$ and $C_3 = 1.04s + 1.04$

Figure 2.11. Nyquist plots of G_5 with PD controller

K_I is in the range of $0 < K_I < 1/2K_D$, the magnitude will decrease monotonically. Then K_P given by

$$\sqrt{\frac{(1+\omega_{c1}^2)(1+T^2\omega_{c1}^2)}{1+(K_D\omega_{c1}-\frac{K_I}{\omega_{c1}})^2}} < K_P < \sqrt{\frac{(1+\omega_{c2}^2)(1+T^2\omega_{c2}^2)}{1+(K_D\omega_{c2}-\frac{K_I}{\omega_{c2}})^2}},$$

is stabilizing and not empty, where the two positive phase crossover frequencies

$\omega_{c1} < \omega_{c2}$ are solved from

$$-L\omega + \arctan\left(K_D\omega - \frac{K_I}{\omega}\right) + \arctan(\omega) - \arctan(T\omega) = 0.$$

For this example, choose $K_D = 1.1$ and $K_I = 0.05$, then K_P is in the range $(1.047,\ 1.0732)$. Let $K_P = 1.06$, the PID controller is $C_4 = 1.166s + 1.06 + 0.053/s$ and the open-loop transfer function turns to be $Q_{54}(s) = \frac{1.166s+1.06+0.053/s}{(0.5s+1)(s-1)}e^{-1.2s}$. The Nyquist plot is given in Figure 2.12(a), which indicates a stable closed-loop. In comparison, let the process delay increase to 2.2 with other settings unchanged, the corresponding Nyquist plot of is given in Figure 2.12(b), which indicates an unstable closed-loop.

2.7 Conclusion

In this chapter, the stabilization of five typical time delay processes is investigated. For each case, the maximum allowable time delay for different controllers is derived, and the procedure for establishing the range of the stabilization gains is also given.

It is manifested from the studies that: for the processes under consideration, the maximum stabilizable time delay with PD/PID controller is larger than that with P/PI controller. At the same time, the maximum stabilizable time delay with P controller is equal to that with PI controller, and the maximum stabilizable time delay with PD is the same as that with PID controller. Hence when only stabilization of these processes is needed, P or PD controller is sufficient.

To deal with practical unstable process with time delay, if the time delay is within the stabilizing range given in this chapter, then the corresponding PID parameters can be determined to stabilize the plant. And then the problem is reduced to controller design for stable process with time delay, where there are many techniques available (Park *et al.*, 1998; Wang *et al.*, 1999*c*; Chen and Seborg, 2002). If the time delay is larger than the maximum, more sophisticated controllers have to be resorted to.

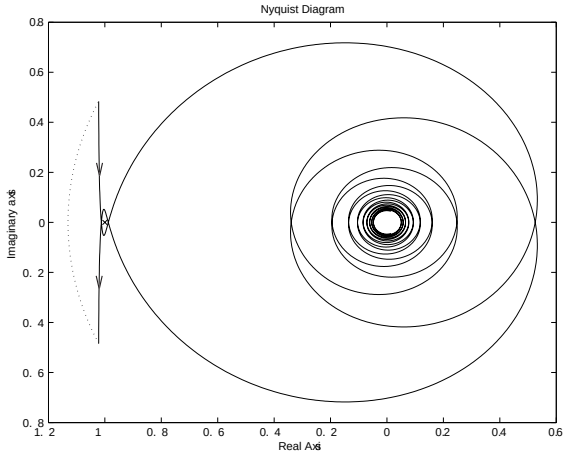

(a) $G_5 = \frac{e^{-1.2s}}{(0.5s+1)(s-1)}$ and $C_4 = 1.166s + 1.06 + 0.053/s$

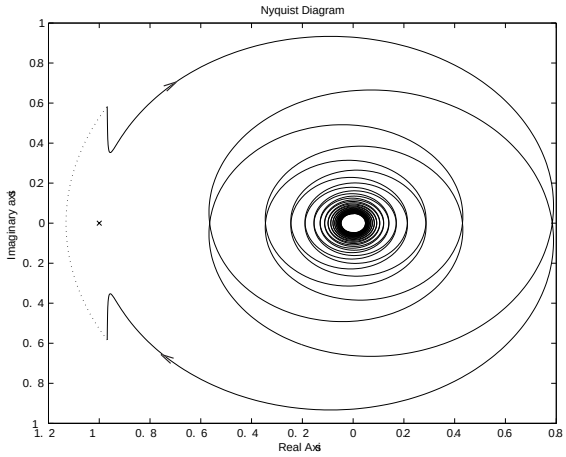

(b) $G_5 = \frac{e^{-2.2s}}{(0.5s+1)(s-1)}$ and $C_4 = 1.166s + 1.06 + 0.053/s$

Figure 2.12. Nyquist plots of G_5 with PID controller

2.8 Appendix

Proof for inequality (2.70).

In order to prove

$$-\frac{\sqrt{1+T^2}+1-T}{T}+\frac{T}{T^2+\delta^2}+\frac{(1+T^2+2\delta^2)T}{\sqrt{(1+T^2+\delta^2)}(T^2+\delta^2)(1+\delta^2)}-\frac{1}{1+\delta^2}<0.$$

it is equivalent to prove the inequality

$$\frac{(1+T^2+2\delta^2)T}{\sqrt{(1+T^2+\delta^2)}(T^2+\delta^2)(1+\delta^2)} < \frac{\sqrt{1+T^2}+1-T}{T} + \frac{\delta^2(1+\delta^2-T^3-\delta^2T)}{T(T^2+\delta^2)(1+\delta^2)}. \tag{2.76}$$

Its left half part is positive, and its right half part is also positive since

$$\frac{\sqrt{1+T^2}+1-T}{T} + \frac{\delta^2(1+\delta^2-T^3-\delta^2T)}{T(T^2+\delta^2)(1+\delta^2)} = \frac{\sqrt{1+T^2}}{T} - \frac{\delta^2}{1+\delta^2} + \frac{\delta^2}{T(T^2+\delta^2)} > 0.$$

To prove (2.76) is thus equivalent to prove the inequality

$$(1+T^2+2\delta^2)^2T^4 - p < q\sqrt{1+T^2} \tag{2.77}$$

where both sides of (2.76) are squared and reorganized, with p and q defined as

$$\begin{aligned} p &= (1+T^2+\delta^2)\left[(1+T^2)(T^2+\delta^2)^2(1+\delta^2)^2 + \delta^4(1+\delta^2-T^3-\delta^2T)^2\right], \\ q &= 2\delta^2(T^2+\delta^2)(1+\delta^2)(1+\delta^2-T^3-\delta^2T)(1+T^2+\delta^2). \end{aligned}$$

The left half side of (2.77) is always negative since

$$\begin{aligned} &(1+T^2+2\delta^2)^2T^4 - p \\ &= (-2T^2+2T-2)\delta^{10} + (-6T^4+4T^3-8T^2+4T-6)\delta^8 \\ &+ (-6T^6+2T^5-13T^4+6T^3-13T^2+2T-6)\delta^6 \\ &+ (-2T^8-9T^6+2T^5-10T^4+2T^3-9T^2-2)\delta^4 + (-2T^8-3T^6-3T^4-2T^2)\delta^2, \end{aligned}$$

where the coefficients for different powers of δ is easily verified negative by either assuming $T \geq 1$ or $0 < T < 1$.

If $T \geq 1$, it follows that the right half part of (2.77) is non-negative since $q \geq 0$, so (2.77) holds.

If $T > 1$, where $q < 0$, (2.77) still holds since $[(1+T^2+2\delta^2)^2T^4 - p]^2 <$

$q^2(1+T^2)$:

$$
\begin{aligned}
&\left[(1+T^2+2\delta^2)^2T^4-p\right]^2-q^2(1+T^2)\\
=&4T^2\delta^{20}+(16T^4+16T^2+16T^3)\delta^{18}+(24T^2+24T^6+68T^5+72T^4+68T^3)\delta^{16}\\
&+(116T^7+116T^3+16T^2+16T^8+128T^4+128T^6+264T^5)\delta^{14}\\
&+(254T^6+113T^4+100T^9+113T^8+404T^5+404T^7+4T^{10}+4T^2+100T^3)\delta^{12}\\
&+(238T^8+50T^4+304T^5+44T^{11}+44T^3+238T^6+536T^7+50T^{10}+304T^9)\delta^{10}\\
&+(112T^5+8T^3+210T^8+332T^9+8T^{13}+106T^6+332T^7+112T^{11}+9T^4\\
&\quad+106T^{10}+9T^{12})\delta^8\\
&+(16T^{13}+16T^5+78T^{10}+18T^6+92T^7+78T^8+92T^{11}+152T^9+18T^{12})\delta^6\\
&+(9T^8+9T^{12}+18T^{10}+8T^{13}+8T^7+24T^9+24T^{11})\delta^4\\
>&0.
\end{aligned}
$$

In consequence, (2.77) and in turn (2.76) hold either for $T \geq 1$ or $0 < T < 1$, and the proof completes.

Chapter 3

PID Control for Regional Pole Placement

3.1 Introduction

In this chapter, an iterative LMI algorithm is presented to calculate PID controller with regional pole placement requirements. Pole placement is one of the fundamental control problems. Much of the literature on the topic focuses on the problem of exact pole placement, where the poles are assigned to or arbitrarily close to specific locations (Wang, 1996). In practice, however, it is often the case that exact closed-loop pole placement is not required. Rather, it may suffice to place the closed-loop poles within a suitable region in the left-half complex plane, which is referred to as regional pole placement (RPP) (Keerthi and Phatak, 1995). However, most works on regional pole placement are restricted to the state-feedback case, or full order dynamic output feedback case (Chilali *et al.*, 1999).

Since it is not always possible to have full access to the state vector, and the full-order dynamic output controllers might be difficult or impossible to implement owing to cost, reliability and hardware implementation constraints, it is of great importance to consider alternative solutions for such a regional pole placement problem. Among most feedback control structures, the PID controllers have been widely used in many industrial control systems due to its its simple structure, con-

venient applicability, and reliable performance (Åström and Hagglünd, 1995). It is thus desirable to investigate the regional pole placement by PID Controllers. As is shown in Zheng *et al.* (2002) and several other literatures, PID controller, as well as other reduced order feedback controllers, is convertible to SOF controllers through state augmentations. Therefore it is useful to form a unifying framework to ease analysis and design of multivariable PID control systems by finding a equivalent SOF controller to meet the specifications.

Despite the simple form of SOF controller, the pole placement problem by SOF remains open, even in the scalar case (Syrmos *et al.*, 1997). Since the celebrated monograph of Boyd *et al.* (1994), many control problems have been synthesized with LMI. It is well known that the static state feedback and the full-order dynamic output feedback control problems result in convex feasibility problems (Gahinet and Apkarian, 1994). In Chilali and Gahinet (1996), the conception of LMI regions is proposed, and then RPP by state feedback or full order dynamic output feedback is formulated as an LMI problem and solved together with H_∞ design. In this chapter, the RPP by SOF controller is formulated as a bilinear matrix inequality problem, which is recast as a quadratic matrix inequality problem and is then solved through an iterative LMI algorithm.

The organization of this chapter is as follows. In Section 3.2, the definition of LMI region and some key results on pole clustering in LMI regions are given first, then the SOF regional pole placement problem is addressed and an ILMI approach is proposed to solve it. Section 3.3 extends the result to reduced order feedback and PI/PID controllers design. Some numerical examples are provided in both Sections to demonstrate the effectiveness of the proposed approach. Finally, Section 3.4 concludes this chapter.

Notation: $\mathbb{R}$ and $\mathbb{C}$ denote the set of real numbers and complex numbers, respectively; and correspondingly, $\mathbb{R}^{m\times n}$ and $\mathbb{C}^{m\times n}$ the set of real $m \times n$ matrices and complex $m \times n$ matrices. I_n denotes the $n \times n$ identity matrix. For a real matrix X, $X > 0$ means X is positive-definite. $\mathrm{tr}(X)$ denotes the trace of X, X^T the transpose, and $\|X\|$ the 2-norm of X. The operator $\otimes$ refers to Kronecker

product, and $\triangleq$ refers to definition. Finally, we use the shorthand

$$\mathrm{Diag}(X_1, \ldots, X_k) \triangleq \begin{bmatrix} X_1 & 0 & \cdots & 0 \\ 0 & X_2 & \ddots & \vdots \\ \vdots & \ddots & \ddots & 0 \\ 0 & \cdots & 0 & X_k \end{bmatrix}.$$

3.2 Regional Pole Placement by Static Output Feedback

In order to achieve satisfactory transients, a custom way is to place the closed-loop poles within a suitable region in the complex plane. Preferable dynamics such as fast decay, good damping, etc. can be ensured by confining the poles in the intersection of a conic sector, a vertical stripe, and a disk, etc.. Consider the linear time-invariant plant:

$$\begin{cases} \dot{x} = Ax + Bu \\ y = Cx + Du \end{cases}, \tag{3.1}$$

with the feedback controller

$$u = Fy,$$

where $x(t) \in \mathbb{R}^n$ is the state, $u(t) \in \mathbb{R}^m$ the control input, and $y(t) \in \mathbb{R}^p$ the output. A, B and C are matrices with appropriate dimensions, and $F \in \mathbb{R}^{m \times p}$ is the feedback gain to be designed. Our goal is to determine F such that the closed-loop poles (or equivalently the eigenvalues of matrix $A_{cl} = A + BFC$) are located within the prescribed regions.

In Chilali and Gahinet (1996), it is demonstrated that any set of convex regions that are symmetric with respect to the real axis can be approximated by LMI region(s), which is a subset $\mathcal{D}$ of the complex plane that can be described by $\mathcal{D} = \{z \in \mathbb{C} : f_{\mathcal{D}}(z) = L + zM + \bar{z}M^T < 0\}$, with $L, M \in \mathbb{R}^{q \times q}$ and $L = L^T$. Specifically, if the region $\mathcal{D}$ is the intersection of j LMI regions $\mathcal{D}_1, \ldots, \mathcal{D}_j$, which are characterized by $f_{\mathcal{D}_i}$ with $f_{\mathcal{D}_i}(z) = L_i + zM_i + \bar{z}M_i^T$, $i = 1 \ldots j$, then $L = \mathrm{Diag}(L_1, \ldots, L_j)$ and $M = \mathrm{Diag}(M_1, \ldots, M_j)$. It follows from Chilali and Gahinet

(1996) that all the closed-loop poles of system (3.1) are placed within the LMI region $\mathcal{D}$ if and only if there exist matrices $X > 0$ and F such that

$$L \otimes X + M \otimes (A_{cl}X) + M^T \otimes (A_{cl}X)^T < 0, \tag{3.2}$$

where $\otimes$ denotes Kronecker product.

In order to have a more clear vision of (3.2), for a matrix $Y \in \mathbb{R}^{q\times q}$, let

$$\hat{Y} \triangleq \begin{bmatrix} y_{11}I_n & y_{12}I_n & \cdots & y_{1q}I_n \\ \vdots & \ddots & \ddots & \vdots \\ y_{q1}I_n & y_{q2}I_n & \cdots & y_{qq}I_n \end{bmatrix}_{nq\times nq}, \tag{3.3}$$

where y_{ij} is the ijth element of Y. Also, for a matrix $Z \in \mathbb{R}^{k\times l}$, let

$$\bar{Z} \triangleq \begin{bmatrix} Z & 0_{k\times l} & \cdots & 0_{k\times l} \\ 0_{k\times l} & Z & \cdots & 0_{k\times l} \\ \vdots & \ddots & \ddots & \vdots \\ 0_{k\times l} & 0_{k\times l} & \cdots & Z \end{bmatrix}_{kq\times lq}. \tag{3.4}$$

Matrices $\hat{L}$, $\hat{M}$, $\bar{A}$, $\bar{B}$, $\bar{C}$, $\bar{F}$, $\bar{X}$, and $\overline{A_{cl}}$ are defined accordingly. It is easy to verify the following facts:

$$\begin{aligned} \overline{A_{cl}X} = \overline{A_{cl}}\bar{X} &= (\bar{A} + \bar{B}\bar{F}\bar{C})\bar{X}, \\ L \otimes X = \hat{L}\bar{X}, \quad M \otimes (A_{cl}X) &= \hat{M}\overline{A_{cl}}\bar{X}, \\ M^T \otimes (A_{cl}X)^T = (M \otimes (A_{cl}X))^T &= (\hat{M}\overline{A_{cl}}\bar{X})^T. \end{aligned}$$

By substituting these terms into (3.2), the RPP problem with SOF is recast as the the existence of matrices $X > 0$ and F such that the following inequality holds:

$$\hat{L}\bar{X} + \hat{M}(\bar{A} + \bar{B}\bar{F}\bar{C})\bar{X} + (\hat{M}(\bar{A} + \bar{B}\bar{F}\bar{C})\bar{X})^T < 0. \tag{3.5}$$

However, (3.5) is a bilinear matrix inequality due to the existence of term $\hat{M}\bar{B}\bar{F}\bar{C}\bar{X}$, and is difficult to solve generally.

In Cao *et al.* (1998), the SOF stabilization problem is studied and solved through an iterative approach. Enlightened by their thoughts, the following theorem for RPP with SOF can be obtained.

Theorem 3.1. *The closed-loop poles of LTI system* (3.1) *are placed within LMI region* $\mathcal{D}$ *if and only if there exist matrices* $X > 0$, $P > 0$ *and* F *such that the following inequality holds:*

$$\hat{L}\bar{X}+\tilde{A}\bar{X}+\bar{X}\tilde{A}^T-\bar{P}\bar{C}^T\bar{C}\bar{X}^T-\bar{X}\bar{C}^T\bar{C}\bar{P}^T+\bar{P}\bar{C}^T\bar{C}\bar{P}^T+(\tilde{B}\bar{F}+\bar{X}\bar{C}^T)(\tilde{B}\bar{F}+\bar{X}\bar{C}^T)^T<0, \tag{3.6}$$

where $\tilde{A}=\hat{M}\bar{A}$, $\tilde{B}=\hat{M}\bar{B}$, *and* $\bar{P}$ *is defined similarly to* (3.4) *with* $P\in\mathbb{R}^{n\times n}$.

In order to prove Theorem 3.1, the following lemma is needed.

Lemma 3.1. *The necessary and sufficient condition* (3.5) *for RPP problem with SOF is equivalent to the existence of matrices* $X > 0$ *and* F *for the following inequality*

$$\hat{L}\bar{X} + \tilde{A}\bar{X} + \bar{X}\tilde{A}^T - \bar{X}\bar{C}^T\bar{C}\bar{X}^T + (\tilde{B}\bar{F} + \bar{X}\bar{C}^T)(\tilde{B}\bar{F} + \bar{X}\bar{C}^T)^T < 0. \tag{3.7}$$

Proof. Sufficiency: rewrite (3.5) *as follows:*

$$\hat{L}\bar{X} + (\tilde{A} + \tilde{B}\bar{F}\bar{C})\bar{X} + \bar{X}^T(\tilde{A} + \tilde{B}\bar{F}\bar{C})^T < 0. \tag{3.8}$$

It follows that:

$$\begin{aligned}
&\hat{L}\bar{X} + (\tilde{A} + \tilde{B}\bar{F}\bar{C})\bar{X} + \bar{X}^T(\tilde{A} + \tilde{B}\bar{F}\bar{C})^T \\
&\quad\le \hat{L}\bar{X} + (\tilde{A} + \tilde{B}\bar{F}\bar{C})\bar{X} + \bar{X}^T(\tilde{A} + \tilde{B}\bar{F}\bar{C})^T + \tilde{B}\bar{F}\bar{F}^T\tilde{B}^T \\
&\quad= \hat{L}\bar{X} + \tilde{A}\bar{X} + \bar{X}\tilde{A}^T - \bar{X}\bar{C}^T\bar{C}\bar{X}^T + (\tilde{B}\bar{F} + \bar{X}\bar{C}^T)(\tilde{B}\bar{F} + \bar{X}\bar{C}^T)^T \\
&\quad< 0.
\end{aligned}$$

Necessity. suppose $\bar{X} > 0$ *and* $\bar{F}$ *such that* (3.8) *holds, then there exist a scalar* $\rho > 0$ *such that*

$$\hat{L}\bar{X} + (\tilde{A} + \tilde{B}\bar{F}\bar{C})\bar{X} + \bar{X}^T(\tilde{A} + \tilde{B}\bar{F}\bar{C})^T + \frac{1}{\rho^2}\tilde{B}\bar{F}\bar{F}^T\tilde{B}^T < 0, \tag{3.9}$$

i.e.

$$\rho^2\hat{L}\bar{X}+\rho^2\tilde{A}\bar{X}+\rho^2\bar{X}\tilde{A}^T-\rho^4\bar{X}\bar{C}^T\bar{C}\bar{X}+(\tilde{B}\bar{F}+\rho^2\bar{X}\bar{C}^T)(\tilde{B}\bar{F}+\rho^2\bar{X}\bar{C}^T)^T<0. \tag{3.10}$$

which is equivalent to (3.7) *by substituting* $\rho^2\bar{X}$ *with* $\bar{X}$.□

Now turn back to Theorem 3.1.

Proof. Sufficiency: it's easy to check $(\bar{X}-\bar{P})\bar{C}^T\bar{C}(\bar{X}-\bar{P})^T \geq 0$, for any $\bar{X}$ and $\bar{P}$ of the same dimension, i.e.

$$\bar{X}\bar{C}^T\bar{C}\bar{X}^T - \bar{P}\bar{C}^T\bar{C}\bar{X}^T - \bar{X}\bar{C}^T\bar{C}\bar{P}^T + \bar{P}\bar{C}^T\bar{C}\bar{P}^T \geq 0, \tag{3.11}$$

with equality holds when when $\bar{P}=\bar{X}$. Combining inequalities (3.6) and (3.11) yields (3.7), according to Lemma 3.1, the sufficiency is proven.

Necessity. Assume there exist $\bar{X}>0$ and $\bar{F}$ such that (3.7) holds, then there exists a real number $\varepsilon>0$ such that:

$$\hat{L}\bar{X} + \tilde{A}\bar{X} + \bar{X}\tilde{A}^T - \bar{X}\bar{C}^T\bar{C}\bar{X}^T + (\tilde{B}\bar{F}+\bar{X}\bar{C}^T)(\tilde{B}\bar{F}+\bar{X}\bar{C}^T)^T + \varepsilon I < 0. \tag{3.12}$$

Choose $\Lambda \geq \bar{C}^T\bar{C}$, $\Delta P = \varepsilon^{1/2}\Lambda^{-1/2}$, and set $\bar{P}=\bar{X}-\Delta P$, then

$$(\bar{X}-\bar{P})\bar{C}^T\bar{C}(\bar{X}-\bar{P})^T \leq \varepsilon I,$$

Hence (3.6) holds, and necessity is proven. Then the proof for Theorem 3.1 completes

Using Schur complement, inequality (3.6) is equivalent to the following quadratic matrix inequality

$$\begin{bmatrix} \hat{L}\bar{X} + \tilde{A}\bar{X} + \bar{X}\tilde{A}^T - \bar{P}\bar{C}^T\bar{C}\bar{X}^T - \bar{X}\bar{C}^T\bar{C}\bar{P}^T + \bar{P}\bar{C}^T\bar{C}\bar{P}^T & (\tilde{B}\bar{F}+\bar{X}\bar{C}^T) \\ (\tilde{B}\bar{F}+\bar{X}\bar{C}^T)^T & -I \end{bmatrix} < 0. \tag{3.13}$$

Once $\bar{P}$ is fixed, (3.13) reduces to an LMI problem, and obviously there always exist a real number α, matrices $X>0$ and F such that

$$\begin{bmatrix} \hat{L}\bar{X} + \tilde{A}\bar{X} + \bar{X}\tilde{A}^T - \bar{P}\bar{C}^T\bar{C}\bar{X}^T - \bar{X}\bar{C}^T\bar{C}\bar{P}^T + \bar{P}\bar{C}^T\bar{C}\bar{P}^T - \alpha\bar{X} & (\tilde{B}\bar{F}+\bar{X}\bar{C}^T) \\ (\tilde{B}\bar{F}+\bar{X}\bar{C}^T)^T & -I \end{bmatrix} < 0. \tag{3.14}$$

Specifically, $\alpha \leq 0$ indicates the feasibility of (3.13). In order to find a negative α, Cao *et al.* (1998) proposed an iterative LMI algorithm that always leads to a convergent reducing series of α but can not ensure the convergence of α to its minimum. With some modifications, the iterative LMI algorithm that follows is given to solve the RPP problem by SOF.

Algorithm 3.1. Initial data: the state space realization (A, B, C), and desired LMI region characterized by L, M. Augment these matrices to form $\hat{L}$, $\hat{M}$, $\bar{A}$, $\bar{B}$, $\bar{C}$, and then compute $\tilde{A}$ and $\tilde{B}$.

Step 1. Choose an initial block diagonal $\bar{X} > 0$, set $i = 1$ and $\bar{P}_1 = \bar{X}$;

Step 2. Solve the following optimization problem for $\bar{X}_i$, $\bar{F}$ and α_i. OP1: Minimize α_i subject to the following LMI constraints

$$\begin{bmatrix} \Sigma_i & (\tilde{B}\bar{F} + \bar{X}_i\bar{C}^T) \\ (\tilde{B}\bar{F} + \bar{X}_i\bar{C}^T)^T & -I \end{bmatrix} < 0, \tag{3.15}$$

$$\bar{X}_i = \mathrm{Diag}(X_i, \cdots, X_i), \quad X_i > 0, \quad \bar{F} = \mathrm{Diag}(F, \cdots, F),$$

where $\Sigma_i = \hat{L}\bar{X}_i + \tilde{A}\bar{X}_i + \bar{X}_i\tilde{A}^T - \bar{P}_i\bar{C}^T\bar{C}\bar{X}_i^T - \bar{X}_i\bar{C}^T\bar{C}\bar{P}_i^T + \bar{P}_i\bar{C}^T\bar{C}\bar{P}_i^T - \alpha_i\bar{X}_i$. Denote by α^* the minimum value of α_i;

Step 3. If $\alpha^* \leq 0$, the matrix pair $(\bar{X}_i, \bar{F})$ solves the RPP problem, stop, and F is the static output feedback gain for the regional pole placement. Otherwise go to Step 4;

Step 4. Solve the following optimization problem for $\bar{X}_i$ and $\bar{F}$. OP2: Minimize $\mathrm{tr}(\bar{X}_i)$ subject to LMI constraints (3.15) with $\alpha_i = \alpha_i^*$. Denote by $\bar{X}_i^*$ the optimal $\bar{X}_i$.

Step 5. If $\|\bar{P}_i\tilde{B} - \bar{X}_i^*\tilde{B}\| < \varepsilon$, where ε is a prescribed threshold, go to Step 6; otherwise set $i = i + 1$, $\bar{P}_i = \bar{X}_i^*$, and go to Step 2;

Step 6. It cannot be decided by this algorithm whether the RPP problem is solvable. Stop.

In this algorithm, OP1 is a generalized eigenvalue minimization problem, and OP2 is a linear objective minimization problem, both of which can be solved efficiently with LMI toolbox in Matlab (Gahinet *et al.*, 1995). The initial choice of $\bar{X}$ in step 1 will affect the convergence process of the algorithm. If the algorithm fails to produce a solution, we may run the algorithm again with another initial $\bar{X}$. In our simulation examples, an initial setting of $\bar{X} = I$ is adopted.

We also need to comment on the stop of this algorithm. Desired regional pole placement will be ensured when $\alpha_i < 0$. However, due to the iterative nature of the algorithm, as the iteration goes and α_i decreases, the pole clustering may have been achieved before α_i drops below zero. Hence we can check the eigenvalues of $(A + BFC)$ with current F once after several iterations, which may reduce the iterations noticeably. An example is given as follows to demonstrate the effectiveness of the algorithm.

Example 3.1. For the system:

$$A = \begin{bmatrix} -0.0366 & 0.0271 & 0.0188 & -0.4555 \\ 0.0482 & -1.01 & 0.0024 & -4.0208 \\ 0.1002 & 0.3681 & -0.707 & 1.42 \\ 0 & 0 & 1 & 0 \end{bmatrix}, \quad B = \begin{bmatrix} 0.4422 & 0.1761 \\ 3.5446 & -7.5922 \\ -5.52 & 4.49 \\ 0 & 0 \end{bmatrix},$$

$$C = \begin{bmatrix} 0 & 1 & 0 & 0 \end{bmatrix},$$

design an SOF controller with the desired pole region: the intersection of the left half plane $\mathrm{Re}(z) < -0.1$, and the conic sector with apex at the origin and inner angle $\frac{140}{180}\pi$. After 4 iterations, when $\alpha = 0.0333$, the closed-loop poles are assigned at $p_{1,2} = -0.2021 \pm 0.4863i$, $p_3 = -205.85$, $p_4 = -0.3274$, with feedback gain $K = [8.4516, 30.9240]^T$. After 5 iterations, when $\alpha = -0.0561$, the closed-loop poles are assigned at $p_{1,2} = -0.2133 \pm 0.4960i$, $p_3 = -2165.5$, $p_4 = -0.3130$, with the feedback gain $K = [87.2134, 325.8051]^T$.

3.3 Regional Pole Placement by PID Controller

The SOF problem is important not only in its own right, but also because many other problems are reducible to some variations of it. For example, it is well known that the reduced order dynamic output feedback design is readily transformed into an SOF problem through simple augmentations. Another example is PID control.

PID controller is the most commonly used algorithm in process control industry, and many approaches have been proposed for PID tuning, see, e.g., Åström and

Hagglünd (1995) and Tan *et al.* (1999). However, in spite of the great efforts on LMI synthesis, there are relatively little literature that addresses the PID design problem under the LMI framework, to mention some of them, see Mattei (2001), Zheng *et al.* (2002) for example. In Zheng *et al.* (2002), an iterative LMI algorithm is employed to design PID controller which guarantees the closed-loop system with stability, H_2 or H_∞ performance, or maximum output control requirement. The result in the preceding section can be employed to design a PID controller with regional pole placement specifications, and it is briefly described as follows.

Consider again the LTI system (3.1) with the following PID control law:

$$u = K_p y + K_i \int_0^t y \, \mathrm{d}\tau + K_d \frac{\mathrm{d}y}{\mathrm{d}t}. \tag{3.16}$$

The PID gains K_p, K_i, $K_d \in \mathbb{R}^{m\times p}$ are to be designed. For simplicity of the analysis, the set point input r has been omitted, and D is assumed 0. The procedure that readily transforms the PID controller into SOF structure is as follows (Zheng *et al.*, 2002):

Define the state of the augmented system as $x_a \triangleq \begin{bmatrix} x_1^T & x_2^T \end{bmatrix}^T$, where $x_1 = x$, $x_2 = \int_0^t y \, \mathrm{d}t$. Also define the output of augmented system as $y_a \triangleq \begin{bmatrix} y_1^T & y_2^T & y_3^T \end{bmatrix}^T$, where $y_1 = \begin{bmatrix} C & 0_{p\times p} \end{bmatrix} x_a$, $y_2 = \begin{bmatrix} 0_{p\times n} & I_p \end{bmatrix} x_a$, $y_3 = \begin{bmatrix} CA & 0_{p\times p} \end{bmatrix} x_a$. Then the augmented system is:

$$\begin{cases} \dot{x}_a = A_a x_a + B_a u \\ y_a = C_a x_a \\ u = K y_a \end{cases}, \tag{3.17}$$

where

$$A_a = \begin{bmatrix} A & 0_{n\times p} \\ C & 0_{p\times p} \end{bmatrix}, \quad B_a = \begin{bmatrix} B \\ 0_{p\times m} \end{bmatrix}, \quad C_a = \begin{bmatrix} C & 0_{p\times p} \\ 0_{p\times n} & I_p \\ CA & 0_{p\times p} \end{bmatrix},$$

$$K = \begin{bmatrix} K_1 & K_2 & K_3 \end{bmatrix}.$$

and K_p, K_i and K_d can be solved from K:

$$\begin{cases} K_d = K_3(I + CBK_3)^{-1} \\ K_i = (I - K_dCB)K_2 \\ K_p = (I - K_dCB)K_1 \end{cases} . \tag{3.18}$$

Then the problem of PID controller design for system (3.1) transforms to that of SOF controller design for system (3.17) with the closed-loop system $\dot{x}_a = (A_a + B_aKC_a)x_a$. Algorithm 3.1 yields K, and it in turn gives K_p, K_i, and K_d.

Example 3.2. For the plant:

$$G(s) = \frac{1}{s^2},$$

design a PID controller with the desired pole region: the intersection of disk centered at the origin with the radius 3, and the conic sector with apex at the origin and inner angle $\pi/3$. After 6 iterations, when $\alpha = 1.0462$, the closed loop poles are assigned at $p_{1,2} = -0.5524 \pm 0.8533i$, $p_3 = -0.7004$, with $K_p = -1.8071$, $K_i = -0.7237$ and $K_d = -1.8052$. After 24 iterations, when $\alpha = -0.0199$, the closed loop poles are assigned at $p_{1,2} = -1.1945 \pm 1.4626i$, $p_3 = -0.8753$, with $K_p = -5.6575$, $K_i = -3.1217$ and $K_d = -3.2644$.

3.4 Conclusion

In this chapter, an iterative LMI algorithm has been proposed to solve the regional pole placement problem by SOF, PID controller, or other reduced order feedback controllers. Several numerical examples are given to demonstrate the effectiveness of the proposed method. This proposed approach can also be extended to multivariable process. Compared with the existing methods on the regional pole placement, ours imposes no specific requirement on either system structure or system order. It should be pointed out that the iterative algorithm developed in this chapter is based on sufficient criteria, and if the algorithm fails to provide a solution, one cannot determine whether or not such a solution exists.

Chapter 4

A Two-degree-of-freedom Smith Control for Stable Delay Processes

4.1 Introduction

In process control, the Smith predictor (Smith, 1957) is a well known and very effective dead-time compensator. One major concern with the normal Smith control is that its disturbance rejection performance is usually limited due to its one-degree-of-freedom nature. In order to cater to disturbance rejection and robustness as well, a double-controller scheme is presented in Tian and Gao (1998) for stable first order processes with dominant delay, but the improvement of disturbance rejection is not significant, and its performance deteriorates when the process time delay is relative small. Recently, several 'modified Smith predictor' control schemes have been proposed (Majhi and Atherton, 2000*a*; Chien *et al.*, 2002; Kaya, 2003) to extend applicability of the Smith predictor to unstable processes. They handle integral or first-order unstable plants by employment of more controllers, and can be applied to stable processes as well through scheme simplification. It is however noted that their characteristic equations are all delay dependent, which is in contrast to delay-free one enjoyed by the normal Smith control and which keeps the

stabilization problem as a complicated task. Also, they pay little attention to disturbance rejection. It is undoubtable that disturbance rejection is most important in process control and good solutions have been sought for long time.

In this chapter, the two-degree-of-freedom Smith predictor control scheme (Wong and Seborg, 1986; Huang *et al.*, 1990; Palmor, 1996) is investigated for improved disturbance rejection. This scheme is featured by delay free nominal stabilization. The resulting set-point response remains the same as in the normal Smith scheme, but the disturbance response can be tuned by one additional controller separately with no effects on the set-point response. Furthermore, a novel method is presented to design this disturbance controller easily and yield substantial control performance improvement.

The rest of the chapter is organized as follows. In Section 4.2, the proposed disturbance controller design is presented. Stability analysis is given in Section 4.3. Typical designs are detailed for first-order plus dead time (FOPDT) and second-order plus dead time (SOPDT) processes in Section 4.4. In Section 4.5, two examples are provided to demonstrate our methods. In Section 4.6, the issue of periodic disturbance rejection is investigated, with modification of the design presented to further improve the performance. An example is also provided. Finally, Section 4.7 concludes this chapter.

4.2 The Proposed Method

In this chapter, our goal is to seek a new control design which can keep the nominal delay-free stabilization of the delay system like that in the normal Smith control, yet, provide some additional means to improve disturbance rejection, and hopefully tune the set-point and disturbance responses separately and easily. After many trials, we decide to use the two-degree-of-freedom Smith control scheme as depicted in Figure 4.1. In Figure 4.1, $G(s) = G_0(s)e^{-Ls}$ and $\hat{G}(s) = \hat{G}_0(s)e^{-\hat{L}s}$ are a stable and minimal phase process and its model respectively. Suppose that the model matches the plant dynamics perfectly, i.e., $\hat{G}_0 = G_0$ and $\hat{L} = L$. It follows that the

closed-loop transfer function from the set-point to the output is given by

$$H_r = \frac{G_0 C_1}{1 + G_0 C_1} e^{-Ls} \triangleq H_{r0} e^{-Ls}, \tag{4.1}$$

where H_{r0} denotes the delay-free part of H_r. For the disturbance path from $D(s)$ to $Y(s)$, it can be shown that the transfer function is

$$H_d = \frac{1 + G_0 C_1 - G_0 C_1 C_2 e^{-Ls}}{1 + G_0 C_1}, \tag{4.2}$$

which shares the same delay-free denominator as in H_r.

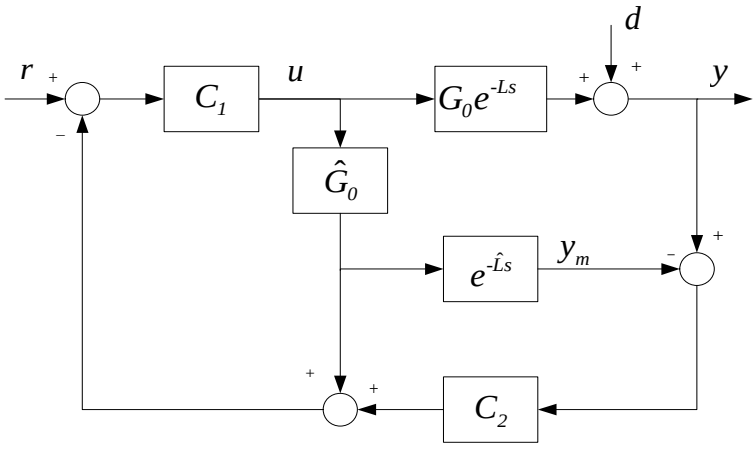

Figure 4.1. Two-degree-of-freedom Smith control structure

To compare this scheme with the Smith one, letting $C_2 = 1$ reduces the scheme to the normal Smith system which has the same set-point transfer function as in (4.1) but a different disturbance transfer function as

$$H_{d1} = \frac{1 + G_0 C_1 - G_0 C_1 e^{-Ls}}{1 + G_0 C_1}.$$

Obviously, with C_1 designed for closed-loop stability and the set-point response, the normal Smith scheme simply does not have any freedom to manipulate the disturbance response. Owing to great importance of disturbance rejection in process control industry, it is definitely desirable to have a means to improve it. In the scheme of Figure 4.1, C_2 appears in the numerator of H_d, and thus can be utilized to reduce or minimize H_d. It is also noted that C_2 is not in the set-point

transfer function (4.1). Hence, C_1 and C_2 can be tuned separately as follows. C_1 is designed to have the desired stability and set-point response. This is a standard task and there are many solutions already. Our focus here is on C_2, that is, design it to achieve best disturbance rejection. In Huang *et al.* (1990), C_2 is composed of a first order lag and a delay term to approximate the inverse of time delay in low frequency range, however, its disturbance performance improvement is not significant, and a novel design for C_2 is proposed in this chapter.

In view of (4.2), intuitively, one might attempt to determine C_2 by frequency response fitting, i.e., by minimizing

$$|H_d| = \left|1 - \frac{G_0 C_1 e^{-j\omega L}}{1 + G_0 C_1} C_2\right| = |1 - H_r C_2|$$

for some working frequency range $\omega \in [\underline{\omega}, \bar{\omega}]$, so that the disturbance response is attenuated. Such optimization falls into the model matching category and sounds reasonable. However, it is actually difficult to produce expected performance. This is because the optimization tends to get C_2 as $C_2 = 1/H_r$ over $[\underline{\omega}, \bar{\omega}]$. The resulting C_2 would mimic the behavior of $1/H_r$ that contains pure time leading $e^{j\omega L}$ with counter-clockwise Nyquist curve, and would exhibit large magnitude for $\omega > \bar{\omega}$. This increases the corresponding $|H_d|$, and may even make the scheme more susceptible to unmodelled high frequency dynamics or uncertainties.

In order to attain better disturbance rejection in face of the delay term in the numerator of H_d, our novel method proceeds as follows. For a given type of disturbance, say $D(s)$, it follows from (4.2) that the disturbance response is

$$\begin{aligned} Y_d =& \frac{1 + G_0 C_1 - G_0 C_1 C_2 e^{-Ls}}{1 + G_0 C_1} D \\ =& Y_{da} - Y_{db}, \end{aligned} \tag{4.3}$$

where

$$Y_{da} = D \tag{4.4}$$

is fixed and

$$Y_{db} = H_{r0} C_2 D e^{-Ls} \tag{4.5}$$

is manipulatable by C_2. Suppose that the disturbance occurs at $t = 0$. Then non-zero responses in $y_{da}(t)$ and $y_{db}(t)$ come in at $t = 0$ and $t = L$, respectively.

Obviously, the disturbance response during $t = 0$ to $t = L$ is solely from $y_{da}(t)$ and fixed. Any effort to change it during this time period is useless but causes the problem on controller design. The best achievable disturbance rejection is to zero the disturbance response from $t = L$ onwards:

$$y_d(t) = y_{da} - y_{db} = \begin{cases} y_{da}(t), & 0 < t < L, \\ 0, & t \geq L, \end{cases}$$

which requires the compensating response $y_{db}(t)$ to be

$$y_{db}(t) = \left\{ \begin{array}{cc} 0, & 0 < t < L \\ y_{da}(t), & t \geq L \end{array} \right\} = y_{da}(t)1(t-L), \tag{4.6}$$

as displayed in Figure 4.2. We now derive an analytical solution for $C_2(s)$ to meet (4.6). In view of (4.4), Y_{da} can be expressed using the partial fraction expansion as, say,

$$Y_{da}(s) = \frac{\alpha_0}{s} + \sum_i \frac{\alpha_i}{s + \beta_i},$$

and its time domain form is

$$y_{da}(t) = \alpha_0 + \sum_i \alpha_i e^{-\beta_i t}.$$

It follows that

$$\begin{aligned} y_{da}(t)1(t-L) &= \left[\alpha_0 + \sum_i \alpha_i e^{-\beta_i t}\right] 1(t-L) \\ &= \left[\alpha_0 + \sum_i \alpha_i e^{-\beta_i L} e^{-\beta_i (t-L)}\right] 1(t-L) \\ &\triangleq \hat{y}_{da}(t-L)1(t-L), \end{aligned} \tag{4.7}$$

where

$$\hat{y}_{da}(t) = \alpha_0 + \sum_i \alpha_i e^{-\beta_i L} e^{-\beta_i t},$$

with

$$\hat{Y}_{da}(s) = \frac{\alpha_0}{s} + \sum_i \frac{\alpha_i e^{-\beta_i L}}{s + \beta_i}. \tag{4.8}$$

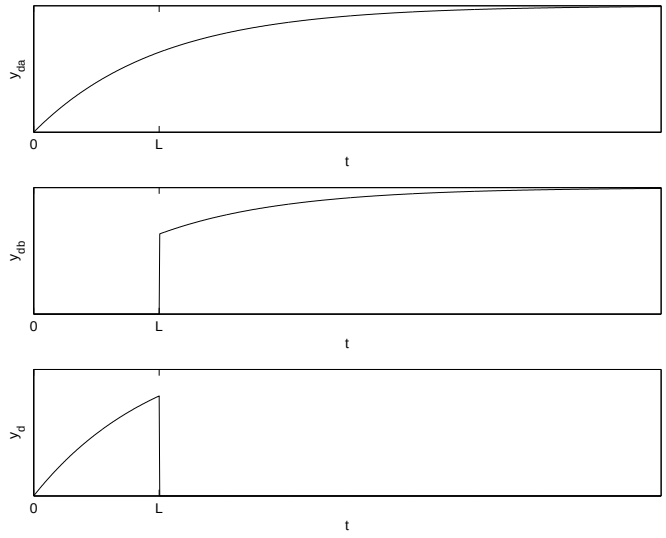

Figure 4.2. Illustration of desired disturbance rejection

It is obvious that $\hat{Y}_{da}e^{-Ls} = Y_{db}$. Laplace transform of (4.6) with help of (4.5) and (4.7) gives

$$H_{r0}C_2De^{-Ls} = \hat{Y}_{da}(s)e^{-Ls},$$

and its solution is

$$C_2^* = \frac{\hat{Y}_{da}(s)}{D(s)}H_{r0}^{-1}. \tag{4.9}$$

Since C_2^* is improper in general, a low-pass filter should be added for practical implementation so that the actual C_2 is given by

$$C_2 = \frac{\hat{Y}_{da}(s)H_{r0}^{-1}}{(\tau s+1)^n D(s)}. \tag{4.10}$$

Then the actual $Y_{db}(s)$ and $Y_d(s)$ are

$$Y_{db}(s) = \frac{\hat{Y}_{da}(s)}{(\tau s+1)^n}e^{-Ls}, \tag{4.11}$$

and

$$Y_d(s) = Y_{da}(s) - \frac{\hat{Y}_{da}(s)}{(\tau s+1)^n}e^{-Ls}, \tag{4.12}$$

respectively. Detailed controller design will be provided for several typical industrial processes in Section 4.4. Our design yields a C_2 that tends to force the disturbance response to vanish after the time-delay.

Before concluding this section, we would highlight the advantage of our design over the standard two-degree-of-freedom control scheme (either single-loop based or Smith predictor based) where a pre-filter is added between the reference input and the negative feedback. In the standard two-degree-of-freedom control scheme, obviously, the pre-filter does not affect the disturbance response and could only be utilized to tune the set-point response. Then, this leaves its primary controller responsible for both closed-loop stabilization and disturbance response, and thus limits disturbance rejection performance. On the other hand, in our design, C_2 deals solely with the disturbance. It is easier to design and achieve superior disturbance rejection performance. In the extreme case where the process is bi-proper, C_2 may eliminate the disturbance response completely from $t = L$, which is impossible for the standard two-degree-of-freedom control scheme and any other schemes where the controller taking care of disturbance rejection also needs to cope with closed-loop stability and/or pole placement.

4.3 Stability Analysis

Stability is a prerequisite for any control systems. In this section, both the internal and robust stability of the two-degree-of-freedom scheme are investigated.

The two-degree-of-freedom structure in Figure 4.1 is an interconnected system that consists of five subsystems and each of them is of single input and single output (SISO). Such a system is internally stable (Wang *et al.*, 1999*b*) if and only if

$$p_c(s) \triangleq \Delta \prod_i p_i(s)$$

has all its roots in the open left half of the complex plane, where $p_i(s)$ are the denominators of the respective subsystem transfer functions and the Δ is the system determinant as defined in the Mason's formula. The five subsystems in Figure 4.1 are: $C_1(s)$, $C_2(s)$, $\hat{G}_0$, $G_0 e^{-Ls}$ and $e^{-\hat{L}s}$. Let $C_1(s) = f_1(s)/g_1(s)$, $C_2(s) = f_2(s)/g_2(s)$ and $\hat{G}_0(s) = G_0(s) = f(s)/g(s)$. Their respective p_i are $p_1 = g_1(s)$, $p_2 = g_2(s)$, $p_3 = p_4 = g(s)$ and $p_5 = 1$. The system determinant Δ is

given by

$$\Delta = 1 + \hat{G}_0 C_1 + (G_0 e^{-Ls} - \hat{G}_0 e^{-\hat{L}s}) C_1 C_2.$$

It follows that

$$p_c(s) = g_2(s) g(s) [g_1(s) g(s) + f_1(s) f(s)].$$

The polynomial, $g_1(s)g(s) + f_1(s)f(s)$, reflects stabilization of delay-free G_0 by the controller C_1, which is always possible, say, by pole placement. The controller C_2 must be stable for the stability of $g_2(s)$, and is used to achieve best disturbance response. With the above two constraints, the overall system is internally stable.

For robust stability analysis, let the total uncertainty be given in the form of multiplicative one as

$$\Delta_G(s) = \frac{G(s) - \hat{G}(s)}{\hat{G}(s)}. \tag{4.13}$$

According to Mason's formula, the transfer function for the remaining part $M(s)$, as is illustrated in Figure 4.3, is

$$M(s) = \frac{C_1 C_2 \hat{G}}{1 + C_1 \hat{G}_0}.$$

Thus a sufficient condition for the robust stability is obtained by the small gain theorem as

$$|M\Delta_G|_\infty < 1, \text{ or equivalently } \left| \frac{C_1 C_2}{1 + C_1 \hat{G}_0} \hat{G} \Delta_G \right|_\infty < 1.$$

Assume nominal stability, then a sufficient condition for the robust stability of the closed-loop system is obtained as

$$\left| \frac{C_1 C_2}{1 + C_1 \hat{G}_0} \hat{G} \Delta_G \right|_\infty < 1 \tag{4.14}$$

according to the small gain theorem (Morari and Zafiriou, 1989). By invoking (4.1) and (4.10), (4.14) reduces to

$$\left| \frac{D(j\omega)}{\hat{Y}_{da}(j\omega)} \right| (\tau^2 \omega^2 + 1)^{n/2} > |\Delta_G|, \ \forall \omega > 0. \tag{4.15}$$

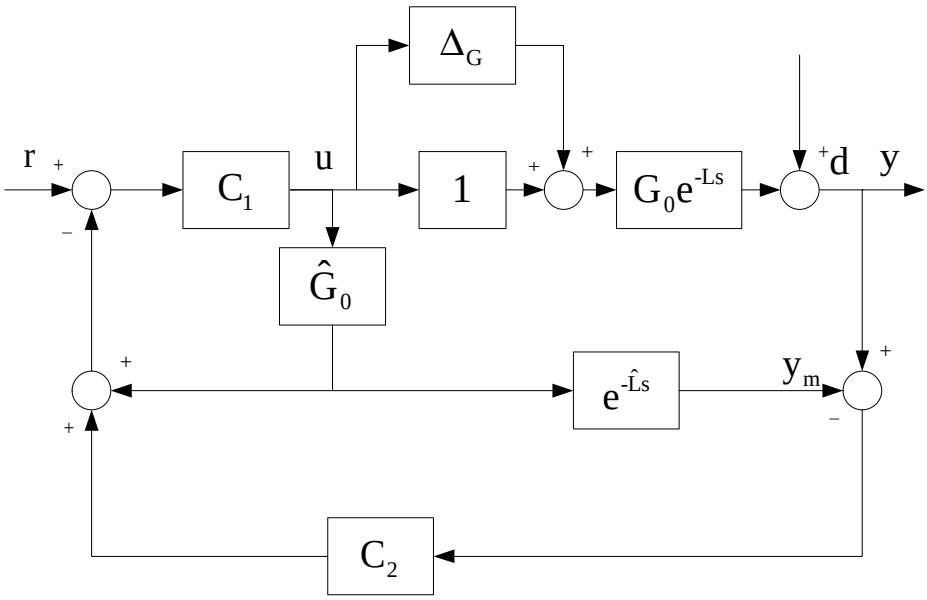

Figure 4.3. System structure with multiplicative uncertainty

In specific, when the disturbance is of step type, $\hat{Y}_{da}(s) = D(s)$ and thus the robust stability requirement turns out to be $(\tau^2\omega^2 + 1)^{n/2} > |\Delta_G|$ for $\forall\omega > 0$, or

$$\frac{|\Delta_G|}{(\tau^2\omega^2 + 1)^{n/2}} < 1, \ \forall\omega > 0. \tag{4.16}$$

It can been seen from (4.10) and (4.15) that a trade-off is to be made by C_2, or tuning of the parameter τ: a decrease in τ will improve the disturbance rejection performance but reduce the robust stability, and vice versa.

4.4 Typical design cases

It follows from the preceding sections that in our scheme, C_1 is designed to have stable closed-loop and good set-point response, and C_2 has to be stable and meet (4.10). In control textbooks, step disturbances are usually assumed when disturbance responses in output are considered. In the control research literature, step disturbances are also the most commonly investigated type for industrial process control. The reasons are that such a disturbance is simple, representative, contains rich frequency components, and has a direct adverse effect on the process

output. Thus, it is viewed as the worst case disturbance. Moreover, if the type of disturbance cannot be known, one typically adopts step disturbance. Due to these considerations, one can say that the step disturbance is the most common benchmark for study of disturbance rejection control. And thus the typical controller designs in this section are based on step disturbance. It should be stressed that our general method in Section 4.2 can deal with any type of disturbance and improve disturbance rejection performance if the type or other information of the disturbance dynamics is known and different from step one, and the corresponding design is illustrated by an example in Section 4.5. Moreover, even for periodic disturbances, our scheme is still applicable.

Now, assume that the disturbance is of step type with unknown magnitude of A so that $D(s) = A/s$. It then follows from (4.8) that $\hat{Y}_{da}(s)$ is also equal to A/s and thus

$$C_2 = \frac{H_{r0}^{-1}}{(\tau s + 1)^n}. \tag{4.17}$$

By (4.12), one gets

$$Y_d(s) = A\frac{(\tau s + 1)^n - e^{-Ls}}{s(\tau s + 1)^n}, \tag{4.18}$$

so that $y_d(t)$ will decay to 0 by invoking the final value theorem

$$y_d(\infty) = \lim_{s \to 0} sY_d(s) = 0.$$

In case that the type or other information of the disturbance dynamics is available, design of the disturbance controller C_2 can be changed accordingly by incorporating the corresponding $D(s)$ and $\hat{Y}_{da}(s)$ (4.7) into (4.10). The design procedure is explained in Section 4.5 by an example.

It is noted that most typical industrial processes of interests could be approximated by FOPDT or SOPDT ones. Detailed controller design will thus be carried out for each case and closed-form formulas for controller parameters are given as follows for easy reference.

FOPDT Processes Consider the following stable FOPDT process:

$$G(s) = G_0(s)e^{-Ls} = \frac{k_0}{T_0 s + 1}e^{-Ls},$$

where all coefficients are positive. The closed-loop transfer function for set-point tracking is chosen to be

$$H_r = \frac{k_0 C_1}{T_0 s + 1 + k_0 C_1} e^{-Ls} = \frac{1}{T_r s + 1} e^{-Ls}, \tag{4.19}$$

where T_r is the desired closed-loop time constant and $T_r \geq T_0$ is recommended. This gives rise to

$$C_1 = \frac{T_0 s + 1}{k_0 T_r s}. \tag{4.20}$$

For step disturbance, $D(s) = A/s$, it follows from equations (4.17) and (4.19) that

$$C_2 = \frac{T_r s + 1}{\tau s + 1}, \tag{4.21}$$

by choosing $n = 1$ to make C_2 proper. A large τ will increase the system robustness, and a small one will yield better disturbance rejection. The recommended range for τ is $\tau = 0.1T_r \sim 0.5T_r$.

SOPDT Processes Consider the following stable SOPDT process:

$$G(s) = G_0(s)e^{-Ls} = \frac{k_0}{a_2 s^2 + a_1 s + 1} e^{-Ls},$$

where all coefficients are positive. Choose the desired set-point transfer function as

$$H_r = \frac{\omega_n^2}{s^2 + 2\xi_n \omega_n s + \omega_n^2} e^{-Ls}, \tag{4.22}$$

and C_1 is given by

$$C_1 = \frac{\omega_n^2 (a_2 s^2 + a_1 s + 1)}{k_0 s (s + 2\xi_n \omega_n)}. \tag{4.23}$$

For step disturbance $D(s) = A/s$, it follows from equations (4.17) and (4.19) that

$$C_2 = \frac{s^2 + 2\xi_n \omega_n s + \omega_n^2}{\omega_n^2 (\tau s + 1)^2}, \tag{4.24}$$

with $\tau = 0.1/\omega_n \sim 0.5/\omega_n$ recommended.

4.5 Examples

In this section, two examples are presented for FOPDT and SOPDT processes respectively.

Example 1: Consider an stable FOPDT process

$$G(s) = \frac{1}{10s+1}e^{-3s}$$

from Huang *et al.* (1990), where they gave

$$C_1 = \frac{s+0.1}{s},$$

and two different settings of C_2 as

$$C_{2a} = \frac{60s+7}{60s+1+6e^{-7s}} \text{ and } C_{2b} = \frac{60s+11}{60s+1+10e^{-3s}}.$$

For our design, choose $T = T_0 = 10$ for the same C_1 as Huang's and let $\tau = 0.3T_0 = 3$. It follows from (4.21) that

$$C_2 = \frac{10s+1}{3s+1}.$$

Step set-point change of magnitude 1 and step disturbance of negative magnitude -0.5 are applied at $t = 1$ and $t = 100$ respectively. The responses of four different controllers (including normal Smith scheme) are then compared in Figure 4.4. The performance improvement of the proposed design is clear. Note that in this example, the normalized time delay is small. In general, the performance improvement of our proposed design will be more significant when the normalized time delay increases.

To see robust performance with respect to modelling errors, consider the process model perturbations of: a) $L = 0.5L_0 = 1.5$, b) $k = 0.5k_0 = 0.5$ and $L = 2L_0 = 6$ simultaneously. It is easy to verify that the system is robustly stable by checking (4.16), where the corresponding left-hand-sides are well below 1 as plotted in Figure 4.5. The corresponding responses are given in Figure 4.6, and the proposed design is robustly stable in both cases and provides better disturbance rejection again.

To illustrate robust performance with respect to different disturbance, suppose that the same step disturbance is now injected into the process input instead of at output. The controllers remain unchanged. The performance is depicted in Figure 4.7. The proposed design performs reasonably well. For more comparison, the feedforward design (Seborg *et al.*, 2004) with accurate disturbance model is also

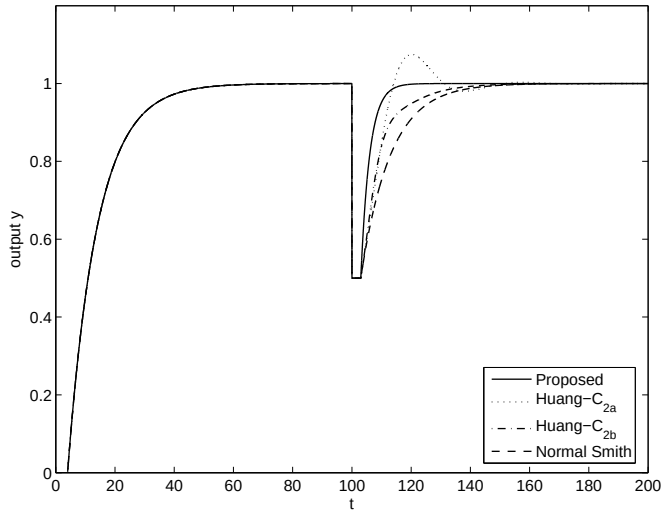

(a) *Output*

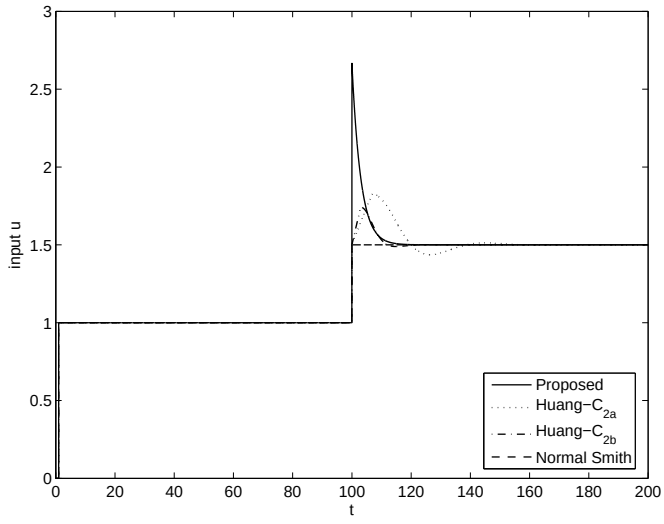

(b) *Input*

Figure 4.4. Responses of Example 1 for step disturbance

included in the figure. Then the feedforward disturbance compensator is calculated as

$$G_f = \frac{13s+1}{2s(10s+1)}.$$

It leads to a faster disturbance response owing to the precise nature of feedforward control. At the same time, its overshoot is relative larger, which is caused by the

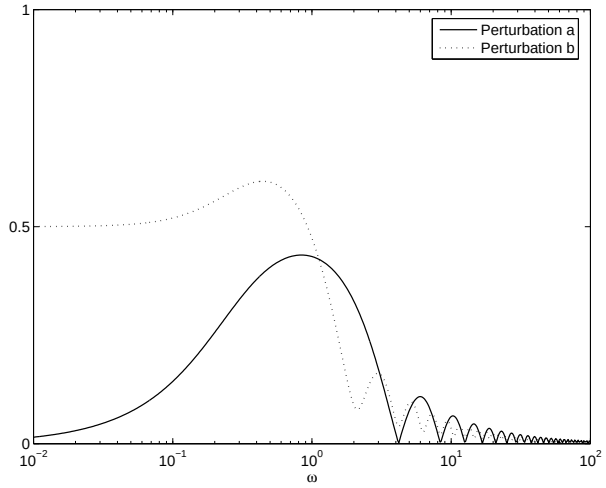

Figure 4.5. Left-hand-sides of (4.16) for Example 1

approximation of time lead. In fact, the feedforward scheme and our proposed design are different and suit different situations. When the disturbance is measurable and an accurate model of the disturbance channel is available, the feedforward design can be applied to improve the disturbance rejection. if this is not the case, one has to use feedback schemes.

To demonstrate that our control design is capable of handling other types of disturbance than the step, let us revisit the above case. The above step disturbance at input is equivalent to the following disturbance at the process output:

$$D(s) = \frac{0.5}{s(10s+1)}. \tag{4.25}$$

Suppose that we know this $D(s)$ except its magnitude (its magnitude does not matter). Then, controller C_2 can be redesigned accordingly to get better performance than the previous one designed for the step as we have better information on the disturbance. It follows from equations (4.7)-(4.10) that

$$\begin{aligned} y_{da}(t) &= 0.5[1 - e^{-0.1t}], \\ \hat{y}_{da}(t) &= 0.5[1 - e^{-0.3}e^{-0.1t}], \\ \hat{Y}_{da}(s) &= 0.5\left(\frac{1}{s} - \frac{e^{-0.3}}{s+0.1}\right), \end{aligned}$$

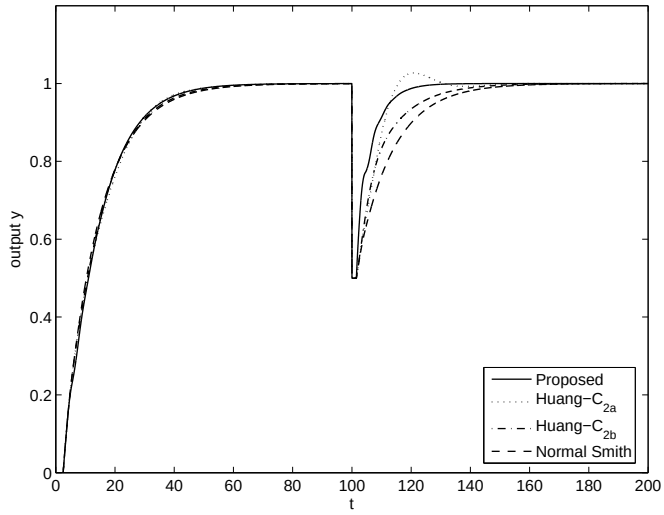

(a) $L = 0.5L_0 = 1.5$

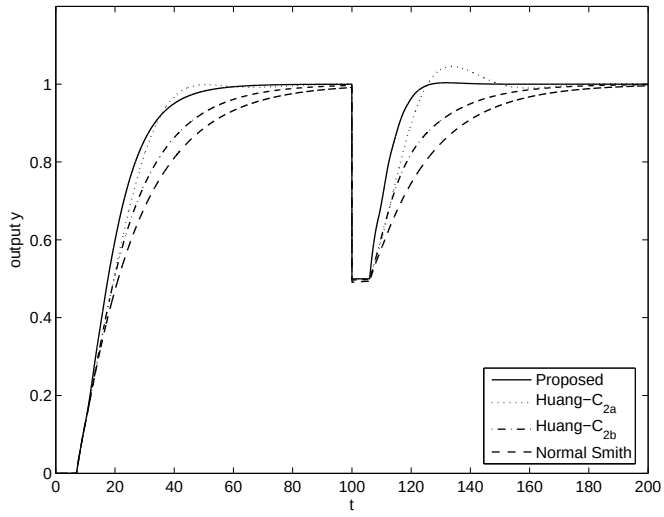

(b) $k = 0.5k_0 = 0.5$, $L = 2L_0 = 6$

Figure 4.6. Responses of Example 1 against model change

and

$$C_2^* = (10s + 1)(2.592s + 1).$$

C_2 is implemented as

$$C_2 = \frac{25.92s^2 + 12.59s + 1}{(3s + 1)^2}$$

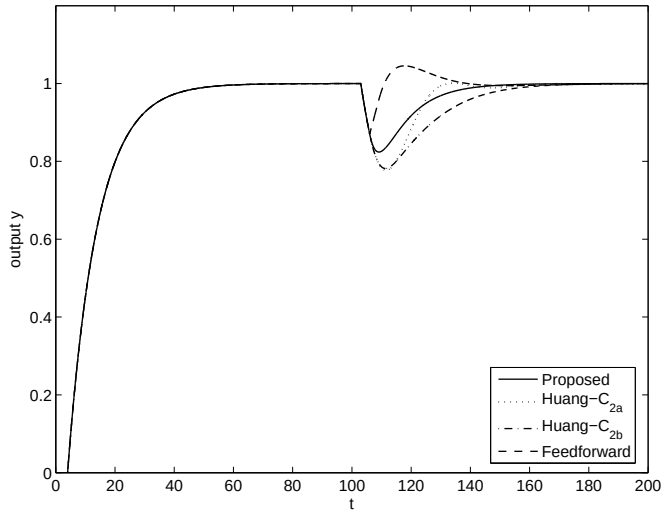

Figure 4.7. Responses of Example 1 against disturbance change

by choosing $\tau = 3$.

For comparison, the generalized analytical predictor (Wong and Seborg, 1986) is also simulated. Its system structure is the same, but the controller C_2 is designed as:

$$C_{gap}(z) = B^N + \frac{1 - B^N}{1 - B}(1 - Bz^{-1}),$$

where $B = e^{-T_s/T_0}$, $N = L/T_s$, T_s the sampling time, and T_0 the process time constant. For this example, by take the sampling time as $T_s = 0.5$, controller $C_{gap}(z)$ is calculated as

$$C_{gap}(z) = \frac{6.0551z - 5.0551}{z}.$$

The performance of the two designs are compared in Figure 4.8, and it is obvious that the proposed one provides better disturbance rejection.

Analytically, in this example, the equivalent disturbance transfer function of the generalized analytical predictor scheme is

$$H_{dgap} = \frac{10s + 1 - (2.528s + 1)e^{-3s}}{10s + 1}$$

by matching $C_{gap}(z)$ as an ideal PD controller $2.528s + 1$. Its corresponding dis-

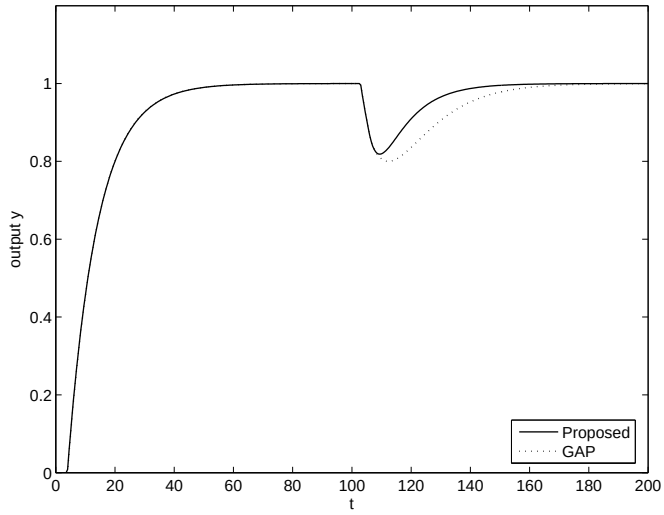

Figure 4.8. Responses of Example 1 with C_2 redesigned

turbance response becomes

$$\begin{aligned} y_{dgap}(t) &= 0.5\left[e^{-t/10} - 1 + \left(1 - e^{-(t-3)/10} - 0.075(t-3)e^{-(t-3)/10}\right)\cdot 1(t-3)\right] \\ &= 0.5\left[e^{-t/10} - 1 + \left(1 - 1.35e^{-t/10} - 0.101(t-3)e^{-t/10}\right)\cdot 1(t-3)\right]. \end{aligned}$$

In comparison, the disturbance transfer function of our scheme is

$$H_d = 1 - \frac{2.592s+1}{(\tau s+1)^2}e^{-3s},$$

and the corresponding disturbance response is

$$\begin{aligned} y_d(t) = 0.5\Bigg[e^{-t/10} - 1 + \Bigg(1 - \frac{74.1}{(\tau-10)^2}e^{-(t-3)/10} - \frac{\tau-2.592}{\tau^2-10\tau}(t-3)e^{-(t-3)/\tau} \\ - \frac{\tau^2-20\tau+25.92}{(\tau-10)^2}e^{-(t-3)/\tau}\Bigg)\cdot 1(t-3)\Bigg]. \end{aligned}$$

In the extreme case that $\tau \to 0$, there hold

$$\lim_{\tau\to 0}\frac{\tau-2.592}{\tau^2-10\tau}(t-3)e^{-(t-3)/\tau} = 0 \text{ and } \lim_{\tau\to 0}\frac{\tau^2-20\tau+25.92}{(\tau-10)^2}e^{-(t-3)/\tau} = 0,$$

and $y_d(t)$ approaches

$$\begin{aligned} y_d(t) &= 0.5\left[e^{-t/10} - 1 + (1 - 0.741e^{-(t-3)/10})\cdot 1(t-3)\right] \\ &= 0.5\left[e^{-t/10} - 1 + (1 - e^{-t/10})\cdot 1(t-3)\right]. \end{aligned}$$

Then the disturbance is rejected completely after $t = 3$, which is not achievable by the generalized analytical predictor scheme.

For generalized analytical predictor, C_{gap} is designed to estimate the disturbance and the output. However, it is not studied how this estimate will affect the disturbance response. In contrast, controller C_2 in our scheme is designed to eliminate the disturbance response from $t = L$ onwards. The information of closed-loop set-point transfer-function is also utilized in the design to compensate for the disturbance. Therefore, our scheme provides better disturbance rejection performance.

Example 2: Consider an stable SOPDT process with distinct real poles:

$$G(s) = \frac{2}{(10s+1)(2s+1)}\, e^{-3s}.$$

By choosing $\omega_n = 0.2$, $\xi = 1$ and $\tau = 0.5/\omega_n = 2.5$, it follows from (4.23) and (4.24) that

$$C_1 = \frac{s^2 + 0.6s + 0.05}{2.5s^2 + s},$$

and

$$C_2 = \frac{25s^2 + 10s + 1}{6.25s^2 + 5s + 1}.$$

The PI-PD Smith scheme from Kaya (2003) is adopted for comparison, whose controller parameters are calculated as $G_{c1} = 0.4 + 0.04/s$ and $G_{c2} = -0.1 - s$ to provide the same set-point response. Step disturbance of negative magnitude -0.5 is applied at $t = 70$. The responses from the two schemes are plotted in Figure 4.9, and the proposed design yields improved disturbance rejection.

In view of these two examples, our proposed design achieves better disturbance rejection. It not only applies for step disturbances, but also is capable to reject other type disturbance as well.

4.6 Rejection of periodic disturbance

Different from the step type disturbance, disturbances acting on the track-following servo systems of an disk drive inherently contain significant periodic components

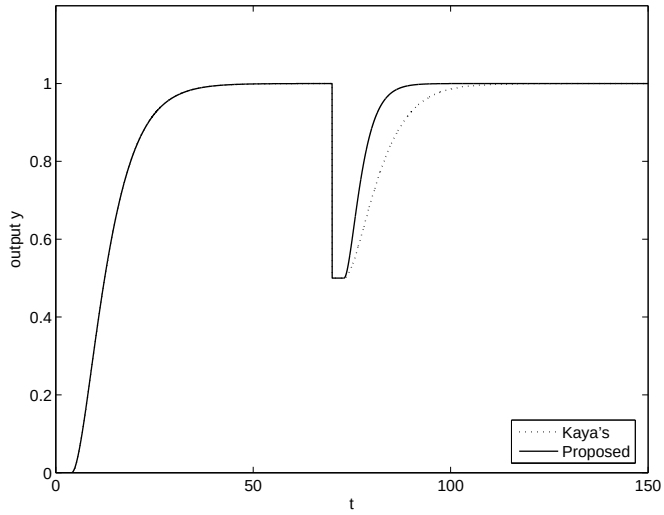

(a) *Output*

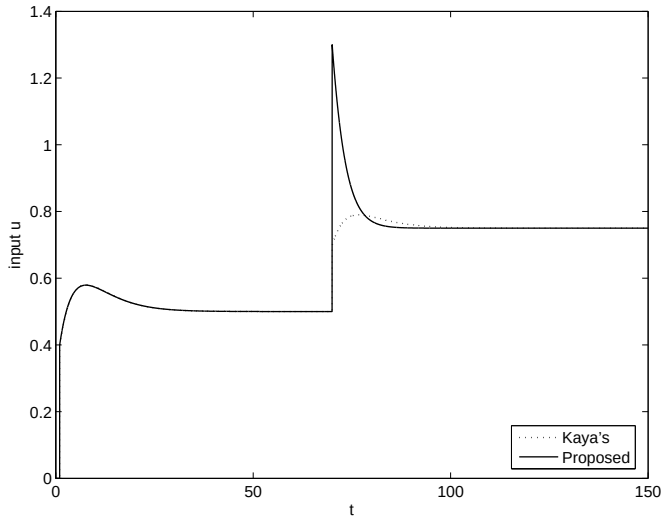

(b) *Input*

Figure 4.9. Responses of Example 2 for step disturbance

that cause tracking errors of a periodic nature (Chew, 1996). Such disturbances are also often encountered in mechanical systems such as industrial robots (Hara *et al.*, 1988). In this section, our proposed scheme is applied to reject periodic disturbances. Furthermore, modifications to the disturbance controller C_2 are investigated to improve the performance.

Assume that the disturbance is a sinusoidal signal with magnitude A and angular frequency ω_d, i.e.

$$d(t) = A\sin(\omega_d t)$$

and

$$D(s) = A\frac{\omega_d}{s^2+\omega_d^2}.$$

It follows from the general design in (4.7)-(4.8) that

$$\hat{Y}_{da}(s) = A\frac{\sin(\omega_d L)s + \omega_d\cos(\omega_d L)}{s^2+\omega_d^2},$$

so that C_2 is implemented by

$$C_2(s) = \frac{\left(\sin(\omega_d L)s + \omega_d\cos(\omega_d L)\right)H_{r0}^{-1}}{\omega_d(\tau s+1)^n}. \tag{4.26}$$

The following example illustrates the design.

Example 3: Consider an stable FOPDT process

$$G(s) = \frac{1}{s+1}e^{-3s}$$

with sinusoidal disturbance $d(t) = 0.3\sin(0.1t)$ injected into the process output at $t = 20$. By choosing the time constant for the set-point transfer-function as $T = T_0 = 1$ and let $\tau = 0.2T_0 = 0.2$. It follows from (4.20) and (4.26) that

$$C_1 = \frac{s+1}{s},$$

and

$$C_2 = \frac{2.955s^2+3.911s+0.9553}{0.04s^2+0.4s+1}.$$

The disturbance response is plotted in Fig 4.10a, Compared with that from the normal Smith design, the performance improvement is obvious. It is also noted that the amplitude and phase of the sinusoidal disturbance does not matter, which is illustrated by Fig 4.10b with $d(t) = 0.4\sin(0.1t+\pi/4)$ and C_2 unchanged.

In order to further investigate the disturbance rejection, let the time constant of the filter be increased to $\tau = 0.8$ and simulate this example again. The corresponding C_2 is

$$C_2 = \frac{2.955s^2+3.911s+0.9553}{0.64s^2+1.6s+1}.$$

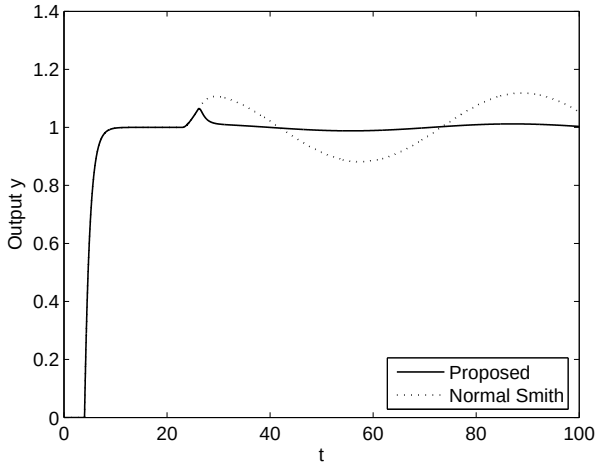

(a) $d(t) = 0.3\sin(0.1t)$

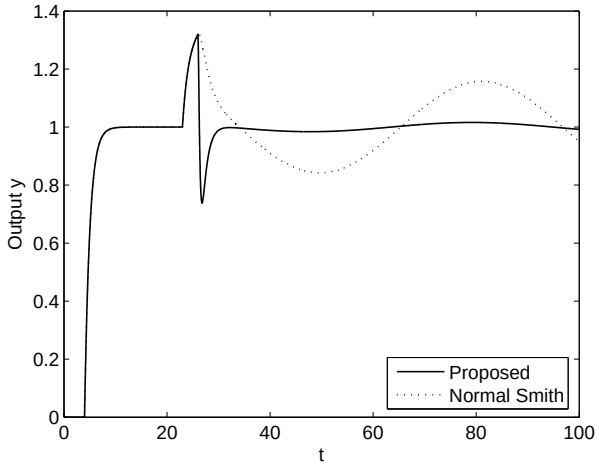

(b) $d(t) = 0.4\sin(0.1t + \pi/4)$

Figure 4.10. Responses of Example 3 for sinusoidal disturbance

Then the response against $d(t) = 0.3\sin(0.1t)$ is plotted in Fig 4.11. It is seen that the performance deteriorates as τ increases. The reason for such performance degradation is explained as follows.

In our general design, C_2^* is expected to make $y_{db} = \hat{y}_{da}$, as is seen from (4.8). In the ideal case, y_{db} is a sinusoid signal and has the same phase and magnitude as $\hat{y}_{da}$. However, the actual controller C_2 contains a filter due to implementation con-

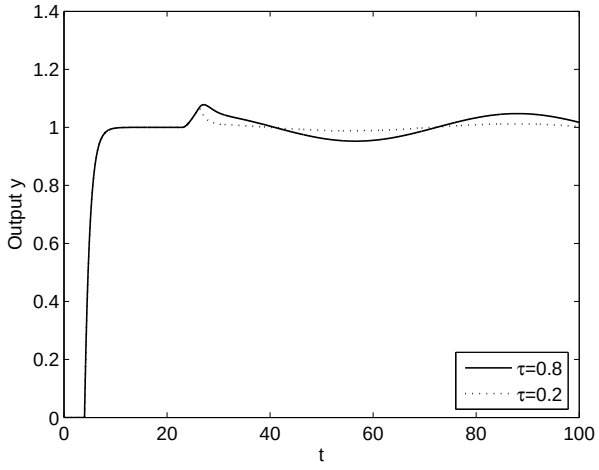

Figure 4.11. Responses comparison for C_2 with different τ

cern, and such discrepancy inevitably leads to deviation of actual outputs. When sinusoidal disturbance is considered, the filter $1/(\tau s+1)^n$ brings forward a phase lag of $n\tan^{-1}(\omega_d\tau)$ and gain magnification of $(1+\omega_d^2\tau^2)^{-n/2}$ to the actual sinusoid y_{db}. In case that $\omega_d\tau$ is small, its effect on y_{db} is negligible. However, as $\omega_d\tau$ increases, y_{db} will deviate from $\hat{y}_{da}$ more significantly and the performance deterioration is obvious. Consequently, counter measures should be taken to improve the disturbance rejection when $\omega_d\tau$ is large. The solution is to modify C_2 as

$$C_2(s)=\frac{\left((1+\omega_d^2\tau^2)^{n/2}\sin(\omega_d L+n\tan^{-1}(\omega_d\tau))s+\omega_d\cos(\omega_d L+n\tan^{-1}(\omega_d\tau))\right)H_{r0}^{-1}}{\omega_d(\tau s+1)^n}, \tag{4.27}$$

so that a pre-compensation for phase and magnitude is included.

Now turn back to the case of $d(t)=0.3\sin(0.1t)$ and $\tau=0.8$, and it follows from (4.27) that

$$C_2=\frac{3.903s^2+4.827s+0.9234}{0.64s^2+1.6s+1},$$

The disturbance response is plotted in Fig 4.12. It is clear that the modified C_2 leads to complete disturbance rejection after process delay L.

In view of the above analysis and example, our proposed scheme is also capable to reject periodic disturbance. Moreover, with compensation in the design of C_2, the disturbance performance is further improved.

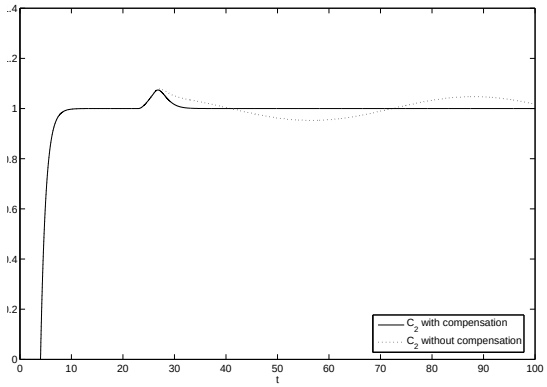

Figure 4.12. Disturbance response with modified design of C_2, $\tau = 0.8$

4.7 Conclusion

Due to great importance of disturbance rejection, a novel disturbance controller design is presented for a two-degree-of-freedom Smith control scheme. This scheme keeps nominal characteristic equation delay-free, and allows separate and easy design of disturbance controller. Our design produces superior disturbance rejection performance, while the set-point response remains the same as in the normal Smith system. In this chapter, the two-degree-of-freedom Smith control applies for minimum-phase time delay processes only. When the unstable process is considered, more sophisticated design is necessary to improve the performance, which is addressed in the next chapter.

Chapter 5

A Double Two-degree-of-freedom Smith Scheme for Unstable Delay Processes

5.1 Introduction

In the previous chapter, a two-degree-of-freedom Smith control is presented to improve the disturbance performance for stable delay process. As we know, the Smith predictor (Smith, 1959) is an effective dead-time compensator for stable processes. However, the original Smith predictor control scheme will be unstable when applied to an unstable process (Wang *et al.*, 1999*b*). To overcome this obstacle, many modifications to the original Smith scheme have been proposed. Åström *et al.* (1994) presented a modified Smith predictor for an integrator plus dead time (IPDT) process and can achieve faster set-point response and better load disturbance rejection with decoupling design of the set-point response from the load disturbance response. Matausek and Micic (1996) considered the same problem with similar results but their scheme is easier to tune. Majhi and Atherton (1999) proposed a modified Smith predictor control scheme suitable for IPDT processes, unstable FOPDT and SOPDT processes. They use the optimal integral time squared error (ITSE) criterion for set-point response design and employ

an optimum stability approach with a proportional controller for stabilization of the given unstable process. With the same control structure, Majhi and Atherton ($2000a$) extends their work for better performance and easy tuning procedure for IPDT, FOPDT and integrating SOPDT processes. Their scheme is displayed in Figure 5.1. The controller G_{c1} is used to stabilize the unstable or integrating process G_0 without delay, while G_c and G_{c2} are designed for set-point tracking and disturbance rejection respectively. In case of perfect modelling, $G_0e^{-Ls} = \hat{G}_0e^{-\hat{L}s}$, the closed-loop responses to set-point and disturbance inputs are given by

$$Y_r(s) = \frac{G_0G_ce^{-Ls}}{1 + G_0(G_c + G_{c1})}R(s) \tag{5.1}$$

and

$$Y_d(s) = \frac{G_0e^{-Ls}}{1 + G_0(G_c + G_{c1})}\frac{1 + G_0(G_c + G_{c1}) - G_0G_ce^{-Ls}}{1 + G_0G_{c2}e^{-Ls}}D(s) \tag{5.2}$$

respectively. It is noted from (5.2) that their G_{c2} only contributes to enhancing the stability of Y_d, and beyond that the disturbance response cannot be taken into consideration. It is well recognized that the disturbance rejection is more important than the set-point tracking for most process control. Hence we aim to provide a Smith scheme for unstable delay processes such that both good set-point and disturbance responses can be achieved with easy tuning of controllers involved by introducing one more degree-of-freedom control in the disturbance loop.

In this chapter, a new modified Smith predictor scheme is proposed. It is actually a double two-degree-freedom control scheme. One two-degree-freedom control configuration with two controllers is provided for the set-point and disturbance, respectively. There are two controllers to tune the denominators and numerators of the respective closed-loop transfer function separately. This innovative scheme eases controller tuning and can lead to substantial control performance improvement, especially for the disturbance rejection. The internal stability is analyzed. Simulations are given to illustrate the effectiveness of the proposed method.

The rest of the chapter is organized as follows. In Section 5.2, a modified Smith structure is proposed and briefly analyzed. The issue of internal stability is addressed in Section 5.3. In Section 5.4, controller design is carried out for three

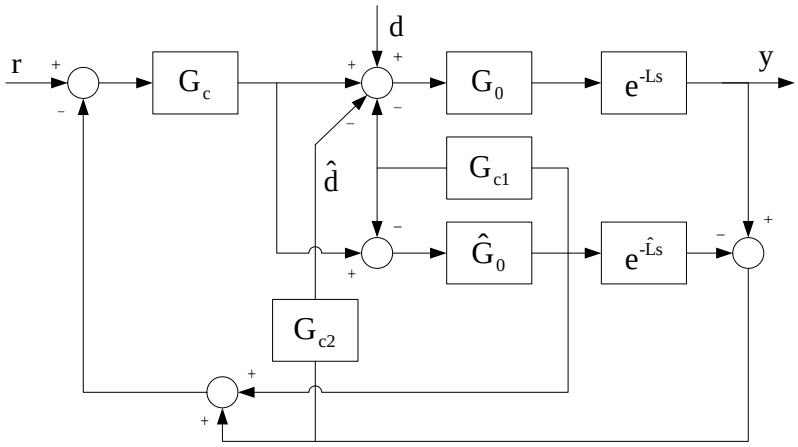

Figure 5.1. Majhi's Smith predictor control scheme

typical industrial processes: IPDT, FOPDT and SOPDT processes. Then three examples are provided in Section 5.5 and compared with Majhi's results. Section 5.6 concludes this chapter.

5.2 The Proposed Scheme

It is noted that in the works by Majhi and Atherton and others on modified Smith control, the disturbance response is not treated with any special care, but just stabilized. Their control schemes simply do not have any freedom to manipulate disturbance response. Owing to great importance of disturbance rejection in process control industry, it is definitely desirable to have a means to improve it. To this end, one more degree-of-freedom of control is needed to enable manipulation of disturbance transient response. At the same time, it should be pointed out that such an addition must not cause any loss of the existing benefits of the previous schemes, rather, all the existing benefits should be kept, and even better, each controller involved should be rationalized in the sense that the rule of each is clearly defined, they together can serve all control objectives, and they can be tuned with ease. Keeping all these in mind, after many try and errors, we come up with a new modified Smith predictor control scheme, as depicted in Figure 5.2,

where $G_0(s)e^{-Ls}$ and $\hat{G}_0(s)e^{-\hat{L}s}$ are a given process and its model, respectively, and G_0 and $\hat{G}_0$ are rational functions with at least one unstable pole. In this new structure, there are four controllers to be designed to meet different objectives. The roles of K_1 and K_3 are similar to those of G_{C1} and G_{C2} in Majhi and Atherton (1999), respectively, i.e., K_1 is designed to stabilize the delay-free process G_0 and K_3 to stabilize the delay process G_0e^{Ls}. However, the proposed structure is of two-degree-of-freedom. K_2 and K_4 are employed to enhance the performance of disturbance rejection and set-point response respectively instead of only one controller G_c as employed in Majhi and Atherton (1999) which generally has a tradeoff to make between performance of disturbance rejection and set-point response. In our new structure, this tradeoff is eliminated by re-constructing the scheme and introducing one more controller.

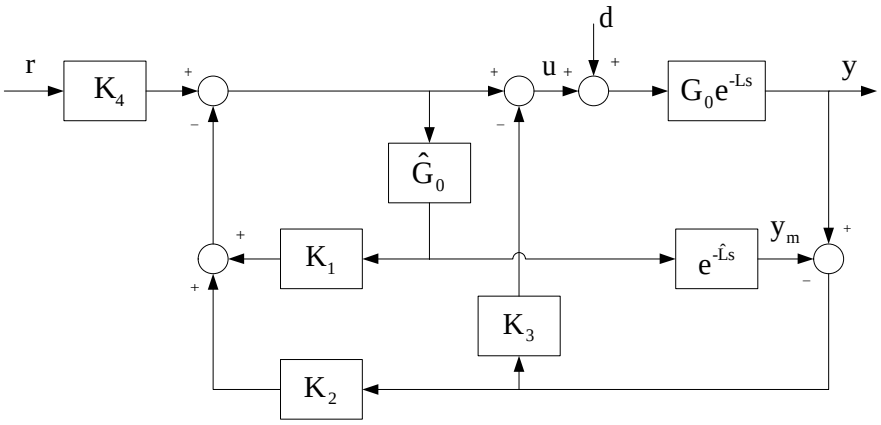

Figure 5.2. Proposed double two-degree-of-freedom control structure

To convince the benefits of the new scheme, suppose that the model perfectly matches the plant dynamics, i.e., $\hat{G}_0 = G_0$ and $\hat{L} = L$. It follows from some algebraic manipulations that the closed-loop transfer function from the set-point to the output is given by

$$H_r = \frac{G_0 K_4}{1 + G_0 K_1} e^{-Ls}. \tag{5.3}$$

One sees that the denominator and numerator of transfer function H_r can be manipulated with K_1 and K_4, respectively. This is essential of two-degree-of-

freedom. Since the transfer function H_r has no time delay in its denominator, K_1 may be designed to place the closed-loop poles to the desired locations using pole placement method. The pre-filter K_4 may be tuned to achieve the optimum set-point response.

For the disturbance path, it can be shown that the transfer function is

$$H_d = \frac{G_0 e^{-Ls}(1 + G_0K_1 - G_0e^{-Ls}K_2)}{(1 + G_0K_1)(1 + G_0e^{-Ls}K_3)}, \tag{5.4}$$

which is also of two-degree-of-freedom once K_1 has been designed as above. The additional factor in its denominator with regard to that of H_r is $(1+G_0e^{-Ls}K_3)$, and the role of K_3 is then to stabilize the delay process, G_0e^{-Ls}. In the numerator, there is the controller K_2, which can be employed for optimum disturbance rejection. Detailed designs of $K_i, i = 1, 2, 3, 4$, will be given in Section 4 below for different processes after stability discussion in the next section.

5.3 Internal Stability

Input/output stability only is not sufficient for practical control systems. The unstable pole-zero cancelations in the system may cause unbounded signals and the system may be damaged by such signals. Thus, internal stability is a prerequisite for any control systems. Our modified Smith predictor scheme is an interconnected system which consists of seven subsystems and each of them is of single input and single output (SISO). It is shown by Wang *et al.* (1999*b*) that an interconnected system consisting only of SISO plants is internally stable if and only if

$$p_c(s) \triangleq \Delta \prod_i p_i(s)$$

has all its roots in the open left half of the complex plane, where $p_i(s)$ are the denominators of the respective subsystem transfer functions and the Δ is the system determinant as defined in the Mason's formula.

Our system in Figure 5.2 has seven subsystems: $K_1(s)$, $K_2(s)$, $K_3(s)$, $K_4(s)$, $\hat{G}_0$, G_0e^{-Ls} and $e^{-\hat{L}s}$. Let $K_1(s) = c_1(s)/d_1(s)$, $K_2(s) = c_2(s)/d_2(s)$, $K_3(s) =$

$c_3(s)/d_3(s)$, $K_4(s) = c_4(s)/d_4(s)$ and $\hat{G}_0(s) = G_0(s) = \alpha(s)/\beta(s)$. Their respective p_i are

$$p_1 = d_1(s),\ p_2 = d_2(s),\ p_3 = d_3(s),\ p_4 = d_4(s),\ p_5 = p_6 = \beta(s) \text{ and } p_7 = 1.$$

It can be shown that the system determinant Δ is given by

$$\Delta = (1 + \hat{G}_0 K_1)(1 + G_0 e^{-Ls} K_3) + K_2(G_0 e^{-Ls} - \hat{G}_0 e^{-\hat{L}s}).$$

It follows that

$$\begin{aligned} p_c(s) &= \Delta(s) \prod_{i=1}^{5} p_i(s) \\ &= [1 + K_1 G_0][1 + K_3 G_0 e^{-Ls}] \cdot d_1(s) \cdot d_2(s) \cdot d_3(s) \cdot d_4(s) \cdot \beta(s) \cdot \beta(s) \cdot 1 \\ &= d_2(s) d_4(s)[d_1(s)\beta(s) + c_1(s)\alpha(s)][d_3(s)\beta(s) + c_3(s)\alpha(s)e^{-Ls}]. \end{aligned}$$

The polynomial, $d_1(s)\beta(s) + c_1(s)\alpha(s)$, reflects stabilization of delay-free G_0 by the controller K_1, which is always possible, say, by pole placement. Both K_2 and K_4 must be stable for the stability of $d_2(s)$ and $d_4(s)$, and are used to achieve best disturbance response and set-point response, respectively. With such constraints, the overall system is internally stable if and only if the delay process, $G_0 e^{-Ls}$, is stabilized by controller K_3. For a general unstable delay system, readers are referred to Bonnet and Partington (1999) for design of a stabilizing controller K_3.

In view of the above analysis, it can be concluded that, unlike the original Smith system where the characteristic equation is of delay-free, the modified Smith scheme gets no simplification as far as stabilization is concerned, that is, the characteristic equation is delay-dependent. In fact, this is the case for all the existing stable modified Smith schemes for unstable processes as we found in Majhi and Atherton (1999), Åström *et al.* (1994), Matausek and Micic (1996), and many others.

5.4 Controller Design

It follows from the discussions in the preceding sections that controller design for the proposed scheme should proceed as follows. K_1 is to stabilize G_0, K_4 is to

shape H_r in (5.3) for desired set-point response, K_3 to stabilize G_0e^{-Ls}, and K_2 to achieve optimum disturbance attenuation of (5.4). Since most typical industrial processes of interests are of IPDT, FOPDT and SOPDT processes, controller design is carried out in detail for each of these three cases as follows.

IPDT Processes Consider the following IPDT model:

$$G(s) = G_0(s)e^{-Ls} = \frac{k_0}{s}e^{-Ls},$$

where all coefficients are non-negative. The closed-loop transfer function for set-point tracking is made to be

$$H_r = \frac{k_0K_4}{s + k_0K_1}e^{-Ls} = \frac{1}{\lambda s + 1}e^{-Ls}, \tag{5.5}$$

where $\lambda > 0$ is an adjustable closed-loop design parameter. A small value of λ produces fast response, and a large value of λ enhances the robustness of the closed-loop system. The guidelines to choose such a parameter is given in Majhi and Atherton (2000*a*) and adopted here. Once λ is determined, K_1 and K_4 are computed from (5.5) as

$$K_1 = \frac{1}{k_0\lambda}, \tag{5.6}$$

and

$$K_4 = \frac{1}{k_0\lambda}. \tag{5.7}$$

This results in the closed-loop transfer function for disturbance:

$$H_d = \frac{k_0\lambda(s + \frac{1}{\lambda} - k_0K_2e^{-Ls})}{(\lambda s + 1)(s + k_0K_3e^{-Ls})}e^{-Ls}.$$

Note that K_3 is designed to stabilize k_0e^{-Ls}/s and the proportional gain is sufficient. According to Matausek and Micic (1996), K_3 is computed to give a phase margin of 60° which gives

$$K_3 = \frac{\pi}{6Lk_0}. \tag{5.8}$$

In order to achieve good disturbance rejection performance, K_2 is selected to minimize the integral squared error (ISE) in case of step type disturbance. We approximate e^{-Ls} by $1 - Ls$ and choose K_2 as a PD controller:

$$K_2 = K_{2P} + K_{2D}s. \tag{5.9}$$

Then, H_d becomes

$$\begin{aligned} H_d &= \frac{k_0\lambda[s+\frac{1}{\lambda}-k_0(K_{2P}+K_{2D}s)(1-Ls)]}{(\lambda s+1)[s+k_0K_3(1-Ls)]}e^{-Ls} \\ &= \frac{k_0\lambda[k_0LK_{2D}s^2+(-k_0K_{2D}+k_0K_{2P}L+1)s+(\frac{1}{\lambda}-k_0K_{2P})]}{\lambda(1-k_0K_3L)s^2+(\lambda k_0K_3+1-k_0K_3L)s+k_0K_3}e^{-Ls}. \end{aligned}$$

To ensure zero steady state error, the constant term $(1/\lambda - k_0K_{2P})$ in the numerator should be equal to zero, which leads to

$$K_{2P} = \frac{1}{k_0\lambda}. \tag{5.10}$$

Then the step disturbance response is given by

$$\begin{aligned} Y_d &= \frac{1}{s}H_d \\ &= Y_0k_0\lambda e^{-Ls}, \end{aligned}$$

where

$$Y_0 = \frac{b_1s+b_0}{a_2s^2+a_1s+a_0},$$

with

$$\begin{aligned} b_1 &= k_0LK_{2D}, \\ b_0 &= -k_0K_{2D}+k_0K_{2P}L+1, \\ a_2 &= \lambda(1-k_0K_3L), \\ a_1 &= \lambda k_0K_3+1-k_0K_3L, \\ a_0 &= k_0K_3. \end{aligned}$$

Since both $k_0\lambda$ and L are fixed, minimizing the ISE of Y_d is equivalent to minimizing the ISE of Y_0. According to Jury and Dewey (1965), the ISE of Y_0 is

$$ISE = \frac{a_2{b_0}^2+a_0{b_1}^2}{2a_2a_1a_0},$$

which is a positive quadratic function of K_{2D}. Then the optimal K_{2D} for minimum ISE is given by

$$K_{2D} = \frac{(6-\pi)(\lambda+L)}{\lambda k_0(6-\pi)+k_0L\pi}, \text{ for } e^{-Ls} \approx 1-Ls. \tag{5.11}$$

If we approximate e^{-Ls} by $(1 - Ls/2)/(1 + Ls/2)$ and repeat the above design, then K_{2P} is still given by (5.10), but K_{2D} is changed to:

$$K_{2D} = \frac{(\frac{1}{2}L + \lambda - \frac{1}{2}\lambda k_0 K_3 L)(1 + \frac{L}{\lambda}) - \frac{1}{4}k_0 K_3 L^2}{k_0(\frac{1}{2}L + \lambda - \frac{1}{2}\lambda k_0 K_3 L) + \frac{1}{4}{k_0}^2 K_3 L^2}, \text{ for } e^{-Ls} \approx \frac{1 - \frac{1}{2}Ls}{1 + \frac{1}{2}Ls}. \quad (5.12)$$

FOPDT Processes Consider the following unstable FOPDT model:

$$G(s) = G_0(s)e^{-Ls} = \frac{k_0}{Ts - 1}e^{-Ls},$$

where all coefficients are non-negative. The closed-loop transfer function for set-point tracking is made to be

$$H_r = \frac{k_0 K_4}{Ts - 1 + k_0 K_1}e^{-Ls} = \frac{1}{\lambda s + 1}e^{-Ls},$$

where $\lambda > 0$ is the adjustable closed-loop design parameter, and this gives rise to

$$K_1 = \frac{1 + T/\lambda}{k_0}, \quad (5.13)$$

and

$$K_4 = \frac{T}{k_0 \lambda}. \quad (5.14)$$

The corresponding closed-loop transfer function for disturbance is

$$H_d = \frac{\lambda G_0(Ts - 1 + k_0 K_1 - k_0 K_2 e^{-Ls})}{T(\lambda s + 1)(1 + K_3 G_0 e^{-Ls})}e^{-Ls}.$$

The controller K_3 is designed to stabilize $G_0 e^{-Ls}$. Based on the optimum phase margin criterion, De Paor and O'Malley (1989) suggested a proportional controller to stabilize an unstable FOPDT process which gives

$$K_3 = \sqrt{\frac{T}{L{k_0}^2}}. \quad (5.15)$$

In order to achieve good disturbance rejection performance, K_2 is determined to minimize the ISE of the disturbance response. With $e^{-Ls} \approx 1 - Ls$ and

$$K_2 = K_{2P} + K_{2D}s \quad (5.16)$$

as chosen before, we have

$$H_d = \frac{\lambda k_0}{T}\frac{k_0 L K_{2D} s^2 + (-k_0 K_{2D} + T + k_0 K_{2P} L)s + (\frac{T}{\lambda} - k_0 K_{2P})}{\lambda(T - k_0 K_3 L)s^2 + (\lambda k_0 K_3 - \lambda + T - k_0 K_3 L)s + k_0 K_3 - 1}e^{-Ls}.$$

Let the constant term $(T/\lambda - k_0 K_{2P})$ be equal to zero, we have

$$K_{2P} = \frac{T}{k_0 \lambda}. \tag{5.17}$$

Following the similar procedure to the IPDT case, the optimal K_{2D} is given by

$$K_{2D} = \frac{\lambda(T - \sqrt{TL})(T + \frac{TL}{\lambda})}{\lambda k_0 (T - \sqrt{TL}) + k_0 L^2 (\sqrt{\frac{T}{L}} - 1)}, \text{ for } e^{-Ls} \approx 1 - Ls. \tag{5.18}$$

Once again, with the approximation of $e^{-Ls} \approx (1 - Ls/2)/(1 + Ls/2)$, K_{2P} keeps the same and K_{2D} becomes

$$K_{2D} = \frac{[\frac{1}{2}TL + \lambda(T - \frac{1}{2}L - \frac{1}{2}\sqrt{TL})](T + \frac{TL}{\lambda}) - \frac{1}{4}TL^2(\sqrt{\frac{T}{L}} - 1)}{k_0[\frac{1}{2}TL + \lambda(T - \frac{1}{2}L - \frac{1}{2}\sqrt{TL})] + \frac{1}{4}k_0 L^2(\sqrt{\frac{T}{L}} - 1)}, \text{ for } e^{-Ls} \approx \frac{1 - \frac{1}{2}Ls}{1 + \frac{1}{2}Ls}. \tag{5.19}$$

SOPDT Processes Consider the following unstable SOPDT model:

$$G(s) = G_0(s)e^{-Ls} = \frac{k_0}{(T_1 s - 1)(T_2 s + 1)} e^{-Ls},$$

where all coefficients are non-negative. The closed-loop transfer function for set-point tracking is made to be

$$H_r = \frac{k_0 K_4}{(T_1 s - 1)(T_2 s + 1) + k_0 K_1} e^{-Ls} = \frac{1}{(\lambda s + 1)^2} e^{-Ls},$$

where $\lambda > 0$ is an adjustable closed-loop design parameter, which gives

$$\begin{aligned} K_1 &= \frac{1}{k_0}(\frac{T_1 T_2}{\lambda^2} + 1) + \frac{1}{k_0}(\frac{2T_1 T_2}{\lambda} - T_1 + T_2)s \\ &\triangleq K_{1P} + K_{1D} s, \end{aligned} \tag{5.20}$$

and

$$K_4 = \frac{T_1 T_2}{k_0 \lambda^2}. \tag{5.21}$$

This results in the closed-loop transfer function for disturbance:

$$H_d = \frac{\lambda^2 G_0[(T_1 s - 1)(T_2 s + 1) + k_0 K_1 - k_0 K_2 e^{-Ls}]}{T_1 T_2 (\lambda s + 1)^2 (1 + K_3 G_0 e^{-Ls})} e^{-Ls}.$$

Using De Paor and O'Malley (1989)'s method again yields

$$K_3 = \sqrt{\frac{T_1}{L {k_0}^2}}(T_2 s + 1). \tag{5.22}$$

Approximate e^{-Ls} by $1 - Ls$ and choose

$$K_2 = K_{2P} + K_{2D}s \tag{5.23}$$

to minimize the ISE of disturbance response. H_d is then calculated as

$$H_d = \frac{\lambda^2 k_0}{T_1 T_2} \frac{b_1 s^2 + b_0 s + (k_0 K_{1P} - k_0 K_{2P} - 1)}{a_4 s^4 + a_3 s^3 + a_2 s^2 + a_1 s + a_0} e^{-Ls},$$

with

$$\begin{aligned}
b_1 &= k_0 L K_{2D} + T_1 T_2, \\
b_0 &= -k_0 K_{2D} + T_1 - T_2 + k_0 K_{1D} + k_0 L K_{2P}, \\
a_4 &= \lambda^2 T_2 (T_1 - \sqrt{T_1 L}), \\
a_3 &= 2\lambda T_2 (T_1 - \sqrt{T_1 L}) + \lambda^2 (T_1 - T_2 + \sqrt{\frac{T_1}{L}} T_2 - \sqrt{T_1 L}), \\
a_2 &= \lambda^2 (\sqrt{\frac{T_1}{L}} - 1) + 2\lambda (T_1 - T_2 + \sqrt{\frac{T_1}{L}} T_2 - \sqrt{T_1 L}) + T_2 (T_1 - \sqrt{T_1 L}), \\
a_1 &= 2\lambda (\sqrt{\frac{T_1}{L}} - 1) + (T_1 - T_2 + \sqrt{\frac{T_1}{L}} T_2 - \sqrt{T_1 L}), \\
a_0 &= \sqrt{\frac{T_1}{L}} - 1.
\end{aligned}$$

Let $k_0 K_{1P} - k_0 K_{2P} - 1 = 0$ and K_{2P} is

$$K_{2P} = K_{1P} - \frac{1}{k_0}. \tag{5.24}$$

The step disturbance response is then given by

$$\begin{aligned}
Y_d &= \frac{\lambda^2 k_0}{T_1 T_2} \frac{b_1 s + b_0}{a_4 s^4 + a_3 s^3 + a_2 s^2 + a_1 s + a_0} e^{-Ls} \\
&\triangleq \frac{\lambda^2 k_0}{T_1 T_2} Y_0 e^{-Ls}.
\end{aligned}$$

According to Jury and Dewey (1965), the ISE of Y_0 is

$$ISE = \frac{(-1)^{(4-1)} |\Omega_1|}{2 a_4 |\Omega|},$$

with

$$\Omega = \begin{bmatrix} a_0 & 0 & 0 & 0 \\ a_2 & a_1 & a_0 & 0 \\ a_4 & a_3 & a_2 & a_1 \\ 0 & 0 & a_4 & a_3 \end{bmatrix} \text{ and } \Omega = \begin{bmatrix} a_0 & 0 & 0 & {b_0}^2 \\ a_2 & a_1 & a_0 & -{b_1}^2 \\ a_4 & a_3 & a_2 & 0 \\ 0 & 0 & a_4 & 0 \end{bmatrix},$$

and is a positive quadratic function of K_{2D}, then the optimal K_{2D} is obtained as

$$K_{2D} = \frac{(a_2a_3 - a_1a_4)(T_1 - T_2 + k_0K_{1D} + k_0K_{1P}L - L) - a_0a_3T_1T_2L}{(a_2a_3 - a_1a_4)k_0 + a_0a_3k_0L}, \text{ for } e^{-Ls} \approx 1 - Ls. \tag{5.25}$$

If we approximate e^{-Ls} by $(1 - Ls/2)/(1 + Ls/2)$, then K_{2P} keeps the same and K_{2D} becomes

$$\begin{aligned} K_{2D} = &\frac{1}{{k_0}^2 f_0 + \frac{1}{4}{k_0}^2L^2f_1}[k_0f_0(T_1 - T_2 - \frac{1}{2}L + \frac{1}{2}k_0LK_{1P} + k_0K_{1D} + \frac{1}{2}k_0K_{2P}L) \\ &-\frac{1}{2}k_0Lf_1(T_1T_2 + \frac{1}{2}LT_1 - \frac{1}{2}LT_2 + \frac{1}{2}k_0LK_{1D}) - \frac{1}{2}k_0T_1T_2Lf_1], \text{ for } e^{-Ls} \approx \frac{1 - \frac{1}{2}Ls}{1 + \frac{1}{2}Ls}, \end{aligned} \tag{5.26}$$

where

$$\begin{aligned} f_1 &= a_0a_3a_4 - a_0a_2a_5, \\ f_0 &= a_2a_3a_4 - {a_2}^2a_5 - a_1{a_4}^2 + a_0a_4a_5, \end{aligned}$$

with

$$\begin{aligned} a_5 =& \frac{1}{2}\lambda^2T_1T_2L, \\ a_4 =& \lambda T_1T_2L + \lambda^2[T_1T_2 + \frac{1}{2}L(T_1 - T_2) - \frac{1}{2}\sqrt{T_1L}T_2], \\ a_3 =& \frac{1}{2}T_1T_2L + \lambda[2T_1T_2 + L(T_1 - T_2) - \sqrt{T_1L}T_2] + \lambda^2(T_1 - T_2 - \frac{1}{2}L + \sqrt{\frac{T_1}{L}}T_2 \\ &- \frac{1}{2}\sqrt{T_1L}), \\ a_2 =& [T_1T_2 + \frac{1}{2}L(T_1 - T_2) - \frac{1}{2}\sqrt{T_1L}T_2] + \lambda(2T_1 - 2T_2 - L + 2\sqrt{\frac{T_1}{L}}T_2 - \sqrt{T_1L}) \\ &+ \lambda^2(\sqrt{\frac{T_1}{L}} - 1), \\ a_1 =& 2\lambda(\sqrt{\frac{T_1}{L}} - 1) + (T_1 - T_2 - \frac{1}{2}L + \sqrt{\frac{T_1}{L}}T_2 - \frac{1}{2}\sqrt{T_1L}), \\ a_0 =& \sqrt{\frac{T_1}{L}} - 1. \end{aligned}$$

Remark 1: We have provided two options for the value of the derivative gain, K_{2D}, in the disturbance rejecting controller K_2. The reason for such options instead of an unique choice is that the better approximation, $e^{-Ls} \approx (1-Ls/2)/(1+Ls/2)$,

does produce better performance over that from $e^{-Ls} \approx 1 - Ls$, but at costs of higher control action, as expected. The size of such extra action varies with process characteristics: biggest for the IPDT case, moderate for the FOPDT case, and smallest for the SOPDT case, as will be seen in the next section.

Remark 2: In all the designs for the above three cases, K_4 has been chosen to fit to some simple target set-point transfer functions. This leads to simple design formulas and the same or very similar set-point performances as from the Majhi and Atherton's method. Such designs seem already sufficiently good for simple processes like the above three cases. They facilitate a fair comparison of disturbance responses between our method and the Majhi and Atherton's method. Note that improvement of disturbance response and its fair comparison with other works are the focus of this chapter. If we would have changed our target set-point transfer function to a different one from the Majhi and Atherton's method, then this difference would also have come to the disturbance transfer function, which could complicate performance comparison of disturbance responses. It should be however pointed out that, in principle, K_4 is a provision in our scheme, which can be utilized to optimize the set-point response in a sense of interests, and the potential improvement of the set-point response from such a best use of K_4 might be significant, say, for complex processes.

5.5 Examples

In this section, we demonstrate our designs in the proceeding section by three examples, one for each case. Note that PD controllers are involved in our designs. As usual, we implement them with an industrial PD form $(k_d s+k_p)/(k_d s/N+1)$ and choose $N = 10$ in all the examples below. Both the set-point and load disturbance are of step signal with the amplitude of 1 and 0.1, respectively. For convenience, the proposed design with $e^{-Ls} \approx 1-Ls$ is referred to as proposed design (A), while the one with $e^{-Ls} \approx (1 - Ls/2)/(1 + Ls/2)$ as proposed design (B).

Example 1: Consider an IPDT process (Majhi and Atherton, 2000*a*):

$$G(s) = \frac{1}{s}e^{-5s}.$$

The controllers from Majhi and Atherton (2000*a*) are $G_c(s) = 0.5(1+1/s)$, $G_{c1} = 1$, which lead to the set-point response of $e^{-Ls}/(2s+1)$; and $G_{c2} = 0.105$, which is designed to stabilize G_0e^{-Ls} with 60° phase margin. For a fair comparison, we choose the same $\lambda = 2$ in their design to produce the same set-point response, and design the same K_3 as their G_{c2}. It follows from (5.6)-(5.12) that $K_1 = 0.5$, $K_3 = 0.105$ and $K_4 = 0.5$, with $K_2 = 0.5 + 0.934s$ for proposed design (A) and $K_2 = 0.5 + 2.723s$ for proposed design (B). The responses of the proposed designs and Majhi's method are shown in Figure 5.3. One sees that that the proposed designs have the same set-point responses but better disturbance rejection compared with Majhi's method.

Example 2: Consider an unstable FOPDT process (Majhi and Atherton, 2000*a*):

$$G(s) = \frac{4}{10s-1}e^{-5s}.$$

The controllers from Majhi and Atherton (2000*a*) are $G_c(s) = 0.25(1+0.5/s)$, $G_{c1} = 0.5 - 2s$ and $G_{c2} = 0.35$. We take the same $\lambda = 2$ as that in Majhi and Atherton (2000*a*) so as to achieve the same set-point response, and design the same K_3 as G_{c2}. It follows from (5.13)-(5.19) that $K_1 = 1.5$, $K_3 = 0.35$, and $K_4 = 1.25$, with $K_2 = 1.25+3.16s$ for proposed design (A) and $K_2 = 1.25+7.93s$ for proposed design (B). The responses of the proposed method and Majhi's method are shown in Figure 5.4. Once again, the proposed method has much better disturbance rejection performance.

Example 3: Consider an unstable SOPDT process (Majhi and Atherton, 1999):

$$G(s) = \frac{2}{(10s-1)(2s+1)}e^{-5s}.$$

The controllers from Majhi and Atherton (1999) are $G_c(s) = 0.1 + 1/s$, $G_{c1} = 5.017+3.408s$, which are designed for ISTE optimal set-point response, and $G_{c2} = 0.707 + 1.414s$ for the optimum stability margin. By choosing $\lambda = 2.5$ for a

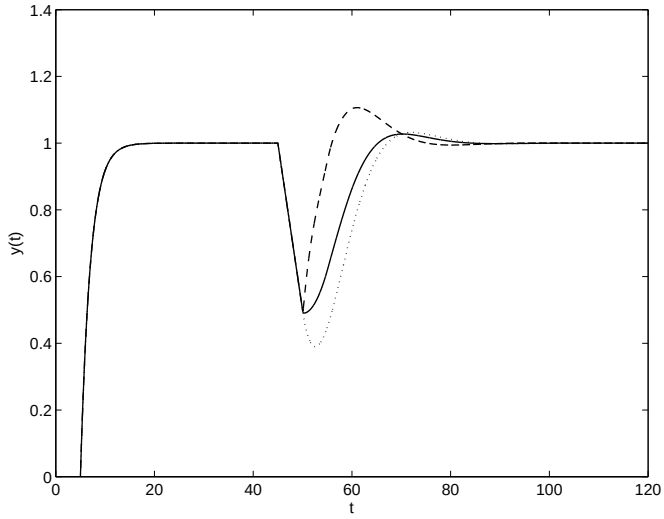

(a) *Output*

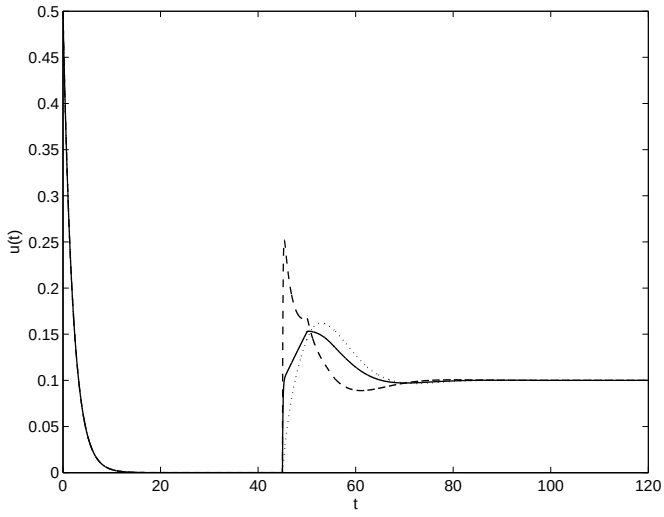

(b) *Input*

Figure 5.3. Step responses for IPDT process
($\cdots\cdots$ Majhi's method; —— proposed design (A);- - - - proposed design (B))

similar set-point response speed, we obtain the controllers from (5.20)-(5.26) as $K_1 = 2.1 + 4s$, $K_3 = 0.707 + 1.414s$ and $K_4 = 1.6$, with $K_2 = 1.6 + 10.44s$ for proposed design (A) and $K_2 = 1.6 + 14.25s$ for proposed design (B). The responses of the proposed method and Majhi's method for nominal plant are shown in Figure

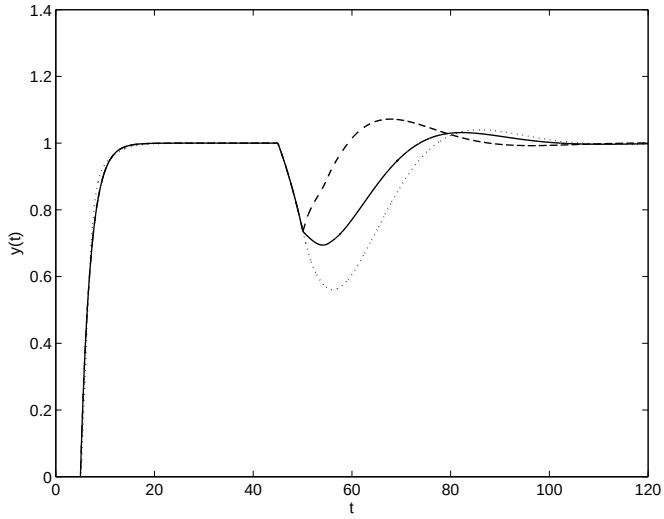

(a) *Output*

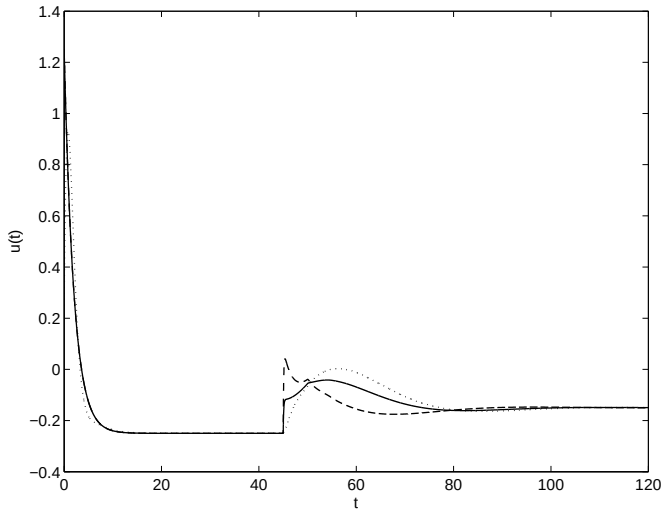

(b) *Input*

Figure 5.4. Step responses for unstable FOPDT process
(· · · · · · Majhi's method; —— proposed design (A);- - - - proposed design (B))

5.5. Obviously, the proposed method has similar set-point response but much better disturbance rejection compared with Majhi's method. Suppose that the model is not accurate and has 10% error at the plant gain, or the gain is 2.2 and 1.8, respectively, while the nominal value is 2. The results are given in Figures

5.6 and 5.7 respectively. Both methods are robust against gain perturbation, but the performance of the proposed method is better, especially for the disturbance response.

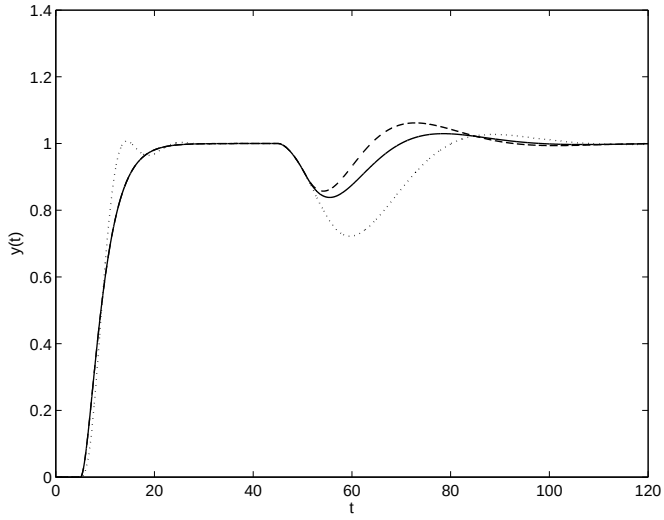

(a) *Output*

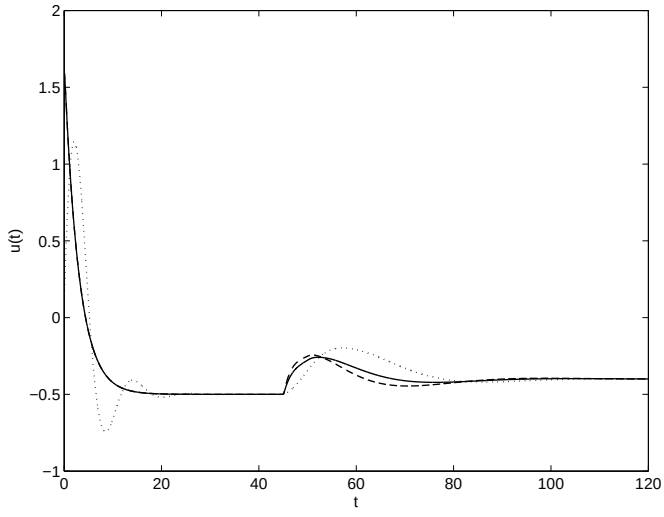

(b) *Input*

Figure 5.5. Step responses for unstable SOPDT process (gain=2)
(· · · · · · Majhi's method; —— proposed design (A);- - - - proposed design (B))

The ISE and maximum error of disturbance responses for the above examples

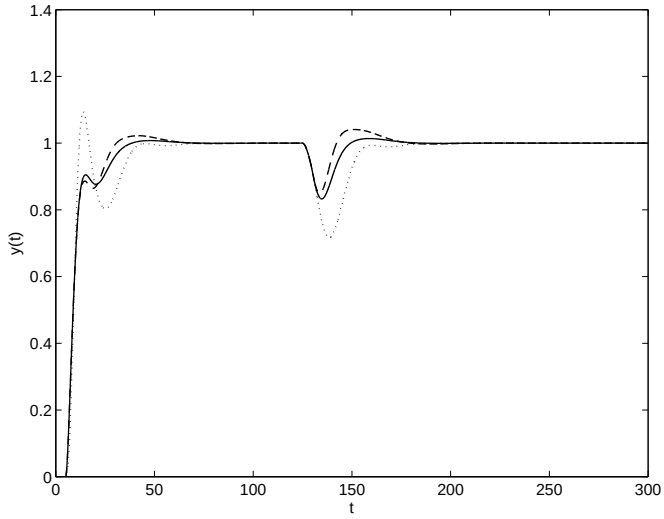

(a) *Output*

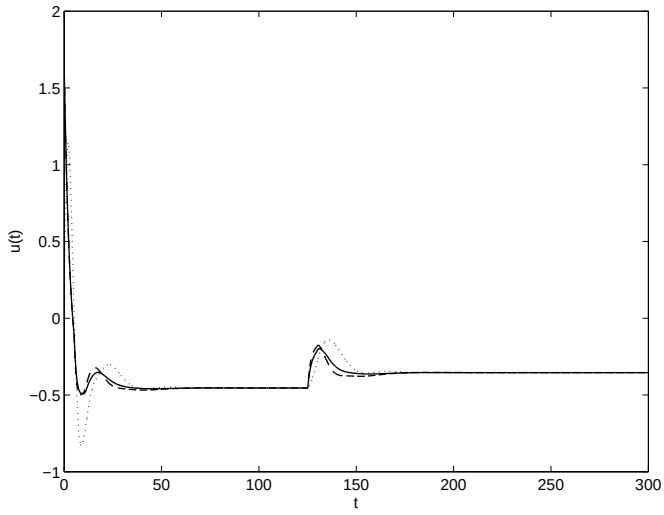

(b) *Input*

Figure 5.6. Step responses for unstable SOPDT process (gain=2.2)
(· · · · · · Majhi's method; —— proposed design (A);- - - - proposed design (B))

are summarized in Table 5.1. It is obvious that the proposed designs have superior performance to Majhi's design. Our design (A) yields better disturbance response than Majhi's with comparable controlled inputs, while our design (B) is even better than design (A) at the cost of a bit more aggressive process inputs. It is noted

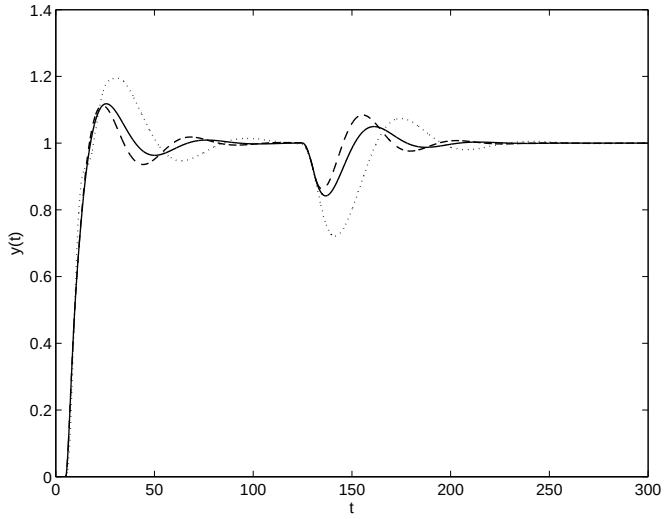

(a) *Output*

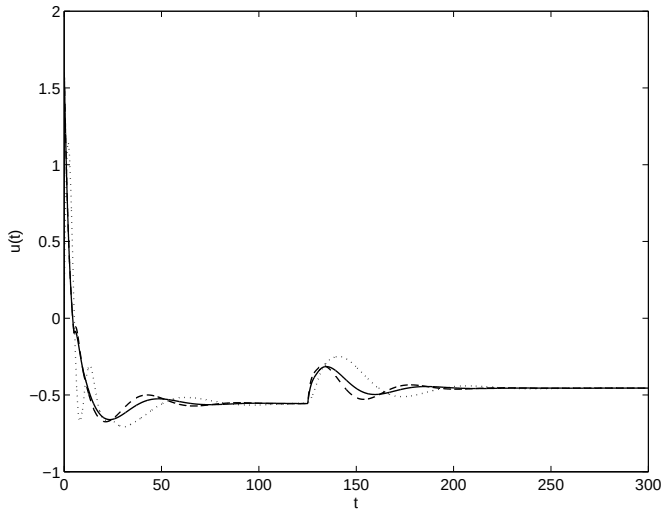

(b) *Input*

Figure 5.7. Step responses for unstable SOPDT process (gain=1.8)
(· · · · · · Majhi's method; —— proposed design (A);- - - - proposed design (B))

that the actual ISE optimal K_2 for three examples without approximation of e^{-Ls} can be found from extensive simulation and is obtained as $K_2^* = 0.5 + 2.83s$, $K_2^* = 1.25 + 7.96s$, and $K_2^* = 1.25 + 14.17s$ respectively, which are almost identical to our design (B). This validates the accuracy of the proposed design (B). The

performance specifications of the actual ISE optimal designs are also included in Table 5.1 for reference.

Table 5.1. Performance Specifications of Disturbance Responses

	Scheme	ISE	Maximum error
Example 1:	Majhi's method	3.130	0.610
	Proposed (A)	1.899	0.509
	Proposed (B)	0.894	0.502
	Actual ISE optimal design	0.891	0.502
Example 2:	Majhi's method	2.510	0.439
	Proposed (A)	1.110	0.306
	Proposed (B)	0.344	0.262
	Actual ISE optimal design	0.344	0.262
Example 3:	Majhi's method	1.032	0.278
$k_0 = 2$	Proposed (A)	0.264	0.162
	Proposed (B)	0.202	0.143
	Actual ISE optimal design	0.202	0.143
Example 3:	Majhi's method	0.902	0.284
$k_0 = 2.2$	Proposed (A)	0.237	0.167
	Proposed (B)	0.177	0.150
	Actual ISE optimal design	0.177	0.150
Example 3:	Majhi's method	1.327	0.279
$k_0 = 1.8$	Proposed (A)	0.311	0.158
	Proposed (B)	0.257	0.137
	Actual ISE optimal design	0.257	0.138

The reasons for better disturbance rejection with reasonable process input sizes are probably as follows: The derivative control is introduced in the disturbance control loop (in K_2) and thus accelerates correction action. This derivative control may not produce extra control action since it compensates for lag present in the process and the path from the disturbance d to control action u has no derivative

term or its equivalent. Our design criterion for this derivative gain is to minimize the integral squared error of disturbance response, which tends to yield quite reasonable control action, compared with those designs for fast response.

5.6 Conclusion

A new control scheme is developed based on previously published works, particularly that of Majhi and Atherton, for better control of unstable process with dead time. By realizing importance of disturbance rejection and non-existence of any control freedom over the disturbance response in the previous schemes, our new scheme has one more degree-of-freedom to manipulate disturbance response, and four controllers involved are well placed to separately tune the denominators and numerators of closed-loop transfer functions from the set-point and disturbance. This allows easy design of each controller and good control performance for both set-point and disturbance responses. The control design for set-point response is handled similarly to that of Majhi and Atherton for three cases considered in the chapter. For disturbance response, we tune the controller parameter to minimize the integral squared error. Two options are provided to suit practical situations of control performance versus available process input limits. Internal stability of the proposed system is analyzed and our designs will always lead to internally stable systems. Simulations show that the proposed scheme yields much better performance for load disturbance responses over the existing methods.

Chapter 6

A Smith-Like Control Design for Processes with RHP Zeros

6.1 Introduction

RHP zeros have been identified in dynamics of many chemical engineering systems such as boilers, simple distillation columns, and coupled distillation column (Holt and Morari, 1985). Characterized by their inverse response to a step input (la Barra S. and León, 1994), RHP zeros have provided challenges to control system design. It is well known that a system with RHP zeros, compared with its minimum phase counterpart, has inherent limitations on achievable feedback system performance such as the closed-loop gain and bandwidth, the integral on sensitivity or complementary sensitivity function (Middleton, 1991; Qiu and Davison, 1993; Seron *et al.*, 1997), loop-transfer recovery (Zhang and Freudenberg, 1990). More specifically, in a conventional unity feedback control scheme, the existence of RHP zeros in the plant prevents use of high gain in the controller and prolongs the settling time to reduce the undershoot.

It is noted that RHP zeros share the same non-minimum phase property as dead time and a popular bridge between RHP zeros and dead time is a first order Páde approximation: $e^{-2zs} = (z-s)/(z+s)$. There has been a dead time compensator, the Smith predictor (Smith, 1957), with which the dead time can be removed

from the characteristic equation of the closed-loop system and the control design is greatly simplified into the dead time free one. For a system whose dead time is large compared with its time constant, it is shown that the Smith Predictor control yields superior performance to single loop control (Ingimundarson and Hägglund, 2002). Naturally, this observation leads us to adapting the Smith scheme to systems with RHP zeros.

In this chapter, a Smith control scheme is adopted to control a stable process with RHP zeros and possible dead time. Both RHP zeros and dead time will be compensated for to ease controller design. Nominal performance (such as undershoot, overshoot, settling time, and ISE) and stability robustness are addressed and necessary relationships are established for easy tuning of a single design parameter in the controller. The performance enhancement of the proposed scheme over the single loop system is analyzed and demonstrated.

The rest of this chapter is organized as follows. In Section 6.2, the proposed design scheme is presented and its nominal performance analyzed. The stability issues are then discussed in Section 6.3. Simulation examples are given in Section 6.4. And then conclusions are drawn in Section 6.5.

6.2 The Control Scheme

Consider the control scheme depicted in Figure 6.1, where G is the process, C the controller to be designed, r, u, and y denote the reference input, control input and the process output respectively. $\hat{G} = G_{\mathrm{L}}G_{\mathrm{R}}$ is a model of the process. If the factorization of $\hat{G}$ into G_{L} and G_{R} is such that $G_{\mathrm{R}} = e^{-Ls}$ represents dead time of $\hat{G}$, while G_{L} is the remaining rational function, then the popular Smith predictor control (Smith, 1957) results. It is well known that with the Smith predictor, the dead time disappears from the characteristic equation of the closed-loop system in the case of $G = \hat{G}$, and the control design problem is reduced to one for the delay-free part only, for which enhanced performance can be achieved.

It is noted that RHP zeros share the same non-minimum phase property with dead time. Thus, it is appealing by adopting the Smith scheme to the RHP zero

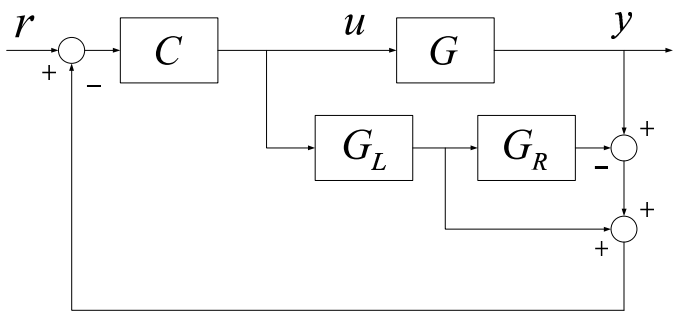

Figure 6.1. Smith control structure

case such that the RHP zeros are removed from the feedback loop and the primary controller is designed for the minimum phase part only, giving performance enhancement over the single loop configuration.

Suppose that a given plant $G(s)$ is stable with k RHP zeros at $z_i > 0$, $i = 1 \cdots k$, and is represented by

$$G = G_0 e^{-L_0 s} \prod_{i=1}^{k} \frac{z_i - s}{z_i + s}, \tag{6.1}$$

where G_0 is a rational, stable and minimum-phase transfer function. It follows from Tan *et al.* (1996) that with the Smith scheme, a deliberately mismatched model may lead to performance improvement over a perfectly matched system while using a simple primary controller, if both the real dead time of the process G and the implicit dead time from high order dynamics of G_0 are condensed to an equivalent total dead time in the low-order model. It is well known that most industrial processes can be approximated by a low-order model. A low-order model is easier to deal with in control design, and a low-order controller is usually adequate for satisfactory performance. Therefore, we approximate G_0 by

$$\hat{G}_0 = \frac{b_1 s + b_0}{a_2 s^2 + a_1 s + a_0} e^{-L_e s}, \quad a_i, b_i > 0 \tag{6.2}$$

Though there are many techniques available for reduced-order modeling (Schoukens and Pintelon, 1991; Obinata and Anderson, 2000), the identification method by Wang and Zhang (2001) is recommended for its accuracy, efficiency and preservation of stability.

In view of the above development, we take

$$\hat{G} = \frac{b_1 s + b_0}{a_2 s^2 + a_1 s + a_0} e^{-Ls} \prod_{i=1}^{k} \frac{z_i - s}{z_i + s}, \quad L = L_0 + L_e. \tag{6.3}$$

Then $\hat{G}$ is factorized as

$$\begin{aligned} G_L &= \frac{b_1 s + b_0}{a_2 s^2 + a_1 s + a_0} \\ G_R &= e^{-Ls} \prod_{i=1}^{k} \frac{z_i - s}{z_i + s} \end{aligned}$$

The primary controller C is chosen as

$$\begin{aligned} C &= G_L^{-1} \frac{1}{\tau s(\tau s + 2)} \\ &= \frac{a_2 s^2 + a_1 s + a_0}{(b_1 s + b_0)\tau s(\tau s + 2)} \end{aligned} \tag{6.4}$$

which is a PID controller cascaded with a second-order lag, and easy to implement. The resultant closed-loop transfer function is

$$H(s) = \frac{C(s)G(s)}{1 + C(s)(G_L(s) - G_L(s)G_R(s) + G(s))} \tag{6.5}$$

If $G = \hat{G}$, then $H(s)$ reduces to the desired closed-loop $H_d(s)$:

$$H_d(s) = \frac{1}{(\tau s + 1)^2} \prod_{i=1}^{k} \frac{z_i - s}{z_i + s} e^{-Ls} \tag{6.6}$$

where the non-minimum phase part (both dead time and RHP zeros) is completely removed from the closed-loop characteristic polynomial. The desired closed-loop performance given by H_d is simple and easy to predict as it is an all-pass transfer function G_R filtered by a double first-order lag, and can be used to well anticipate the actual closed-loop performance as long as the approximation in (6.2) is within a reasonable range, say, a maximum relative error of 10% in the frequency range of closed-loop bandwidth. The design has one tunable parameter only, i.e., the time constant τ, which determines both the nominal performance and robust stability. The relation between τ and time domain specifications of H_d is analyzed in this section, while the issue of stability and robustness is treated in the next section.

For the desired closed-loop transfer function $H_{\rm d}(s)$ in (6.6), one easily finds that the overshoot in response to a step input is zero. According to Morari and Zafiriou (1989), for all transfer functions that contain the same RHP zeros, the one in the form of $\prod_{i=1}^{k} \frac{z_i - s}{z_i + s}$ is of minimum ISE against a step input, with the minimum value of $\sum_{i=1}^{k}(2/z_i)$. Denote by $z_{\min}$ the smallest one of $z_i, i = 1 \cdots k$, if $z_{\min} < 1/\tau$ holds, then the slowest pole in $H_{\rm d}$ is at $-z_{\min}$, and the step response is characterized by a large undershoot, small settling time, and small ISE. In particular, $H_{\rm d}$ is close to $G_{\rm R}$ and is ISE sub-optimal when $z_{\min} << 1/\tau$. For $z_{\min} > 1/\tau$, as τ increases, the dynamic lag due to $\frac{1}{(\tau s+1)^2}$ begins to dominate the transient, and the step response is of small undershoot, large settling time and large ISE.

For illustration, consider the closed-loop transfer function with only one RHP zero z:

$$H_{\rm d}(s) = \frac{1}{(\tau s + 1)^2} \frac{z - s}{z + s}, \quad z > 0 \tag{6.7}$$

By the inverse Laplace transform, the time domain step response is

$$y(t) = 1 - \frac{2}{(c-1)^2} e^{-zt} - \frac{zt(c+1)}{c(c-1)} e^{-\frac{zt}{c}} + \frac{(1 + 2c - c^2)}{(c-1)^2} e^{-\frac{zt}{c}}, \quad c = \tau z \tag{6.8}$$

In order to find the undershoot, letting $\dot{y}(t) = 0$ yields the transcendental equation:

$$\frac{2}{(c-1)^2} e^{-zt} - \frac{(c+1)}{c(c-1)} (1 - \frac{zt}{c}) e^{-\frac{z}{c}t} = 0 \tag{6.9}$$

As z and t always appear together as zt in (6.9), one sees that for a fixed c the solution to (6.9) can be expressed in terms of zt, and the time of achieving the undershoot is inversely proportional to z. When the solution, $(zt)^*$, is substituted to (6.8), the resultant undershoot is uniquely determined by $c = \tau z$. Similar to the time of achieving the undershoot, for a fixed c, both the settling time t_s and the ISE are also inversely proportional to z. The relationships of the undershoot, the 2% settling time and the ISE against the parameter τ are depicted in Figures 6.2(a)-(c) respectively. With the help of Figure 6.2, it is convenient to make a trade-off between the undershoot, settling time and ISE by tuning of τ.

For systems with more than one RHP zeros, no neat relationships between time domain specifications and τ exist due to the different possible relative positions of

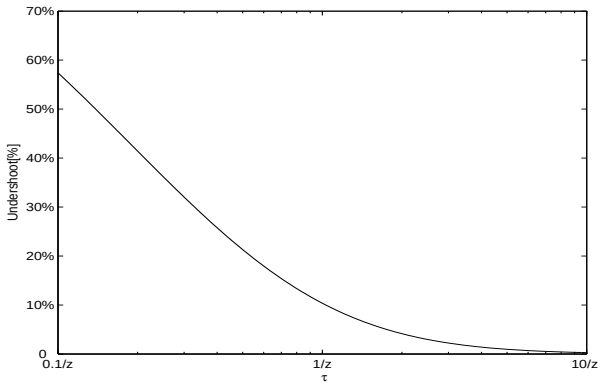

(a) Undershoot

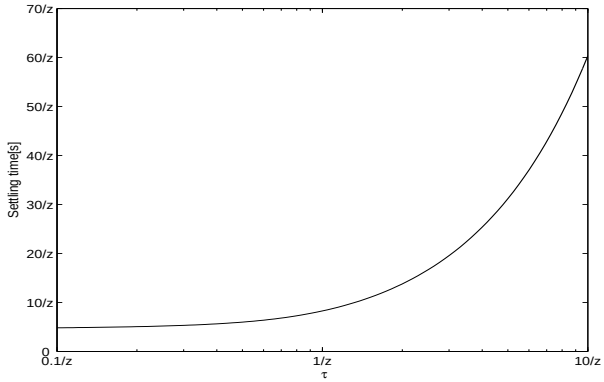

(b) Settling time

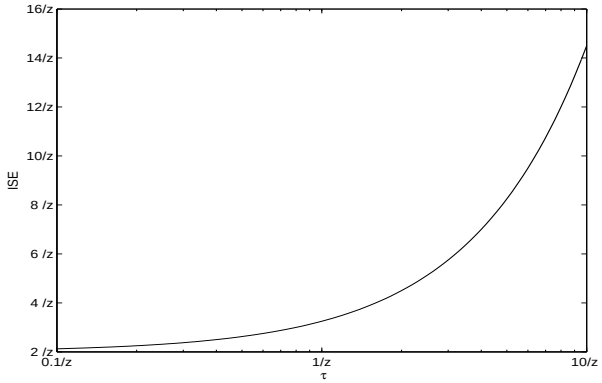

(c) ISE

Figure 6.2. Step response specifications against tuning parameter τ

RHP zeros. However, it is found from simulation that when all the other RHP zeros are at least 1.5 times as large as the smallest one $z_{\min}$, their effects on undershoot and settling time are insignificant, and we can estimate the performance based on $z_{\min}$ as if there would be a single RHP zero at $z = z_{\min}$. This is illustrated by Figure 6.3, where the undershoot and settling time of

$$H_{\rm d}(s) = \frac{1}{(\tau s+1)^2}\frac{(z-s)(z_2-s)}{(z+s)(z_2+s)}, \quad z_2 > z > 0,$$

are depicted, with z_2 chosen as $z_2 = 1.5z$, $z_2 = 2z$ and $z_2 = 5z$ respectively, compared with the single RHP case in (6.7). It follows from Figure 6.3 that, for one thing, both the undershoot and the settling time are increased with the introduction of RHP zero z_2 when $\tau > 0.3/z$; for another, as z_2 increases, its effect diminishes, and is almost negligible when $z_2 = 5z$.

When the dead time L (both from original process and from model reduction) is also taken into account for $H_{\rm d}$, the step response shifts L towards the positive time axis, and the settling time is increased by L, while the undershoot remains unchanged. One concludes that τ can be tuned based on the smallest RHP zero according to the time domain specifications, with some reservation paid if there exist other RHP zeros.

6.3 Stability Analysis

Stability is the primary concern for any controller design. In this section, both the nominal and robust stability of the proposed scheme are investigated.

For nominal stability, the perfect model match, $\hat{G} = G$, is assumed. It follows from Wang *et al.* (1999*b*) that the Smith scheme, Figure 6.1, is internally stable if and only if the controller C stabilizes the minimum-phase model $G_{\rm L}$. In comparison, for the single-loop scheme, the nominal stability requires the process G to be stabilized. From the factorization $G = G_{\rm L}G_{\rm R}$, there hold

$$|G(j\omega)| = |G_{\rm L}(j\omega)G_{\rm R}(j\omega)| = |G_{\rm L}(j\omega)|$$

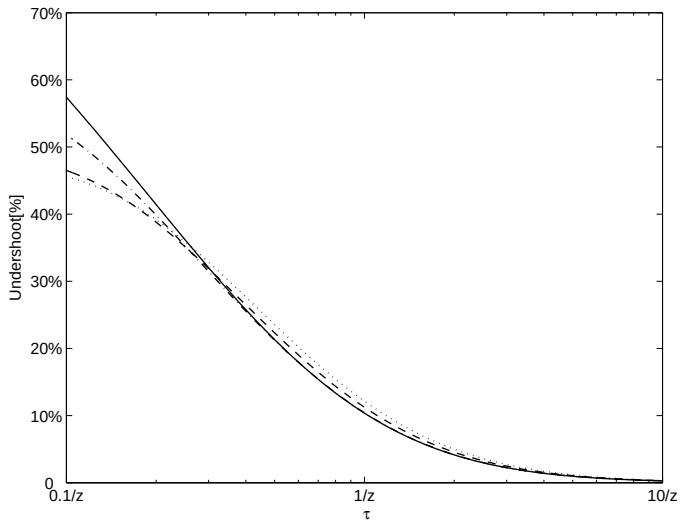

(a) Undershoot

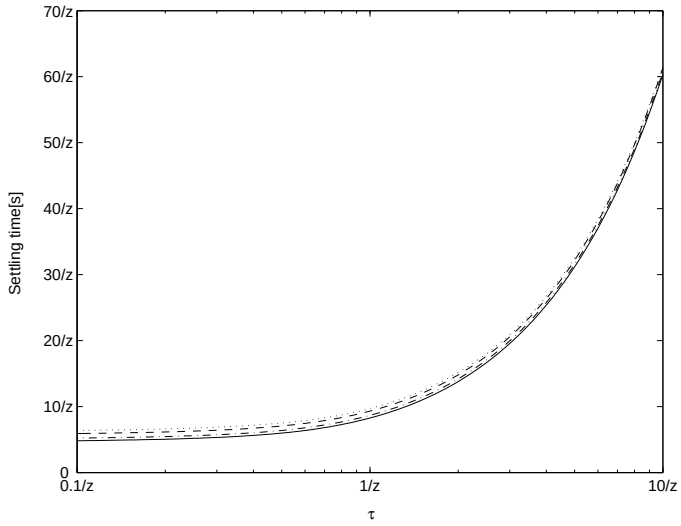

(b) Settling time

Figure 6.3. Performance comparison of processes with 2 RHP zeros
(—— single RHP zero z; $\cdots\cdots$ $z_2 = 1.5z$; - - - $z_2 = 2z$; $-\cdot-$ $z_2 = 5z$)

and

$$\arg(G(j\omega)) = \arg(G_{\mathrm{L}}(j\omega)) - 2\sum_{i=1}^{k} \tan^{-1}\left(\frac{\omega}{z_i}\right) - L\omega$$

At the gain cross-over frequency such that $|G(j\omega_{gc})| = |G_L(j\omega_{gc})| = 1$, $\arg(G) <$

$\arg(G_L)$ always holds; i.e., G always has more phase lag than G_L, leading to less phase margin for G than G_L. At the phase cross-over frequency such that $\arg(G(j\omega_{\rm pc})) = -\pi$, G usually has a finite gain margin, while $G_{\rm L}$ has an infinity gain margin since $G_{\rm L}$ will never reach the phase of $-\pi$. Hence $G_{\rm L}$ is much easier to stabilize and control by the primary controller in the Smith scheme than its counterpart G by a controller in a single-loop feedback scheme. For example, let

$$G(s) = \frac{2(1-s)}{(1+s)^3}$$

so that

$$G_L(s) = \frac{2}{(1+s)^2} \quad \text{and} \quad G_R(s) = \frac{1-s}{1+s}$$

The gain and phase margins for $G(s)$ are 1 and 0 respectively, while those for $G_{\rm L}(s)$ are ∞ and $\pi/2$, respectively.

In robustness analysis, one may view G as the true process dynamics. Then, the mismatch between G and $\hat{G} = G_{\rm L}G_{\rm R}$ can capture both imperfectness of process modeling and model reduction involved in our design procedure. Let the total uncertainty be bounded by

$$\left| \frac{G(s) - \hat{G}(s)}{\hat{G}(s)} \right| < \Delta_{\rm G}(s) \tag{6.10}$$

Then the Smith system is robustly stable (Morari and Zafiriou, 1989) if and only if

$$|H_{\rm d}(j\omega)| \leq \frac{1}{\Delta_{\rm G}(j\omega)}, \quad \forall \omega \geq 0 \tag{6.11}$$

Substituting (6.6) into inequality (6.11) yields

$$\left| \frac{1}{(1+j\omega\tau)^2} \right| \leq \frac{1}{\Delta_{\rm G}(j\omega)}, \quad \forall \omega \geq 0 \tag{6.12}$$

or

$$1 + \omega^2\tau^2 \geq \Delta_{\rm G}(j\omega), \quad \forall \omega \geq 0 \tag{6.13}$$

As for the process gain uncertainty $\Delta_{\rm G}(s) = |\Delta k/k|$ or the process phase uncertainty $\Delta_G(s) = |e^{j\Delta\theta} - 1|$, it follows from (6.13) that a gain margin of 2 and a phase margin of $\pi/3$ are guaranteed, since the left half term of (6.13) is always

larger than 1. For uncertainties in the RHP zeros, assume that the RHP zero, z_0, is perturbed to $z = z_0 + \Delta z$, so that G and $\hat{G}$ are given by

$$G = G_0 e^{-L_0 s} \frac{z - s}{z_0 + s},\ \hat{G} = G_0 e^{-L_0 s} \frac{z_0 - s}{z_0 + s}$$

respectively. Then Δ_G is

$$\Delta_G = \left| \frac{\Delta z}{z_0 - s} \right|$$

and is guaranteed to be less than 1 for $0 \leq z \leq 2z_0$. For uncertainties in the time delay, let the time delay L_0 be perturbed to $L_0 + \Delta L$, so that G and $\hat{G}$ are given by

$$G = G_0 e^{-(L_0 + \Delta L)s} \frac{z_0 - s}{z_0 + s},\ \hat{G} = G_0 e^{-L_0 s} \frac{z_0 - s}{z_0 + s}$$

respectively. Then Δ_G is reduced to

$$\begin{aligned} \Delta_G &= \left| e^{-j\omega \Delta_L} - 1 \right| \\ &= 2 \left| \sin\left(\frac{\omega \Delta L}{2} \right) \right| \end{aligned}$$

The robust stability condition (6.13) becomes

$$2 \left| \sin \theta \right| \leq 1 + \lambda \theta^2,\ \theta = \frac{\omega \Delta L}{2},\ \lambda = \left(\frac{2\tau}{\Delta L} \right)^2$$

Plot the left half side and the right half side of the inequality together in Figure 6.4 with respect to θ. The curve of the left half side is fixed while that of right half side changes for different λ. It is computed that the two curves are tangent when $\lambda = 0.70$, consequently the robust stability condition holds if $(2\tau/\Delta L)^2 \geq 0.7$ or equivalently

$$\tau \geq 0.42 |\Delta L| \tag{6.14}$$

In view of the above robust stability analysis, a larger τ will render the system more robust against the uncertainties, and vise versa. Recalling from the preceding section that a larger τ also dictates a greater ISE and a longer settling time, one concludes that the tuning of τ is also to make the trade-off between nominal performance and robust stability. Therefore the whole control design scheme can be summarized as the following procedure.

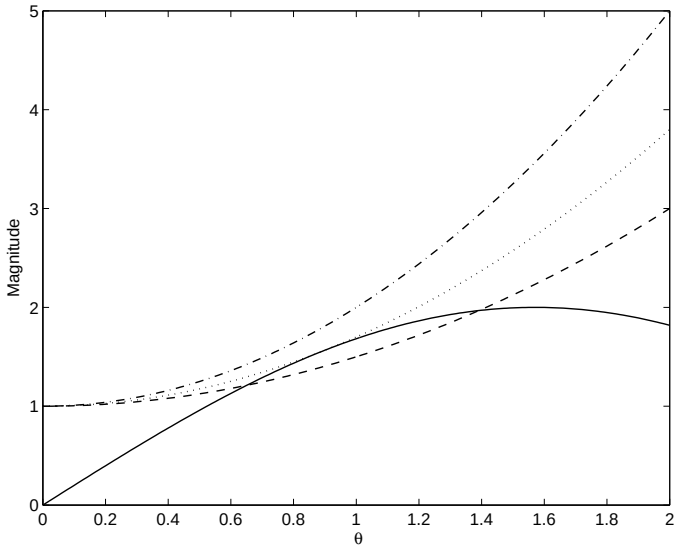

Figure 6.4. Illustration of robust stability condition for uncertain time delay
(—— $2|\sin\theta|$; - - - $1+0.5\theta^2$; $\cdots$ $1+0.7\theta^2$; - · - $1+\theta^2$)

6.3.1 Design procedure

Initial data: the process transfer function G and time domain specifications (undershoot, settling time and ISE) and uncertainty size Δ_{G}.

(i) Rewrite G in the form of (6.1);

(ii) Obtain the second order plus dead time model (6.2) for G_0;

(iii) Tune τ such that the best trade-off between the specifications is made with help of Figure 6.2 and (6.13);

(iv) Form the controller by (6.4).

Regarding step (ii), for any given stable plant G, G_0 can be extracted by (6.1). Then the step response of G_0 can be constructed with the inverse fast Fourier transform (Wang *et al.*, 2004), and is employed with the step identification method in Wang and Zhang (2001) to obtain the reduced order model for G_0. The model reduction algorithm is summarized in the subsequent subsection for ease of reference and use.

6.3.2 Model reduction

Consider a stable and minimum phase process:

$$G(s) = \frac{b_1 s + b_0}{s^2 + a_1 s + a_0} e^{-Ls}$$

(i). Let the input $u(t)$ to G be of step type with size h, then its step response is constructed as

$$y(t) = h[G(0) + \mathcal{F}^{-1}\{\frac{G(j\omega) - G(0)}{j\omega}\}], \tag{6.15}$$

where $\mathcal{F}^{-1}$ may easily be implemented by the inverse fast Fourier transform, see details in Wang *et al.* (2004).

(ii). With the step response $y(t)$, the static gain $K = b_0/a_0$ is computed as $K = y(\infty)/h$. Let

$$\begin{aligned} \Delta y(t) &= y(t) - y(\infty) \\ \gamma(t) &= -\int_0^t \int_0^{\tau_2} \Delta y(\tau_1) d\tau_1 d\tau_2 \\ \phi(t) &= \left[\Delta y(t), \quad \int_0^t \Delta y(\tau_1) d\tau_1, \quad Kh, \quad Kht\right]^T \end{aligned}$$

(iii). Take $t = t_i \geq L$, $i = 1 \cdots N$ to cover the transient time span and arrange the regression form as

$$\Gamma = \Phi\theta$$

with

$$\begin{aligned} \Gamma &= \left[\gamma(t_1) \quad \gamma(t_2) \quad \cdots \quad \gamma(t_N)\right]^T \\ \Phi &= \left[\phi(t_1) \quad \phi(t_2) \quad \cdots \quad \phi(t_N)\right]^T \\ \theta &= \left[\theta_1, \quad \theta_2, \quad \theta_3, \quad \theta_4\right]^T. \end{aligned}$$

(iv). Obtain the ordinary least squares solution:

$$\hat{\theta} = (\Phi^T\Phi)^{-1}\Phi^T\Gamma$$

(v). Find the model parameters:

$$\begin{bmatrix} a_1 \\ a_0 \\ L \\ b_1 \\ b_0 \end{bmatrix} = \begin{bmatrix} \theta_2/\theta_1 \\ 1/\theta_1 \\ \theta_4 - \theta_2 + \sqrt{2(\theta_3 - \theta_1) + (\theta_4 - \theta_2)^2} \\ K\sqrt{2(\theta_3 - \theta_1) + (\theta_4 - \theta_2)^2}/\theta_1 \\ K/\theta_1 \end{bmatrix}$$

6.4 Simulation Examples

In this section, two numerical examples are presented to demonstrate the effectiveness of the proposed scheme.

Example 6.1. Consider a high-order oscillatory process with a single RHP zero:

$$G(s) = \frac{k(1-s)}{(s+2)^4(s^2+s+1)^2}, \quad k = k_0 = 1 \tag{6.16}$$

$G(s)$ is rewritten in form of (6.1) as

$$G = G_0\frac{1-s}{1+s}, \quad G_0 = \frac{1+s}{(s+2)^4(s^2+s+1)^2}$$

The algorithm in the Appendix is applied to G_0 and gives

$$\hat{G}_0(s) = \frac{0.0412}{s^2+0.6983s+0.6601}e^{-1.97s}.$$

The time and frequency responses of both G_0 and the reduced-order model are exhibited in Figures 6.5(a),(b), and the modelling error $\Delta_{\rm G}(j\omega)$ in Figure 6.6. Since at the phase cross-over frequency of G, $\omega_{\rm pc} = 0.588$ rad/s, the corresponding $\Delta_{\rm G}(j\omega)$ is very small from Figure 6.6, this indicates that the model reduction result is reasonably good. Then, by our factorization, $G_{\rm L}$ and $G_{\rm R}$ become

$$G_{\rm L} = \frac{0.0412}{s^2+0.6983s+0.6601} \quad \text{and} \quad G_{\rm R} = \frac{1-s}{1+s}e^{-1.97s} \tag{6.17}$$

Suppose that the design specification are such that the undershoot should be less than 5%, and others be as good as possible. It follows from Figure 6.2(a) that $\tau > 1.5/z = 1.5$ is required, and is chosen as 1.88 here so as to produce the same

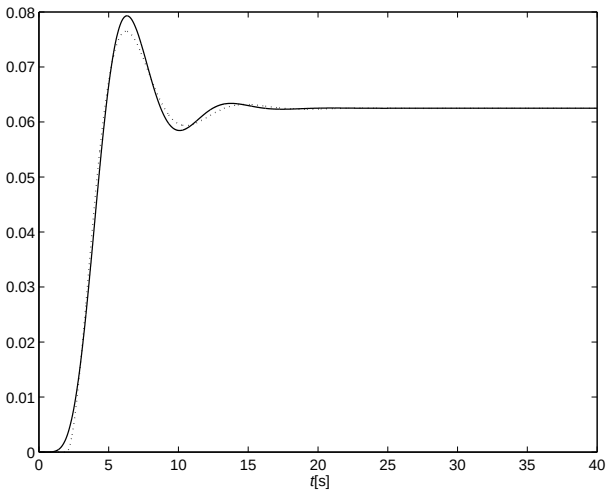

(a) Step responses of G_0 and its model

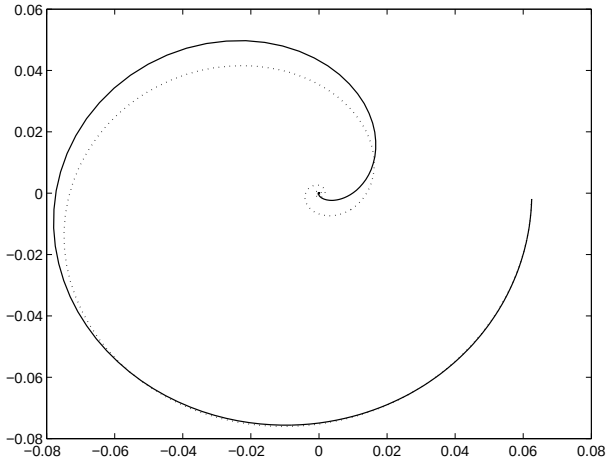

(b) Nyquist curves of G_0 and its model

Figure 6.5. Time and frequency responses of G_0 and its model in Example 1 (—— G_0; $\cdots\cdots$ reduced model of G_0)

undershoot with the single-loop PI control below. The controller is obtained from (6.4) as

$$C(s) = \frac{s^2 + 0.6983s + 0.6601}{0.0412 \times 1.88s(1.88s + 2)} = \frac{12.8998s^2 + 9.0086s + 8.5147}{s(1.88s + 2)} \tag{6.18}$$

With G in (6.16), G_{L} and G_{R} in (6.17) and C in (6.18), the system in Figure 6.1 is simulated, and the step response is depicted in Figure 6.7. The robustness

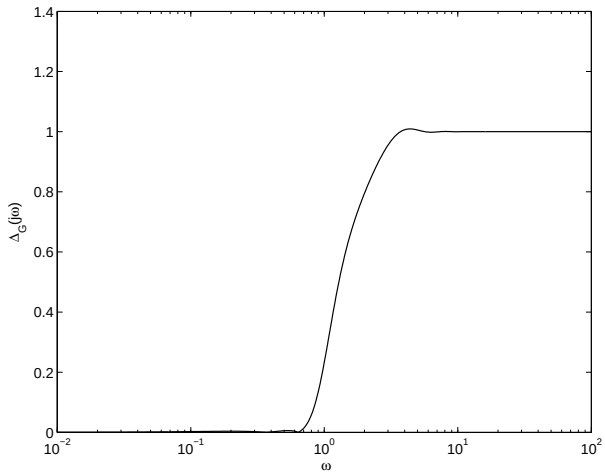

(a) Modelling error $\Delta_G(j\omega)$

Figure 6.6. Modelling error for the process in Example 1

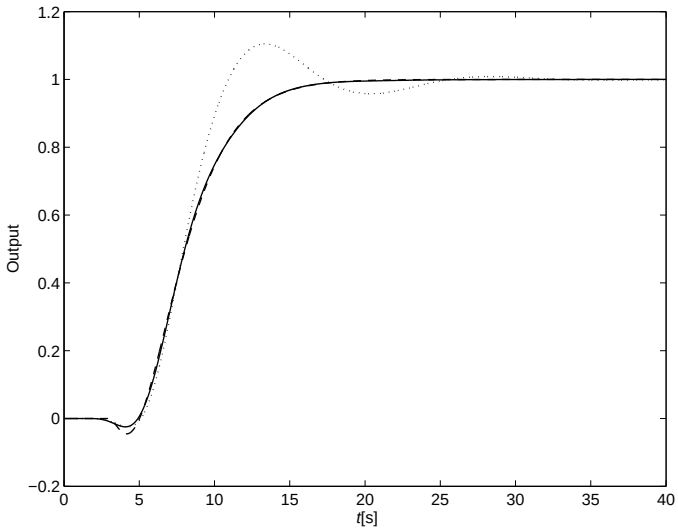

Figure 6.7. Closed-loop step response of Example 1
(—— proposed; $\cdots$ PI; - - - desired)

issue is examined by increasing the static gain as $k = 1.25$, 1.5, 2 in (6.16), and their respective responses are depicted in Figure 6.8(a). In order to make comparison, the exact gain and phase margin method (Fung *et al.*, 1998) is applied. For gain margin of 2 and phase margin of $\pi/3$, the PI controller is obtained as

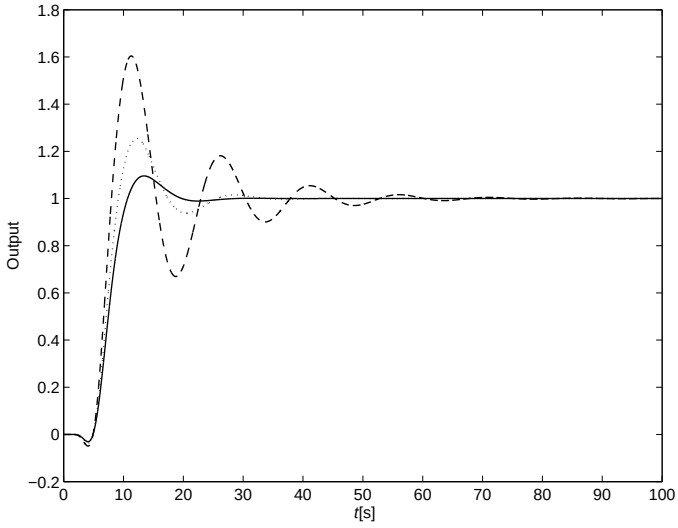

(a) Proposed Smith scheme

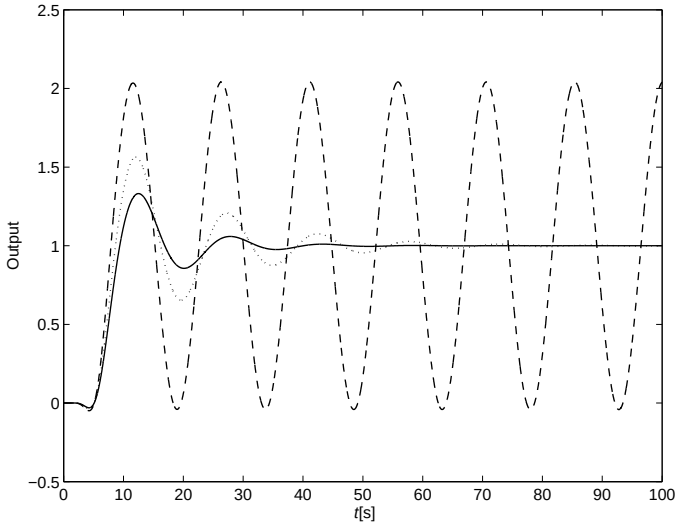

(b) Single-loop PI control

Figure 6.8. System robustness of Example 1
(—— $k = 1.25$; $\cdots\cdots$ $k = 1.5$; - - - $k = 2$)

$K(s) = 4.028 + 2.358/s$, with its step response compared in Figures 6.7 and 6.8(b). Performance enhancement from the proposed scheme is substantial. Compared with PI control, its time response has the same undershoot but no overshoot, much smaller settling time, and greater robustness since it remains stable even

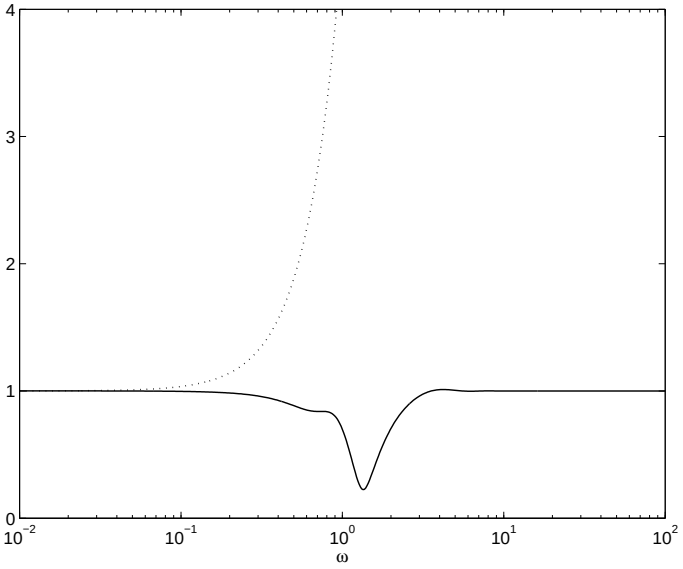

Figure 6.9. Robust stability check against uncertain RHP zero of Example 1 (—— Δ_G for $z = 2z_0$; $\cdots\cdots$ $1 + \omega^2\tau^2$)

when $k = 2$. For uncertainty in RHP zero, the robust stability is ensured for $z = 2z_0$ as is demonstrated by Figure 6.9, where the curve of $1 + \omega^2\tau^2$ is above that of Δ_{G}. The step responses for different uncertain RHP zeros are given in Figure 6.10. In case of uncertain time delay, since $\tau/0.42 = 4.47$, robust stability is ensured against $\Delta L = 4.47$ by (6.14), as is verified by the robust stability check in Figure 6.11. The step responses for $\Delta L = 1, 2, 4.47$ are also provided in Figure 6.12. At last, consider the combined uncertainty of $k = 1.25$, $z = 1.25$ and $\Delta L = 2$, the robust stability condition (6.13) is checked and verified in Figure 6.13, then the step response is given in Figure 6.14 and compared with the PI design. All these results against various uncertainties demonstrate the good robust stability of the proposed design and validates the stability analysis in Section 3.

Example 6.2. Consider another high-order process with two RHP zeros:

$$G(s) = \frac{k(1-2s)(1-3s)}{(s+1)^{10}}, \quad k = k_0 = 1$$

It follows that

$$G = G_0 \frac{(0.5-s)(0.33-s)}{(0.5+s)(0.33+s)}$$

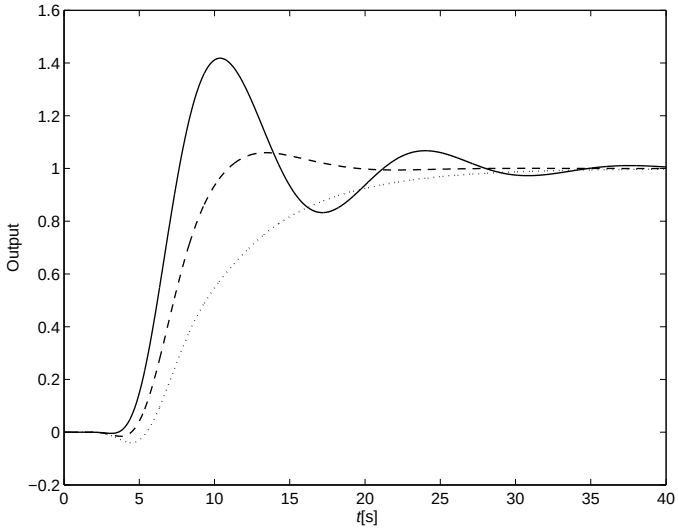

Figure 6.10. Step responses against uncertain RHP zero of Example 1
(—— $z = 2z_0$; $\cdots$ $z = 0.75z_0$; - - - $z = 1.25z_0$)

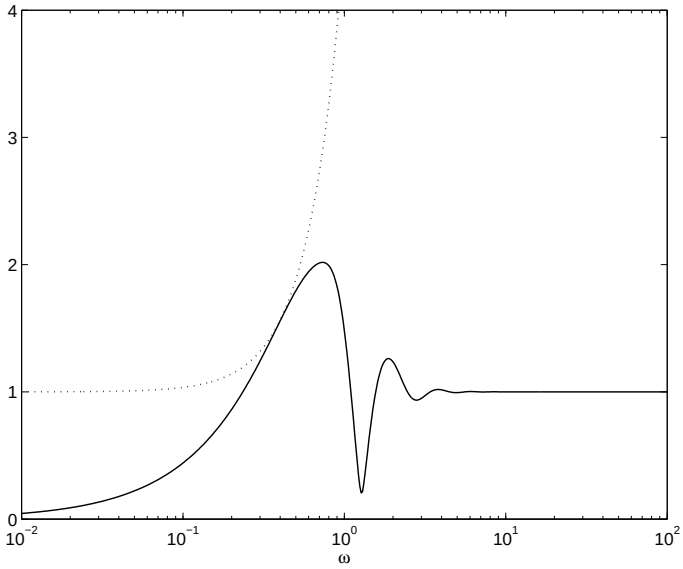

Figure 6.11. Robust stability check against uncertain time delay of Example 1
(—— Δ_G for $\Delta L = 4.47$; $\cdots$ $1 + \omega^2\tau^2$)

with

$$G_0 = \frac{(1+2s)(1+3s)}{(s+1)^{10}}$$

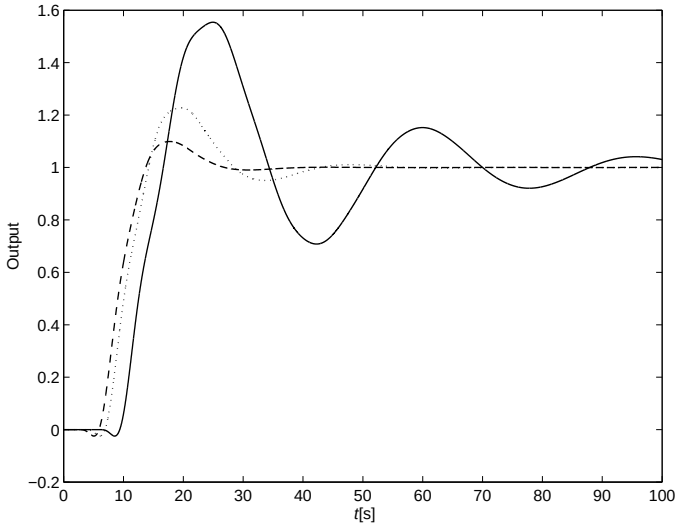

Figure 6.12. Step responses against uncertain time delay of Example 1
(—— $\Delta L = 4.47$; $\cdots$ $\Delta L = 2$; - - - $\Delta L = 1$)

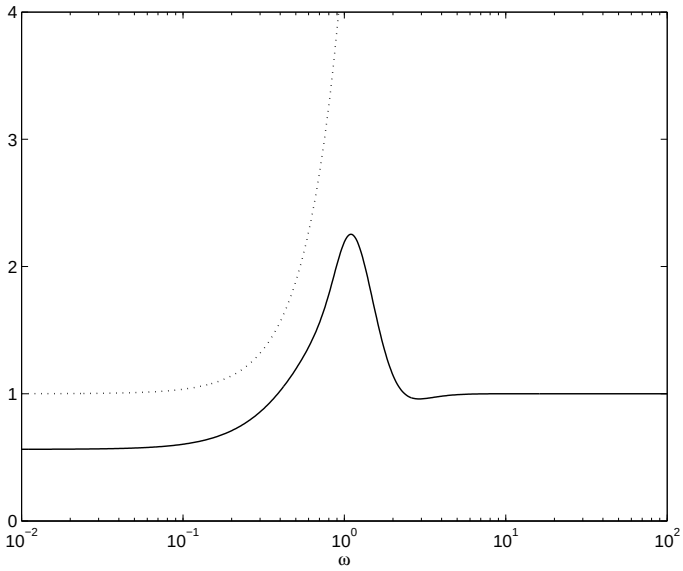

Figure 6.13. Robust stability check against combined uncertainties of Example 1
(—— Δ_G for $k = 1.25$, $z = 1.25z_0$ and $L = 2$; $\cdots$ $1 + \omega^2\tau^2$)

The reduced-order model for G_0 is obtained as

$$\hat{G}_0(s) = \frac{0.3114}{s^2 + 0.6601s + 0.3109} e^{-2.98\text{s}}$$

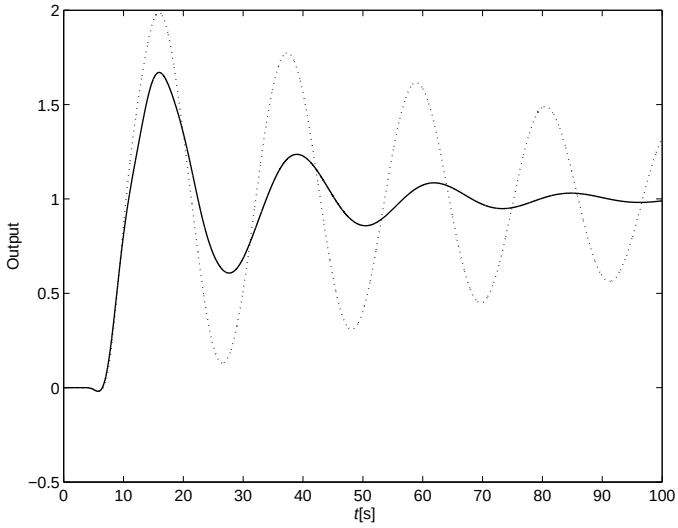

Figure 6.14. Step responses against combined uncertainties of Example 1 (—— proposed; $\cdots$ PI)

so that

$$G_L = \frac{0.3114}{s^2 + 0.6601s + 0.3109} \quad \text{and} \quad G_R = \frac{(0.5 - s)(0.33 - s)}{(0.5 + s)(0.33 + s)} e^{-2.98s}$$

The smallest RHP zero is $z = 0.33$. Suppose that the design specification are such that the undershoot should be less than 15%, and others be as good as possible. It follows from Figure 6.2(a) that $\tau > 0.7/z = 2.1$, and we choose $\tau = 3$, taking care of the effect from another RHP zero. Then the controller is configured from (6.4) as

$$C(s) = \frac{s^2 + 0.6601s + 0.3109}{0.3114 \cdot 3s(3s + 2)} = \frac{1.0704s^2 + 0.7066s + 0.3328}{s(3s + 2)}$$

The nominal step response is given in Figure 6.15 and the responses under a static gain perturbation of $k = 1.25, 1.5, 2$, are depicted in Figure 6.16(a). In comparison, the exact gain and phase margin method, with gain margin of 2 and phase margin of $\pi/3$, yields the controller of $K(s) = 0.349 + 0.055/s$, which leads to the responses in Figures 6.15 and 6.16(b). And the performance improvement of the proposed scheme is obvious.

The performance specifications of the simulation examples are measured and summarized in Table 6.1, from which one sees that the transient performance

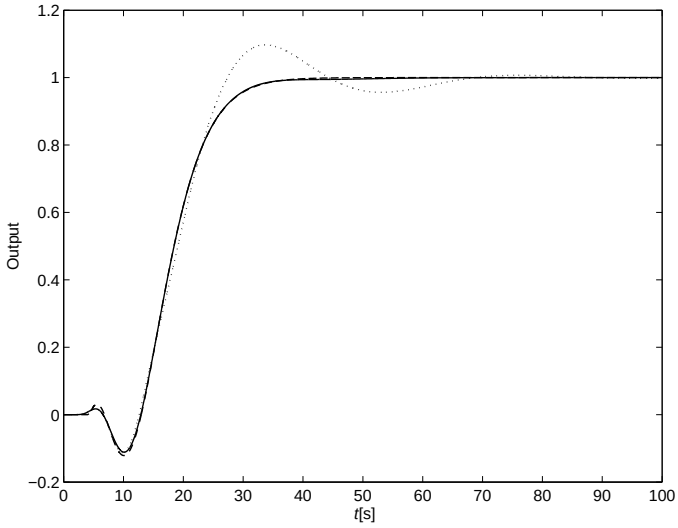

Figure 6.15. Closed-loop step response of Example 2
(—— proposed; · · · · PI; - - - desired)

of the proposed scheme is superior to that of the single-loop PI design. With almost the same undershoot and ISE, the proposed scheme not only gives a smaller settling time without overshoot for nominal performance, but also better robustness to uncertainties. Moreover, from Figures 6.7 and 6.15, the step response of the proposed scheme tracks the desired one closely, and it is hence convenient to design controller based on the desired one.

6.5 Conclusion

In this chapter, a Smith-like control scheme is proposed for control performance enhancement of stable processes with RHP zeros. Compared with the single-loop scheme, it has the following advantages: (i) controller design is simplified to one for a delay-free, second-order minimum phase process; (ii) a single tuning parameter is devised and the resulting trade-off between various nominal and robustness specifications is graphically exhibited and straightforward to make; (iii) performance of the designed system is predictable from the desired closed-loop transfer function and can be enhanced over popular PI control.

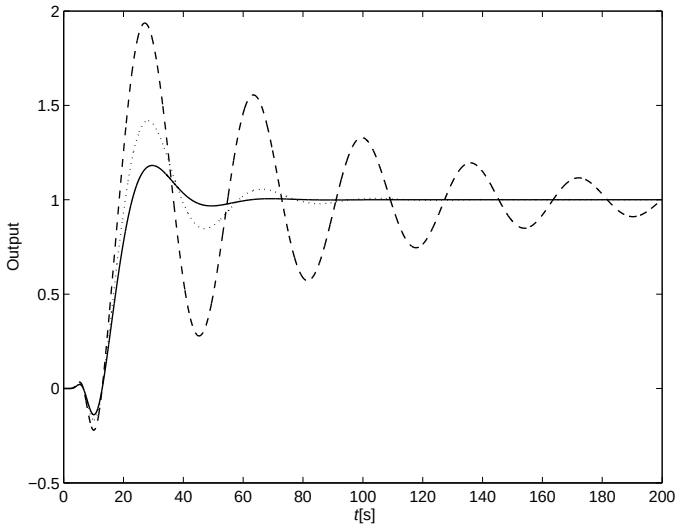

(a) Proposed Smith scheme

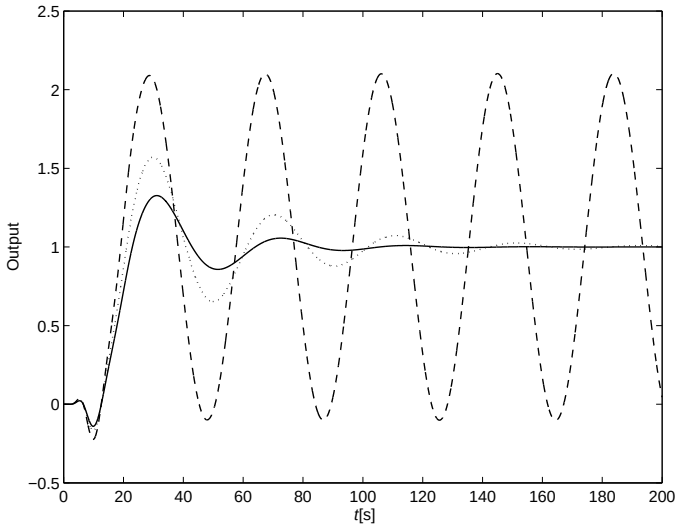

(b) Single-loop PI control

Figure 6.16. System robustness of Example 2
(—— $k = 1.25$; $\cdots\cdots$ $k = 1.5$; - - - $k = 2$)

Table 6.1. Performance Specification Comparison for Systems with RHP Zero(s)

	Scheme	US(%)	OS(%)	TS	ISE
Example 1:	Proposed	2.46%	0%	14.98	7.29
$k = 1$	PI	2.46%	10.52%	22.43	7.26
	Proposed	3.08%	9.59%	17.16	6.88
$k = 1.25$	PI	3.07%	33.25%	36.12	7.41
	Proposed	3.70%	25.4%	23.15	6.86
$k = 1.5$	PI	3.70%	56.5%	58.62	8.63
	Proposed	4.93%	60.44%	49.66	8.25
$k = 2$	PI	NA	NA	NA	NA
$k = 1.25$, $\Delta L = 2$	Proposed	1.95%	60.71%	87.03	12.08
and $z = 1.25z_0$	PI	1.87%	98.75%	371.95	33.34
Example 2:	Proposed	11.14%	0%	31.79	17.66
$k = 1$	PI	11.26%	9.72%	61.11	17.84
	Proposed	13.89%	18.19%	54.39	20.61
$k = 1.25$	PI	14.06%	32.65%	95.63	25.41
	Proposed	16.64%	41.93%	85.23	25.06
$k = 1.5$	PI	16.84%	57.09%	154.69	35.43
	Proposed	22.10%	93.62%	283.42	63.51
$k = 2$	PI	NA	NA	NA	NA

US: undershoot; OS: overshoot; TS: Settling time

Chapter 7

Deadbeat Tracking Control with Hard Input Constraints

7.1 Introduction

One of the fundamental problems associated with the discrete-time systems is deadbeat control, i.e., drive some signal to zero in finite time and keep it zero for all discrete times thereafter. The problem of deadbeat control received attention since 1950s, and has been extensively studied in the 1980s (Kimura and Tanaka, 1981; Emami-Naeini and Franklin, 1982; Schlegel, 1982). However, the minimum time deadbeat control usually suffers from the problem of large control magnitude, which prevents the practical implementation. On the other hand, due to technological and safety reasons, the actuators cannot inject an unlimited energy into the plant, which imposes bounds on controlled inputs. Consequently, investigating hard input constraints for deadbeat control is of practical importance. To the author's knowledge, there are few works concerning this issue. In Henrion *et al.* (2001), a polynomial approach (Kučera, 1979) is employed to solve the problem of maximizing the initial stability region with stabilizing controller under hard input constraints. The paper assumes that the input sequence is a finite one when dealing with the hard constraints. This assumption enables easier formulation of input constraints, since only finite enumerable inequalities are involved. However,

such circumstance is rare, since the control input sequence is infinite for general deadbeat control problems.

In this chapter, the constrained deadbeat tracking problem is investigated by employing the polynomial approach. Firstly, the general solution for deadbeat control with bounded inputs is derived as a function of a free polynomial. After that, by taking the hard input constraints into consideration, the candidate deadbeat controllers are formulated as feasible solutions subjecting to a infinite series of linear inequalities. Through extensive analysis of these infinite inequalities, it is proven that the hard input constraints can be ensured approximately with arbitrary accuracy by choosing a suitable finite subset of the inequalities. Then the problem is reduced to finding a feasible solution subjecting to finite linear inequality constraints, and could be solved with ease. Furthermore, the controller parameters can be optimized for some time domain performance benchmarks, say for example, the integral of squared error.

The rest of this chapter is organized as follows. Section 7.2 prepares some basic algebraic backgrounds for the discussion. In Section 7.3, the general solution for deadbeat controllers with bounded inputs is derived, with an example given to illustrate the time-optimal deadbeat solution. Then in Section 7.4, deadbeat controller design subjecting to hard input constraints is addressed. The reduction to finite linear inequality constraints is presented in detail, and the controller design procedure is summarized, with a numerical example provided to indicate the design procedure. Finally, Section 7.5 concludes this chapter.

7.2 Preliminaries

Let us recall several algebraic notions (Kučera, 1979). Denote, respectively, by $\mathcal{R}$ the field of real numbers, by $\mathcal{R}[z^{-1}]$ the ring of polynomials in the indeterminate z^{-1} with the coefficients in $\mathcal{R}$, such as

$$a(z^{-1}) = a_0 + a_1 z^{-1} + a_2 z^{-2} \cdots + a_n z^{-n}.$$

The degree of $a(z^{-1})$, represented by ∂a, denotes the highest power of z^{-1} in a with a non-zero coefficient. Notation (a, b) represents the greatest monic common divisor of polynomials $a(z^{-1})$ and $b(z^{-1})$. One can always write $a = a_b(a, b)$ and $b = b_a(a, b)$ with a coprime pair of polynomials a_b and b_a. A polynomial $a(z^{-1})$ is called stable if all its roots, λ_i such that $a(\lambda_i) = 0$, satisfy $|\lambda_i| > 1$. A polynomial can be factorized into $a(z^{-1}) = a^-(z^{-1})a^+(z^{-1})$, where $a^-(z^{-1})$ is stable with the highest possible degree. In addition, a polynomial $a(z^{-1})$ is called marginally stable if all its roots satisfy $|\lambda_i| \geq 1$ and those roots with $|\lambda_i| = 1$ are distinct. A polynomial can also be factorized into $a(z^{-1}) = a^{\ominus}(z^{-1})a^{\oplus}(z^{-1})$, where $a^{\ominus}$ is marginally stable with the highest possible degree.

The equation:

$$a(z^{-1})\alpha(z^{-1}) + b(z^{-1})\beta(z^{-1}) = c(z^{-1}) \tag{7.1}$$

with given polynomials $a(z^{-1})$, $b(z^{-1})$ and $c(z^{-1})$, and unknown polynomials $\alpha(z^{-1})$ and $\beta(z^{-1})$, is called a linear Diophantine equation in polynomials. It is solvable if and only if (a, b) divides c. If α^* and β^* form a particular solution of (7.1), then the general solution is expressed as

$$\begin{aligned} \alpha &= \alpha^* + b_a\theta, \\ \beta &= \beta^* - a_b\theta, \end{aligned} \tag{7.2}$$

where θ is an arbitrary polynomial. The minimum degree solution of (7.1) with respect to β can be derived as follows. Suppose that α_0 and β_0 are a particular solution. If $\partial\beta_0 < \partial(a_b)$, then $\alpha^* = \alpha_0$ and $\beta^* = \beta_0$ are already the minimum degree one; Otherwise, by reducing β_0 modulo a_b, β_0 can be written as

$$\beta_0 = \beta^* + \gamma a_b, \quad \text{with} \quad \partial\beta^* < \partial a_b,$$

so that the minimum degree solution is obtained as $\alpha^* = \alpha_0 + \gamma b_a$ and β^*.

Consider now the field of real rational functions, which is expressed as the ratio of two polynomials: $G(z^{-1}) = b(z^{-1})/a(z^{-1})$. $G(z^{-1})$ is causal if $G(0) < \infty$. Let $\mathcal{R}_c[z^{-1}]$ be the ring of causal real rational functions. A causal $G(z^{-1})$ can be expanded by long polynomial division as an infinite series:

$$G(z^{-1}) = \frac{b(z^{-1})}{a(z^{-1})} = g_0 + g_1 z^{-1} + g_2 z^{-2} + \cdots .$$

It is stable (marginally stable respectively) if $a(z^{-1})$ is a stable (marginally stable respectively) polynomial. Obviously, the sequence, $g_i, i = 1, 2, \cdots$, from a causal G, is convergent to zero (respectively bounded) if G is stable (respectively marginal stable). In case of no confusion, G is called convergent or bounded accordingly. Note that a polynomial $a(z^{-1})$ is a special case of causal rational functions. It has a finite terms in its expansion series, and thus always stable in the sense of stability of causal rational functions.

7.3 Bounded Input Constraints Case

In this section, we will solve the deadbeat tracking control for deterministic discrete-time linear SISO systems with internal stability, which leads to bounded inputs. The problem is formally stated as follows.

Problem 7.1. Consider the single-variable feedback system in Figure 7.1. Suppose that the plant G and reference input R are given causal rational functions with coprime fractions: $G = b(z^{-1})/a(z^{-1})$, and $R = h(z^{-1})/p(z^{-1})$. Find a deadbeat controller C such that the closed-loop system is internally stable, and the error E vanishes in a finite time.

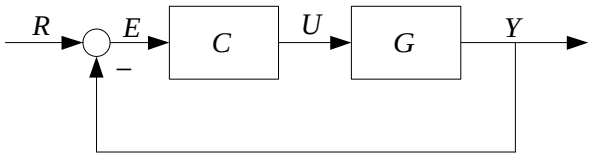

Figure 7.1. Single loop feedback system

We are now in a position to state the main result of this section as follows.

Theorem 7.1. *Problem 7.1 is solvable if and only if p_a, the coprime factor of polynomial p with respect to a, is marginally stable, which is equivalent to the solvability of the linear Diophantine equation*

$$(b, h^+)(b_h p_a)^{\oplus}\alpha + p a_p^+ \beta = h^-. \tag{7.3}$$

If the polynomials, α and β, solve the above equation, it follows that

$$\begin{aligned} E &= h^+ a_p^+ \beta, \\ U &= \frac{h^+ a_p}{(b, h^-)(b_h p_a)^\ominus}\alpha, \\ C &= U/E. \end{aligned} \tag{7.4}$$

Proof: The system in Figure 7.1 is internally stable if and only if the transfer matrix

$$\begin{bmatrix} \dfrac{1}{1+CG} & \dfrac{C}{1+CG} \\ \dfrac{G}{1+CG} & \dfrac{1}{1+GC} \end{bmatrix} \tag{7.5}$$

is stable (Zhou and Doyle, 1998). Notice that

$$\frac{1}{1+CG} = \frac{E}{R} = \frac{pE}{h}. \tag{7.6}$$

Since E is a polynomial due to the deadbeat requirement and p/h is coprime, h^+ must divide E for stability of $1/(1+CG)$. Similarly, one sees that

$$\frac{G}{1+CG} = \frac{E}{R}G = E\frac{p}{h}\frac{b}{a} = E\frac{p_a b_h}{h_b a_p} \tag{7.7}$$

and $h_b^+ a_p^+$ must divide E for stability of $G/1+CG$. Equations (7.6) and (7.7) imply that

$$E = h^+ a_p^+ E_1 \tag{7.8}$$

for some polynomial E_1. Besides, one writes

$$\frac{C}{1+CG} = \frac{U}{R} = \frac{U}{R} = \frac{Up}{h}.$$

Then, U should contain h^+ in its numerator for stability of $C/(1+CG)$, or

$$U \;=\; h^+ U_1, \tag{7.9}$$

for some bounded U_1 whose denominator is coprime with h^+. It follows from Figure 7.1 that $E = R - GU$. Substituting (7.8) and (7.9) into the above equation yields

$$\begin{aligned} U_1 &= \frac{a_p(h^- - p a_p^+ E_1)}{b p_a} \\ &= \frac{a_p(h^- - p a_p^+ E_1)}{b_h (b, h^-)(b, h^+) p_a} \\ &= \frac{a_p}{(b, h^-)(b_h p_a)^\ominus}\frac{h^- - p a_p^+ E_1}{(b, h^+)(b_h p_a)^\oplus}. \end{aligned} \tag{7.10}$$

In order for U_1 to be bounded, $(b, h^+)(b_q p_a)^{\oplus}$ should divide $(h^- - pa_p^+ E_1)$, which leads to the linear Diophantine equation (7.3) with U and E given as (7.4).

It is noticed that

$$\begin{aligned}((b, h^+)(b_h p_a)^{\oplus}, pa_p^+) &= ((b, h^+)(b_h p_a)^{\oplus}, p) \\ &= ((b_h p_a)^{\oplus}, p) \\ &= p_a^{\oplus},\end{aligned}$$

which is always coprime with h^-. Hence (7.3) is solvable if and only if $p_a^{\oplus} = 1$, in other words, p_a is marginal stable. Then the proof is completed.

It follows from the preceding section that if (7.3) is solvable and the minimum degree solution with respect to β is solved as α^* and β^*, then the general solution for (7.3) is expressed as

$$\alpha = \alpha^* + pa_p^+ \theta, \quad \beta = \beta^* - (b, h^+)(b_h p_a)^{\oplus} \theta, \tag{7.11}$$

where α^* and β^* form a particular solution, and θ is an arbitrary polynomial. This leads to the general solution for Problem 7.1 as follows:

$$E = E^* - h^+ a_p^+ (b, h^+)(b_h p_a)^{\oplus} \theta, \quad U = U^* + \frac{h^+ a_p p a_p^+}{(b, h^-)(b_h p_a)^{\ominus}} \theta, \tag{7.12}$$

respectively. Then the settling time is

$$t_s = \partial E + 1.$$

Obviously, the time optimal solution results if

$$E^* = h^+ a_p^+ \beta^*, \quad U^* = \frac{h^+ a_p}{(b, h^-)(b_h p_a)^{\ominus}} \alpha^*. \tag{7.13}$$

The following example is given to illustrate the results.

Example 1 Consider the plant

$$G = \frac{2 + z^{-1} - z^{-2}}{19 - 2z^{-1} - 16z^{-2}},$$

with the reference input

$$R = \frac{2 - z^{-1}}{1 - z^{-1}}.$$

It follows that $a = 19 - 2z^{-1} - 16z^{-2}$, $b = 2 + z^{-1} - z^{-2}$, $p = 1 - z^{-1}$ and $h = 2 - z^{-1}$. Since $p_a^{\oplus} = 1$, the problem is solvable. The resultant linear Diophantine equation is

$$\alpha + (1 - z^{-1})\beta = 2 - z^{-1}.$$

One easily checks that the minimum degree solution with respect to β is $\alpha^* = 1$ and $\beta^* = 1$. Consequently, the time optimal control is obtained as

$$\begin{aligned} E^* &= 1, \\ U^* &= \frac{19 - 2z^{-1} - 16z^{-2}}{2 - z^{-1} - 2z^{-2} + z^{-3}}, \\ C^* &= \frac{U^*}{E^*} = U^*. \end{aligned}$$

The simulation result for this example is displayed in Figure 7.2. One notices that E vanishes only after one step. However, the magnitude of the controlled input is rather big.

7.4 Hard Input Constraints Case

In this section, the deadbeat tracking problem with hard input constraints is considered, and the problem is stated as follows.

Problem 7.2. Consider the single variable feedback system (Figure 7.1). Given the plant $G = b(z^{-1})/a(z^{-1})$ and the reference input $R = h(z^{-1})/p(z^{-1})$, with $a, b, p, h \in \mathcal{R}[z^{-1}]$. Find a controller $C \in \mathcal{R}_c[z^{-1}]$ such that the system is internally stable, the tracking error $E = R - Y$ vanishes in a finite time. Moreover, the input sequence U,

$$U(z^{-1}) = u_0 + u_1 z^{-1} + u_2 z^{-2} \cdots,$$

satisfies the hard constraints,

$$\underline{u} \le u_i \le \overline{u}, \ i = 0, 1, \cdots \tag{7.14}$$

for all nonnegative integers i, where $\underline{u}$ and $\overline{u} \in \mathcal{R}$ are given scalars. Without loss of generality, $\underline{u} = -\overline{u}$ is assumed, since otherwise, we can always define $U' = U - (\underline{u} + \overline{u})/(2 - 2d)$, $\underline{u}' = \underline{u} - (\underline{u} + \overline{u})/2$ and $\overline{u}' = \overline{u} - (\underline{u} + \overline{u})/2$ so that $\underline{u}' = -\overline{u}'$.

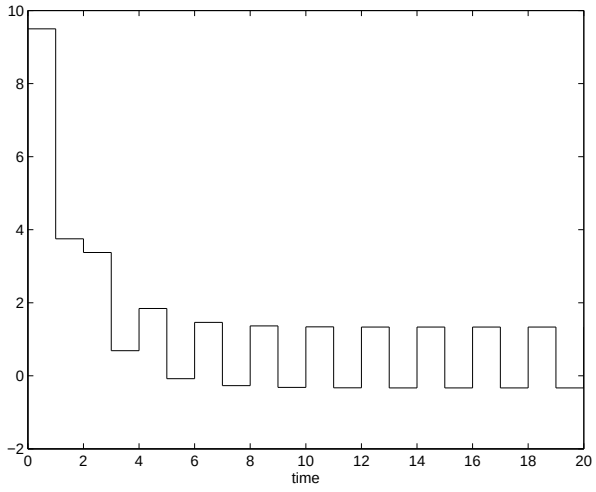

(a) *Input* U^*

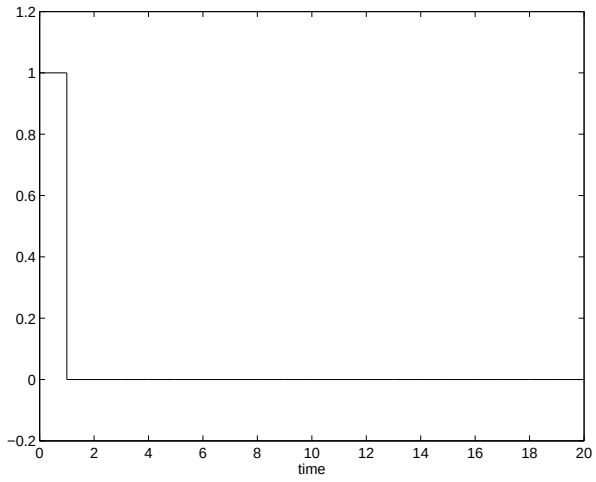

(b) *Error* E^*

Figure 7.2. Minimum-time deadbeat control for Example 1

The constraints in (7.14) is referred to as original hard input constraints. Obviously, U must be a bounded sequence in order to be within hard constraints. It follows from the preceding section that, under the solvability condition of $p_a^{\oplus} = 1$, the general solutions (7.12) for deadbeat controller design with bounded inputs can be written as

$$U = \delta + \lambda\theta, \tag{7.15}$$

$$E = f + l\theta, \tag{7.16}$$

with known polynomials f and l of

$$f = h^+ a_p^+ \beta^*, \quad l = h^+ a_p^+ (b, h^+)(b_h p_a)^{\oplus},$$

marginally stable causal rational functions δ and λ of

$$\delta = \frac{h^+ a_p}{(b, h^-)(b_h p_a)^{\ominus}} \alpha^*, \quad \lambda = \frac{h^+ a_p p a_p^+}{(b, h^-)(b_h p_a)^{\ominus}}, \tag{7.17}$$

and a free polynomial θ. We seek a polynomial θ to meet $\underline{u} \le u_i \le \overline{u}$. Let

$$\delta = \sum_{i=0}^{+\infty} \delta_i z^{-i}, \tag{7.18}$$

$$\lambda = \sum_{i=0}^{+\infty} \lambda_i z^{-i}, \tag{7.19}$$

where the expression for δ_i and λ_i can be easily calculated from the residues of (7.17), and similarly let

$$\theta = \sum_{i=0}^{\partial\theta} \theta_i z^{-i}.$$

One readily verifies that

$$\begin{aligned} u_i &= \delta_i + \textstyle\sum_{j=0}^{i} \lambda_{i-j}\theta_j, \quad \text{for} \quad i < \partial\theta, \\ u_i &= \delta_i + \textstyle\sum_{j=0}^{\partial\theta} \lambda_{i-j}\theta_j, \quad \text{for} \quad i \ge \partial\theta. \end{aligned} \tag{7.20}$$

Then (7.15) is arranged into the matrix form as

$$\mathbf{u} = \mathbf{\Delta} + \mathbf{\Lambda\Theta}, \tag{7.21}$$

where

$$\mathbf{u} = \begin{bmatrix} u_0 \\ u_1 \\ \vdots \\ \vdots \\ \vdots \\ u_k \\ \vdots \end{bmatrix}, \boldsymbol{\Delta} = \begin{bmatrix} \delta_0 \\ \delta_1 \\ \vdots \\ \vdots \\ \vdots \\ \delta_k \\ \vdots \end{bmatrix}, \boldsymbol{\Theta} = \begin{bmatrix} \theta_0 \\ \theta_1 \\ \vdots \\ \theta_{\partial\theta} \end{bmatrix}, \text{ and}$$

$$\boldsymbol{\Lambda} = \begin{bmatrix} \lambda_0 & 0 & \dots & 0 \\ \lambda_1 & \lambda_0 & \dots & 0 \\ \vdots & \vdots & \ddots & \vdots \\ \lambda_{\partial\theta} & \lambda_{(\partial\theta-1)} & \ddots & \lambda_0 \\ \vdots & \vdots & \ddots & \vdots \\ \lambda_k & \lambda_{(k-1)} & \cdots & \lambda_{(k-\partial\theta+1)} \\ \vdots & \vdots & \vdots & \vdots \end{bmatrix}. \tag{7.22}$$

Also define

$$\bar{\mathbf{u}} = \begin{bmatrix} \bar{u} & \bar{u} & \bar{u} & \cdots \end{bmatrix}^T,$$

and then (7.14) becomes

$$|\boldsymbol{\Delta} + \boldsymbol{\Lambda}\boldsymbol{\Theta}| \leq \bar{\mathbf{u}}. \tag{7.23}$$

Noting the constraint (7.23) is composed of infinite number of linear inequalities. Deriving its feasible solution falls into the category of semi-infinite programming with enumerable index sets. However, this problem does not satisfy the usual assumption of compactness for typical semi-infinite optimization, and there is no convenient algorithm to solve it directly. In order to overcome the difficulty of manipulating infinite inequalities, it is desirable to develop a simple procedure for Problem 7.2 where only finite inequality constraints are involved. At the same time, the corresponding solution should still match the hard constraints with good accuracy.

Consider the sequences $\{\delta_i\}$ and $\{\lambda_i\}$ in (7.18) and (7.19), which are derived from the marginally stable causal rational functions δ and λ (7.17). It is noted that by splitting the decaying components (which converge to 0 as index i increases to ∞) with the periodical components therein, $\{\delta_i\}$ and $\{\lambda_i\}$ are arranged as the summation of power series as

$$\begin{aligned}\delta_i &= \sum_{j=1}^{m} w_j {\gamma_j}^i + \sum_{j=m+1}^{n} w_j {\gamma_j}^i, \\ \lambda_i &= \sum_{j=1}^{m} v_j {\gamma_j}^i + \sum_{j=m+1}^{n} v_j {\gamma_j}^i,\end{aligned} \tag{7.24}$$

where $|\gamma_j| = 1$ for $1 \le j \le m$ and $|\gamma_j| < 1$ for $m+1 \le j \le n$. Let

$$\begin{aligned}\delta_i &= \delta_{p,i} + \delta_{d,i}, \quad \delta_{p,i} = \sum_{j=1}^{m} w_j {\gamma_j}^i, \quad \delta_{d,i} = \sum_{j=m+1}^{n} w_j {\gamma_j}^i, \\ \lambda_i &= \lambda_{p,i} + \lambda_{d,i}, \quad \lambda_{p,i} = \sum_{j=1}^{m} v_j {\gamma_j}^i, \quad \lambda_{d,i} = \sum_{j=m+1}^{n} v_j {\gamma_j}^i.\end{aligned} \tag{7.25}$$

Then $\{\delta_i\}$ is decomposed into the summation of a periodical sequence $\{\delta_{p,i}\}$ and a decaying sequence $\{\delta_{d,i}\}$, and it is the same case for $\{\lambda_i\}$. Denote by δ_p, δ_d, λ_p and λ_d the corresponding rational functions for the sequences $\{\delta_{p,i}\}$, $\{\delta_{d,i}\}$, $\{\lambda_{p,i}\}$ and $\{\lambda_{d,i}\}$, it follows that U could also be decomposed into periodical components and decaying components as

$$\begin{aligned}U &= U_p + U_d, \\ U_p &= \delta_p + \lambda_p \theta, \\ U_d &= \delta_d + \lambda_d \theta,\end{aligned}$$

with the corresponding matrix form being

$$\begin{aligned}\mathbf{u} &= \mathbf{u}_p + \mathbf{u}_d, \\ \mathbf{u}_p &= \boldsymbol{\Delta}_p + \boldsymbol{\Lambda}_p \boldsymbol{\Theta}, \\ \mathbf{u}_d &= \boldsymbol{\Delta}_d + \boldsymbol{\Lambda}_d \boldsymbol{\Theta},\end{aligned}$$

where $\boldsymbol{\Delta}_p$, $\boldsymbol{\Delta}_d$, $\boldsymbol{\Lambda}_p$ and $\boldsymbol{\Lambda}_d$ are defined in a similar fashion as in (7.22). Since $\boldsymbol{\Theta}$ represents the coefficients of a finite real polynomial, the resultant $\mathbf{u}_p$ is a periodical sequence, and $\mathbf{u}_d$ is a decaying sequence which converges to 0 as its index

approaches infinity. Thus $\mathbf{u}$ converges to $\mathbf{u}_p$ as the index approaches infinity. If we can make sure that $|u_{d,i}|$ is smaller than $\forall \varepsilon > 0$ for $i \geq k$, then $|u_i| \leq |u_{p,i}| + \varepsilon$ always holds for $i \geq k$. This motivates us to modify the hard input constraints requirement with some relaxation as:

A. $|u_i| \leq \bar{u}$ for $i = 0, 1 \ldots k-1$, where k is an integer such that $|u_{d,i}| \leq \varepsilon$ for $i \geq k$,

B. $|u_{p,i}| \leq \bar{u}$ for $\forall i$.

Constraints A and B combine to ensure that $|u_i| \leq \bar{u}$ for $0 \leq i \leq k-1$ and $|u_i| \leq \bar{u} + \varepsilon$ for $i \geq k$. When ε decreases, the constraints are exactly equivalent to the original hard constraint (7.14). Due to the periodicity, only finite linear inequalities are involved for Constraint B. As for Constraint A, given arbitrary small $\varepsilon > 0$, there always exist an integer k such that $|u_{d,i}| \leq \varepsilon$ for $i \geq k$ (as may be expected, a smaller ε leads to a larger k), as will be demonstrated later. Consequently only k linear inequalities are to be examined for Constraint A. Therefore, the pros and cons for this modification are, reduction in the number of inequality constraints and relaxation of hard constraints to $|u_{p,i}| \leq \bar{u} + \varepsilon$ for $i \geq k$, respectively. In addition, Constraint B can also be revised as ' $|u_{p,i}| \leq \bar{u} - \varepsilon$ for $\forall i$'. In this case, it is ensured that $|u_i| \leq \bar{u}$ for $i \geq 0$ at the cost of conservativeness in the feasible solution set, since the original hard constraints only lead to $|u_{p,i}| \leq \bar{u}$. In fact, the difference of the two different Constraint B's is not significant in most cases. In case that the hard constraints is stringent and no violation is allowed, choosing $|u_{p,i}| \leq \bar{u} - \varepsilon$ is necessary. In the following contents, Constraint B of $|u_{p,i}| \leq \bar{u}$ is always employed for analysis and simulation.

Now turn back to Constraint A. In view of (7.25), it is seen that

$$\delta_{d,i} \leq \sum_{j=m+1}^{n} |w_j||\gamma_{max}|^i \triangleq w_{sum}|\gamma_{max}|^i,$$

$$\lambda_{d,i} \leq \sum_{j=m+1}^{n} |v_j||\gamma_{max}|^i \triangleq v_{sum}|\gamma_{max}|^i,$$

where $\gamma_{max} = max(\gamma_j)$ for $j = m+1, \cdots, n$, $w_{sum} = \sum_{j=m+1}^{n} |w_j|$, and $v_{sum} =$

$\sum_{j=m+1}^{n} |v_j|$. It follows from (7.20) that for $i \geq \partial\theta$,

$$|u_{d,i}| = \left| \delta_{d,i} + \sum_{j=0}^{\partial\theta} \lambda_{d,i-j}\theta_j \right| \leq w_{sum}|\gamma_{max}|^i + v_{sum}|\gamma_{max}|^i \sum_{j=0}^{\partial\theta} |\theta_i|. \tag{7.26}$$

Since any feasible θ of (7.23) also satisfies a finite subset of the constraints. Hence an estimate for the upper bound of $\sum_{j=0}^{\partial\theta} |\theta_i|$ is obtainable through the following linear programming optimization.

Optimization 1. Calculate the maximum of $\sum_{j=0}^{\partial\theta} |\theta_i|$:

Objective: maximize $\sum_{j=0}^{\partial\theta} |\theta_i|$ for given degree $\partial\theta$.

Constraints: $|u_i| \leq \bar{u}$ for $0 \leq i \leq n$.

The maximum value could be made more accurate by increasing the numbers of inequality constraints. Denote by θ_{sum} the maximum value, it follows from (7.26) that

$$|u_{d,k}| \leq (w_{sum} + v_{sum}\theta_{sum}) |\gamma_{max}|^k,$$

and an integer k given by

$$k = \frac{\ln \varepsilon - \ln(w_{sum} + \theta_{sum} v_{sum})}{\ln \gamma_{max}} \tag{7.27}$$

suffices to ensure $|u_{d,i}| \leq \varepsilon$ for $i \geq k$. Then Condition A is arranged as the matrix form linear inequalities

$$\begin{bmatrix} \mathbf{\Lambda}_k \\ -\mathbf{\Lambda}_k \end{bmatrix} \mathbf{\Theta} \leq \overline{u} I_{2k\times 1} + \begin{bmatrix} -\mathbf{\Delta}_k \\ \mathbf{\Delta}_k \end{bmatrix}, \tag{7.28}$$

where $I_{2k\times 1}$ is a length $2k$ column vector with all the elements equal to 1, $\mathbf{\Lambda}_k$ and $\mathbf{\Delta}_k$ are truncations of the first k rows from $\mathbf{\Lambda}$ and $\mathbf{\Delta}$, respectively.

For condition B, assume for simplicity that the period of U_p is an integer T, then it suffices to check $|u_{p,i}| \leq \overline{u} - \varepsilon$ for finite terms $i \leq T + \partial\theta$, which is readily arranged as

$$\begin{bmatrix} \mathbf{\Lambda}_{p,(T+\partial\theta)} \\ -\mathbf{\Lambda}_{p,(T+\partial\theta)} \end{bmatrix} \mathbf{\Theta} \leq (\overline{u} - \varepsilon) I_{2(T+\partial\theta)\times 1} + \begin{bmatrix} -\mathbf{\Delta}_{p,(T+\partial\theta)} \\ \mathbf{\Delta}_{p,(T+\partial\theta)} \end{bmatrix}, \tag{7.29}$$

where $\mathbf{\Lambda}_{p,(T+\partial\theta)}$ and $\mathbf{\Delta}_{p,(T+\partial\theta)}$ are truncations of the first $(T + \partial\theta)$ rows from $\mathbf{\Lambda}_p$ and $\mathbf{\Delta}_p$, respectively. Then the finite linear inequalities from Conditions A (7.28)

and B (7.29) constitute the hard input constraints, and any feasible $\mathbf{\Theta}$ leads to a solution for the deadbeat controller. In order to calculate a unique $\mathbf{\Theta}$ instead of just one of the feasible solutions, some time-domain performance benchmarks could be chosen as the objective for optimization. For example, the error signal E (7.15) is a polynomial determined by $\mathbf{\Theta}$, and it can be arranged into the matrix form as

$$\mathbf{e} = \mathbf{F} + \mathbf{L}\mathbf{\Theta},$$

where

$$\mathbf{e} = \begin{bmatrix} e_0 \\ e_1 \\ \vdots \\ \vdots \\ \vdots \\ \vdots \\ e_{\partial E} \end{bmatrix}, \mathbf{F} = \begin{bmatrix} f_0 \\ f_1 \\ \vdots \\ f_{\partial f} \\ 0 \\ \vdots \\ 0 \end{bmatrix}, \mathbf{L} = \begin{bmatrix} l_0 & 0 & \dots & 0 \\ l_1 & l_0 & \dots & 0 \\ \vdots & \vdots & \ddots & \vdots \\ l_{\partial l} & l_{(\partial l-1)} & \ddots & l_0 \\ 0 & l_{(\partial l-1)} & \ddots & l_1 \\ \vdots & \vdots & \ddots & \vdots \\ 0 & 0 & \cdots & l_{\partial l} \end{bmatrix}. \tag{7.30}$$

Then the integral of squared error is computed as

$$\text{ISE} = \mathbf{F}'\mathbf{F} + \mathbf{\Theta}'\mathbf{L}'\mathbf{L}\mathbf{\Theta} + 2\mathbf{F}'\mathbf{L}\mathbf{\Theta}. \tag{7.31}$$

It is hence convenient to choose ISE as the objective function for minimization, which leads to a unique deadbeat controller satisfying the input constraints. The optimization is described as follows:

Optimization 2. Calculate a ISE optimal deadbeat controller subjecting to modified hard input constraints:
Objective: Minimize ISE (7.31) over the vector $\mathbf{\Theta}$ with given dimension $\partial\theta$.
Constraints: Inequalities (7.28) and (7.29).

7.4.1 Design procedure and computational aspects

The whole procedure for solving Problem 7.2 with modification of hard constraints is then summarized as follows.

Prior information: process model, reference input, expected settling time (given by $\partial\theta$), and hard constraints $\underline{u}$, $\overline{u}$.

Step i. Solve (7.3) for the minimum-time solution of the deadbeat tracking problem with bounded inputs, and derive the general solution (7.12) for U and E;

Step ii. Derive δ_i, λ_i and then in turn $\delta_{p,i}$, $\delta_{d,i}$, $\lambda_{p,i}$ and $\lambda_{d,i}$ from (7.24)(7.25), compute w_{sum} and v_{sum};

Step iii. Solve Optimization 1 for θ_{sum};

Step iv. Solve k from (7.27);

Step v. Solve Optimization 2 for Θ, then formulate the controlled input, the error, and the controller with $\mathbf{t}$ by (7.12).

In this design procedure, Step i gives the general solution for the bounded stabilizing deadbeat control, and is a prerequisite for Problem 7.2 to be solvable. Step ii only involves with simple algebraic manipulations. In Step iii, a trick is employed to transform the objective of Optimization 1 into a linear one, see Dantzig and Thapa (2003) for details. In Step iv, smaller k could be derived by more elegant handling of inequalities (7.26) and (7.27). In Optimization 2 of Step v, it is straightforward to modify the objective to minimizing IAE, $ITAE$ or $ITSE$ etc. for different benchmarks.

Since Condition A is necessary for either original hard constraints or modified ones, if inequalities (7.28) alone allows no feasible Θ, then Problem 7.2 has no solutions, and one may need to increase the complexity of controller by increasing $\partial\theta$. It also need to be commented on the modified constraints. Although the constraints for $i \geq k$ are relaxed such that $|u_i| \leq \bar{u} + \varepsilon$ is is possible, it is likely that Constraint A will prevent $|u_i|$ from exceeding $\bar{u}$, and the calculated deadbeat controller still satisfies the original hard constraints.

7.4.2 Numerical example

Example 2 Design a deadbeat controller for Example 1 to meet the hard constraints of $|u_i| \leq 2$ with $\partial\theta \leq 10$ and ISE minimized.

Following the results in Example 1, the general solution U is given directly as

$$\begin{aligned} E &= E^* - \theta, \\ U &= U^* + \frac{19 - 2z^{-1} - 16z^{-2}}{2 + z^{-1} - z^{-2}}, \\ C &= \frac{U}{E} \\ &= \frac{(19 - 2z^{-1} - 16z^{-2})(1 + (1 - z^{-1})\theta)}{(2 - z^{-1} - 2z^{-2} + z^{-3})(1 - \theta)}. \end{aligned}$$

The input U can then be decomposed as

$$\begin{aligned} U_1 &= \frac{5}{6(1 + z^{-1})} + \frac{1}{2(1 - z^{-1})} + \frac{5}{3(1 + z^{-1})}\theta, \\ U_2 &= \frac{49}{6(1 - 0.5z^{-1})} + \left(16 - \frac{49}{6(1 - 0.5z^{-1})}\right)\theta \\ &= \delta_2 + \lambda_2\theta. \end{aligned}$$

Optimization 1 is then carried out to estimate θ_{sum}, which yields

$$\sum_{i=0}^{10} |\theta_i| \leq 2.375.$$

Simply choose $\varepsilon = 0.02$. It follows from (7.27) that $k = 20$, and then θ is solved from Optimization 2 as

$$\begin{aligned} \theta = &- 0.7895 - 0.6620z^{-1} - 0.5766z^{-2} - 0.4603z^{-3} - \\ &0.3761z^{-4} - 0.2693z^{-5} - 0.1872z^{-6} - 0.0886z^{-7} - \\ &0.0091z^{-8} - 0z^{-9} - 0z^{-10}, \end{aligned}$$

$$\begin{aligned} E = &1.7895 + 0.6620z^{-1} + 0.5766z^{-2} + 0.4603z^{-3} + \\ &0.3761z^{-4} + 0.2693z^{-5} + 0.1872z^{-6} + \\ &0.0886z^{-7} + 0.0091z^{-8}, \\ t_s = &9, \end{aligned}$$

and $ISE_{min} = 4.4419$. With this θ, the controller can be formulated and then the simulation results for U and E are displayed in Figure 7.3. It verifies that the hard constraint requirements are met.

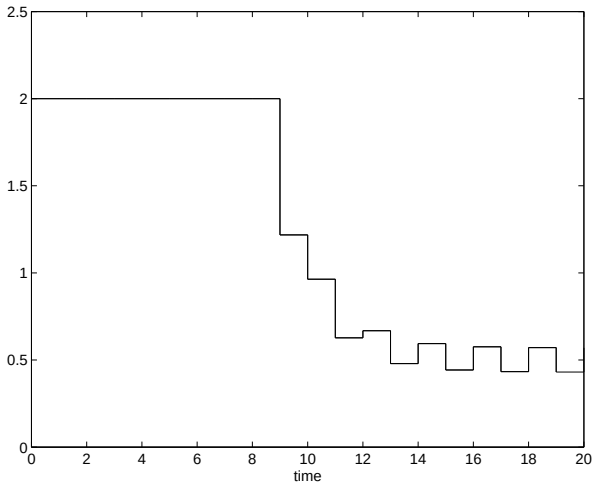

(a) *Input U*

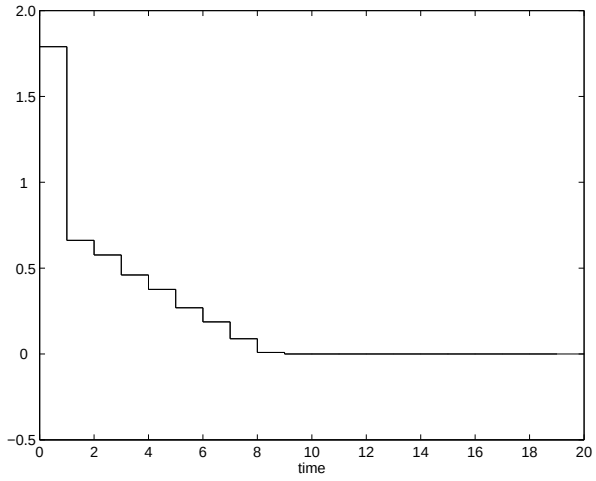

(b) *Error E*

Figure 7.3. Minimum ISE deadbeat control for Example 2 with hard constraints

7.5 Conclusion

In this chapter, a polynomial approach is presented to solve deadbeat tracking control with hard input constraints. The difficulty of infinite inequality constraints is handled by employing the modified hard constraints. This modification could meet the original constraints with arbitrary accuracy, while only finite linear equality constraints are need. Efficient quadratic optimizations are employed to calculate the controller with ISE minimized. Numerical examples are provided to illustrate the effectiveness of the design. This approach can be easily extended to the problems of deadbeat disturbance rejection or deadbeat servo control by adopting a two-degree-of-freedom scheme.

Chapter 8

Conclusions

8.1 Main Findings

In this thesis, several new results are obtained around control system design for better performance and robustness. Briefly, the results are summarized as follows:

A. PID Controller Analysis and Design

In this thesis, the PID stabilization and design issues are covered. For the first topic, the stabilization of five typical time delay processes is investigated. For each case, the maximum stabilizable time delay for different controllers is derived, and the computational method is also given to determine the stabilization gain. The analysis provides theoretical understanding of such stabilization problem. Based on the study, when only stabilization of these processes is needed, P or PD controller is sufficient. On the other hand, the results also yield practical guidelines for actual controller design. When the time delay is within the stabilizing range, the stabilizing PID parameters can be easily determined to stabilize the plant. For the second topic, an iterative LMI algorithm is presented to solve the regional pole placement problem by PID controllers, static output feedback or reduced order feedback controllers. By formulating the requirements on regional pole clustering with LMI regions, the problem is described as a bilinear matrix inequality problem. Then it is reduced to an equivalent quadratic matrix inequality problem and solved using an iterative algorithm. This approach is usefully especially when exact pole

placement or dominant pole placement is not achievable. Compared with the existing methods on the regional pole placement, ours imposes no specific requirement on either system structure or system order. This approach can be extended to multivariable process design.

B. Smith Controller Design and Disturbance Rejection

In this thesis, two Smith predictor designs are presented for stable time delay process and unstable one respectively, both of which pay special attention to disturbance rejection, and a Smith like scheme is also proposed to control system with RHP zeros. A two-degree-of-freedom Smith control scheme is investigated for improved disturbance rejection of minimum-phase delay processes. The novel tuning rule for the additional degree-of-freedom enables convenient design of disturbance controller with superior disturbance rejection, as well as easy trade-off between system robustness and performance. For unstable time delay processes, a double two-degree-of-freedom control scheme is proposed to enhance the performance. The four controllers involved are well placed to separately tune the denominators and numerators of closed-loop transfer functions from the set-point and disturbance. For disturbance response, the one more degree-of-freedom is tuned to minimize the integral squared error. Two options are provided to meet practical situations for the trade-off between control performance and control action limits. It is shown by examples that both two schemes lead to significant improvement of disturbance response.

For systems with RHP zeros, a Smith-like scheme is presented for easy tuning and improved performance. The relationships between the time domain specifications and the tuning parameter are developed to meet the design requirements on performance and robustness. Compared with the conventional single-loop design, the proposed scheme provides robust, improved, and predictable performance than the popular PI control.

C. Deadbeat Controller Design with Hard Constraints

In the thesis, a polynomial approach is employed to solve the deadbeat track-

ing problem with hard input constraints. The deadbeat requirement and hard constraints combine to yield finite linear inequalities constraints. The design could be efficiently solved with quadratic programming optimizations. The deadbeat nature of the error enables easy incorporation of various time-domain optimization objectives, such as ISE, ITSE, etc. This approach can also be extended to the problems of deadbeat disturbance rejection, or even servo control designs by adopting a two-degree-of-freedom scheme.

8.2 Suggestions for Further Work

The thesis has taken the full route from initial ideas, via theoretical developments, to methodologies that can be applied to relevant practical problems. Several new results have been obtained but some topics remain open and are recommended for further work.

A. Multi-variable PID Controller Synthesis and Design

In the thesis, PID stabilizability synthesis is provided for low-order single variable processes. In practice, many processes are multivariable, however, the stability analysis for multivariable PID design remains open. Either the Hermite-Biehler theorem based results (Silva *et al.*, 2004), or the polynomial approach based analysis (Hwang and Hwang, 2004), or the Nyquist stability based analysis presented in the thesis, have substantial difficulty when multivariable systems are concerned. More effective design design specifications, stability margins, and robustness measure of Multi-variable PID control systems are desirable, and they may lead to a large branch of tuning rules similar to the single variable case. Also, a regional pole placement PID design is presented in the thesis, which converts the problem into a equivalent static output feedback problem and solved via LMI. In general, a multivariable PID control system can be converted to an equivalent static output feedback system for which powerful results can be adopted and various PID control problems then solved via LMI, which may form a unifying framework to ease analysis and design of multivariable PID control systems.

B. Multi-variable Smith Predictor Design

Two modified Smith predictor design have been proposed for stable and unstable single variable time delay processes, respectively. Different measures are taken to improve the disturbance rejection. For multi-variable processes, the proposed approaches may encounter problems because of the coupling and different time delay of each element in the processes. One possible method is to develop decoupling controller to make the system decoupled, and then, the schemes presented for single variable processes can be applied for the decoupled loop. Robust issues should be pay special attention in the design, since decoupling is usually sensitive to the process model used. It is desirable to design robust decoupling Smith predictor such that the interaction of the resultant system is kept within a certain tolerance for the whole family of the uncertain processes.

Bibliography

Åström, K. J. and T. Hagglünd (1995). *PID controller: Theory, design, and tuning.* Instrument society of America, research triangle park. North Carolina.

Åström, K. J. and T. Hagglünd (2001). The future of PID control. *Control Engineering Practice* **9**(11), 1163–1175.

Åström, K. J., C. C. Hang and B. C. Lim (1994). A new Smith predictor for controlling a process with an integrator and long dead time. *IEEE Trans. Automatic Control* **39**(2), 343–345.

Åström, K. J., T. Hagglünd, C. C. Hang and W. K. Ho (1993). Automatic tuning and adaptation for PID controllers - a survey. *Control Engineering Practice* **1**(4), 699–714.

Bernstein, D. (1992). Some open problems in matrix theory arising in linear systems and control. *Linear Algebra and its Applications* **162-164**, 409–432.

Bonnet, C. and J. R. Partington (1999). Bezout factors and l^1-optimal controllers for delay systems using a two-parameter compensator scheme. *IEEE Trans. Automatic Control* **44**(8), 1512–1521.

Boyd, S., L. E. Ghaoui, E. Feron and V. Balakrishnan (1994). *Linear matrix inequalities in system and control theory.* SIAM. Philadelphia.

Cao, Y. Y., J. Lam and Y. X. Sun (1998). Static output feedback stabilization: an ILMI approach. *Automatica* **34**(12), 1641–1645.

Chen, D. and D. E. Seborg (2002). PI/PID controller design based on direct synthesis and disturbance rejection. *Ind. Eng. Chem. Res* **41**, 4807–4822.

Chew, K. K. (1996). Control system challenges to high track density magnetic disk storage. *IEEE Trans. on Magnetics* **32**(3), 1799–1804.

Chidambaram, M. (1997). Control of unstable systems: a review. *J. Energy, Heat Mass Transfer* **19**, 49–56.

Chien, I. L. and P.S. Fruehauf (1990). Consider IMC tuning to improve controller performance. *Chem. Eng. Progr.* **86**, 33–41.

Chien, I. L., S. C. Peng and J. H. Liu (2002). Simple control method for integrating processes with long deadtime. *Journal of Process Control* **12**, 391–404.

Chilali, M. and P. Gahinet (1996). H_∞ design with pole placement constraints: An LMI approach. *IEEE Trans. Automatic Control* **41**, 358–367.

Chilali, M., P. Gahinet and P. Apkarian (1999). Robust pole placement in LMI regions. *IEEE Trans. Automatic Control* **44**(12), 2257–2270.

Dantzig, G. B. and M. N. Thapa (2003). *Linear programming: theory and extensions*. Springer-Verlag. New York.

De Paor, A. M. and M. O'Malley (1989). Controllers of ziegler nichols type for unstable processes. *International Journal of Control* **49**, 1273–1284.

Emami-Naeini, A. and G. Franklin (1982). Deadbeat control and tracking of discrete-time systems. *IEEE Trans. Automatic Control* **27**(1), 176–181.

Fung, H. W., Q. G. Wang and T. H. Lee (1998). PI tuning in terms of gain and phase margins. *Automatica* **34**(9), 1145–1149.

Gahinet, P., A. Nemirovski, A. J. laub and M. Chilali (1995). The LMI Control Toolbox.

Gahinet, P. and P. Apkarian (1994). A linear matrix inequality approach to H_∞ control. *International Journal of Robust and Nonlinear Control* **4**, 421–448.

Hang, C. C., K. J. Åström and Q. G. Wang (2002). Relay feedback auto-tuning of process controllers a tutorial review. *Journal of Process Control* **12**(1), 143–162.

Hara, S., Y. Yamamoto, T. Omata and M. Nakano (1988). Repetitive control system: a new type servo system for periodic exogenous signals. *IEEE Trans. Automatic Control* **33**(7), 659–668.

Henrion, D., S. Tarbouriech and V. Kučera (2001). Control of linear systems subject to input constraints: a polynomial approach. *Automatica* **37**, 597–604.

Ho, W. K. and W. Xu (1998). PID tuning for unstable processes based on gain and phase-margin specifications. *IEE proc. Control Theory Appl.* **145**(5), 392–396.

Ho, W. K., C. C. Hang and L. S. Cao (1995). Tuning of PID controllers based on gain and phase margin specifications. *Automatica* **31**(3), 497–502.

Ho, W. K., C. C. Hang, W. Wojsznis and Q. H. Tao (1996). Frequency domain approach to self-tuning PID control. *Control Engineering Practice* **4**(6), 807–813.

Ho, W. K., Y. Hong, A. Hansson, H. Hjalmarsson and J. W. Deng (2003). Relay autotuning of PID controllers using iterative feedback tuning. *Automatica* **39**, 149–157.

Holt, B. R. and M. Morari (1985). Design of resilient processing plants-VI. the effect of right-half-plane zeros on dynamic resilience. *Chemical Engineering Science* **40**(1), 59–74.

Hu, T. and Z. Lin (2001). *Control Systems with Actuator Saturation: Analysis and Design*. Birkhauser. Boston.

Hu, T., Z. Lin and B. M. Chen (2002). An analysis and design method for linear systems subject to actuator saturation and disturbance. *Automatica* **38**(2), 351–359.

Huang, H. P., C. L. Chen, Y. C. Chao and P. L. Chen (1990). A modified Smith predictor with an approximate inverse of dead time. *AIChE Journal* **36**(7), 1025–1031.

Hwang, C. and J. H. Hwang (2004). Stabilisation of first-order plus dead-time unstable processes using PID controllers. *IEE Proc. Control Theory Appl.* **151**(1), 89–94.

Ingimundarson, A. and T. Hägglund (2002). Performance comparison between PID and dead-time compensating controllers. *Journal of Process Control* **12**, 887–895.

Jury, E. I. and A. G. Dewey (1965). A general formulation of the total square integrals for continous systems. *IEEE Trans. Automatic Control* **10**, 119–120.

Kaya, I. (2003). Obtaining controller parameters for a new PI-PD Smith predictor using autotuning. *Journal of Process Control* **13**, 465–472.

Keerthi, S. S. and M. S. Phatak (1995). Regional pole placement of multivariable systems under control structure constraints. *IEEE Trans. Automatic Control* **40**(2), 272–276.

Kharitonov, V. L., S. I. Niculescu, J. Moreno and W. Michiels (2005). Static output feedback stabilization: Necessary conditions for multiple delay controllers. *IEEE Trans. Automatic Control* **50**(1), 82–86.

Kimura, H. (1975). Pole assignment by gain output feedback. *IEEE Trans. Automatic Control* **20**, 509–516.

Kimura, H. and Y. Tanaka (1981). Minimal-time minimal-order deadbeat regulator with internal stability. *IEEE Trans. Automatic Control* **26**(6), 1276–1282.

Kučera, V. (1979). *Discrete linear control: The polynomial equation approach.* John Wiley and Sons. Prague.

Kwak, H. J., S. W. Sung, I. B. Lee and J. Y. Park (1999). Modified Smith predictor with a new structure for unstable processes. *Ind. Eng. Chem. Res.* **38**(2), 405C411.

la Barra S., De and B. A. León (1994). On undershoot in SISO systems. *IEEE Trans. Automatic Control* **39**(3), 578–581.

Luyben, W.L. (1990). *Process modeling, simulation and control for chemical engineers*. McGraw-Hill International Editions. New York.

Majhi, S and D. P. Atherton (1999). Modified Smith predictor and controller for processes with time delay. *IEE Proc. Control Theory Appl.* **146**(5), 359–366.

Majhi, S. and D. P. Atherton (2000*a*). Obtaining controller parameters for a new Smith predictor using autotuning. *Automatica* **36**, 1651–1658.

Majhi, S and D.P. Atherton (2000*b*). Online tuning of controllers for an unstable FOPDT processes. *IEE Proc. Control Theory Appl.* **147**(4), 421–427.

Matausek, M. R. and A. D. Micic (1996). A modified Smith predictor for controlling a process with an integrator and long dead-time. *IEEE Trans. Automatic Control* **41**(8), 1199–1203.

Mattei, M. (2001). Robust multivariable PID control for linear parameter varying systems. *Automatica* **37**, 1997–2003.

Middleton, R. H. (1991). Trade-offs in linear control system design. *Automatica* **27**(2), 281–292.

Morari, M. and E. Zafiriou (1989). *Robust process control*. Prentice Hall. Englewood Cliffs, NJ.

Obinata, G. and B. D. O. Anderson (2000). *Model reduction for control system design*. Springer. New York.

Ogata, K. (1990). *Mordern control Engineering, 2nd edition*. Prentice Hall. Englewood Cliffs, NJ.

Ohnishi, K. (1987). A new servo method in mechatronics. *Trans. Jpn. Soc. Elec. Eng.* **107-D**, 83–86.

Palmor, Z. J. (1996). Time-delay compensation - Smith predictor and its modifications. *The Control handbook* pp. 224–238.

Park, J. H., S. W. Sung and I. Lee (1998). An enhanced PID control strategy for unstable processes. *Automatica* **34**(6), 751–756.

Poulin, E. and A. Pomerleau (1996). PID tuning for integrating and unstable processes. *IEE Proc. Control Theory Appl.* **143**(5), 429–435.

Prashanti, G. and M. Chidambaram (2000). Set-point weighted PID controllers for unstable systems. *Journal of the Franklin Institute* **337**, 201–215.

Qiu, L. and E. J. Davison (1993). Performance limitations of non-minimum phase systems in the sevomechanism problem. *Automatica* **29**(2), 337–349.

Roffel, B. and B.H.L Betlem (2004). *Advanced practical process control*. Springer. Berlin.

Rovira, A. A., P. W. Murrill and C. J. Smith (1969). Tuning controllers for setpoint changes. *Instruments & Control Systems* **42**, 67–69.

Schlegel, M. (1982). Parameterization of the class of deadbeat controllers. *IEEE Trans. Automatic Control* **27**(3), 727–729.

Schoukens, J. and R. Pintelon (1991). *Identification of linear systems: a practical guideline to accurate modeling*. Pergamon Press. Oxford.

Seborg, D. E., T. F. Edgar and D. A. Mellichamp (2004). *Process dynamics and control, 2nd edition*. Wiley. Hoboken, NJ.

Seron, M. M., J. H. Braslavsky and G. C. Goodwin (1997). *Fundamental limitations in filtering and control*. Springer. London.

Shafiei, Z. and A. T. Shenton (1994). Tuning of PID-type controllers for stable and unstable systems with time-delay. *Automatica* **30**(10), 1609–1615.

Shafieia, Z. and A. T. Shentona (1994). Tuning of PID-type controllers for stable and unstable systems with time delay. *Automatica* **30**(10), 1609–1615.

Shinskey, F.G. (1996). *Process control systems. application, design and tuning (4th ed.)*. McGraw-Hill. New York.

Silva, G.J., A. Datta and S.P. Bhattacharyya (2004). *PID controllers for time-delay systems*. Birkhäuser. Boston.

Smith, O. J. (1957). Closed control of loops with dead time. *Chemical Engineering Progress* **53**, 217–219.

Smith, O. J. (1959). A controller to overcome dead time. *ISA J.* **6**(2), 28–33.

Söylemez, M. T., N. Munro and H. Baki (2003). Fast calculation of stabilizing PID controllers. *Automatica* **39**(1), 121–126.

Sree, R. P., M. N. Srinivas and M. Chidambaram (2004). A simple method of tuning PID controllers for stable and unstable FOPTD systems. *Computers and Chemical Engineering* **28**, 2201–2218.

Syrmos, V. L., C. T. Abdallah, P. Dorato and K. Grigoriadis (1997). Static output feedback-a survey. *Automatica* **33**(2), 125–137.

Takatsu, H. and T. Itoh (1999). Future needs for control theory in industry-report of the control technology survey in Japanese industry. *IEEE Trans. Contr. Syst. Technol.* **7**(3), 298–305.

Tan, K. K., Q. G. Wang and C. C. Hang (1999). *Advances in PID control*. Springer. Lundon.

Tan, K. K., Q. G. Wang, T. H. Lee and Q. Bi (1996). A new approach to analysis and design of Smith-Predictor controllers. *AIChE Journal* **42**(6), 1793–1797.

Tian, Y. C. and F. Gao (1998). Double-controller scheme for control of processes with dominant delay. *IEE Proc. Control Theory Appl.* **145**(5), 479–484.

Wang, Q. G. and Y. Zhang (2001). Robust identification of continuous systems with dead-time from step responses. *Automatica* **37**, 377–390.

Wang, Q. G., H. W. Fung and Y. Zhang (1999*a*). PID tuning with exact gain and phase margins. *ISA Transactions* **38**, 243–249.

Wang, Q. G., T. H. Lee and J. B. He (1999*b*). Internal stability of interconnected systems. *IEEE Trans. Automatic Control* **44**(3), 593–596.

Wang, Q. G., T. H. Lee, W. F. Ho, Q. Bi and Y. Zhang (1999*c*). PID tuning for improved performance. *IEEE Transactions on Control Systems Technology* **7**(4), 457–465.

Wang, Q. G., X. P. Yang, M. L., Z. Y. and X. Lu (2004). Stable model reduction for time delay systems. *Journal of Chemical Engineering of Japan*.

Wang, X. and J. Rosenthal (1992). Pole placement by static output feedback. *Journal of Mathematical Systems, Estimation, and Control* **2**(2), 205–218.

Wang, X. C. Alex (1996). Grassmannian, central projection, and output feedback pole assignment of linear systems. *IEEE Trans. Automatic Control* **41**(6), 786–794.

Wong, S. K. P. and D. E. Seborg (1986). A theoretical analysis of Smith and analytical predictors. *AICHE Journal* **32**(10), 101–107.

Zhang, Y., Q. G. Wang and K. J. Åström (2002). Dominant pole placement for multi-loop control systems. *Automatica* **38**, 1213–1220.

Zhang, Z. H. and J. S. Freudenberg (1990). Loop transfer recovery for nonminimum phase plants. *IEEE Trans. Automatic Control* **35**(5), 547–553.

Zheng, F., Q. G. Wang and T. H. Lee (2002). On the design of multivariable PID controllers via LMI approach. *Automatica* **38**, 517–526.

Zhou, K. M. and J. C. Doyle (1998). *Essentials of robust control*. Prentice Hall. Upper Saddle River, New Jersey.

Zhuang, M. and D. P. Atherton (1993). Automatic tuning of optimum PID controllers. *IEE Proc. Control Theory Appl.* **140**(3), 216–224.

Author's Publications

Journal Publications

[1] Lu, Xiang, Yong-Sheng Yang, Qing-Guo Wang and WX Zheng, 'A double two-degree-of-freedom control scheme for improved control of unstable delay processes', Journal of Process Control, 15(5), 2005, 605-614

[2] Wang, Qing-Guo, Xiang Lu, Han-Qin Zhou and Tong-Heng Lee, "Novel Disturbance Controller Design for a Two-degree-of-freedom Smith Scheme", Ind. Eng. Chem. Res., 46(2), 2007, 540-545

[3] Wang, Qing-Guo, Xiang Lu and Tong Heng Lee, 'A Smith-like Control Scheme for Performance Enhancement of Systems with RHP Zeros', Journal of Chemical Engineering of Japan, 40(2), 2007, No. 2, 128-138.

[4] Wang, Qing-Guo, Xiang, Cheng, Xiang Lu and Tong-Heng Lee, "Stabilization of Second-order Unstable Delay Processes by Simple Controllers", Journal of Process Control, accepted.

Conference Publications

[5] Wang, Qing-Guo, Tong Heng Lee and Xiang Lu, 'An Iterative LMI Algorithm

for Regional Pole Placement by Static Output Feedback', 11th IFAC Symposium of Information Control Problems in Manufactory, April 5-7, 2004, Bahia, Brazil.

[6] Wang, Qing-Guo, Xiang Lu and Tong Heng Lee, 'A Smith-like Control Design for Performance Enhancement of Systems with RHP Zeros', 6th Asia-Pacific Conference on Control and Measurement, August 12-19, 2004, Chengdu, China.

[7] Wang, Qing-Guo, Xiang Lu, Hanqin Zhou, and Tong-heng Lee, 'A two-degree-of -freedom Smith control for improved disturbance rejection', 16th IFAC World Congress, Jul 4-8, 2005, Praha, Czech Republic

[8] Wang, Qing-Guo, Xiang Cheng, Xiang Lu, L. A. Nguyen and T. H. Lee, 'Stabilization of Second-order Unstable Delay Processes by Simple Controllers', 7th IFAC Symposium on Advances in Control Education, 21- 23 June 2006, Madrid, SPAIN

Other Publications

[9] Wang, Qing-Guo, Yong-Sheng Yang and Xiang Lu, 'Robust IMC Controller Design in Frequency Domain', First Humanoid, Nanotechnology, Information Technology, Communication and Control Environment and Management (HNICEM) International Conference, March 29-31, 2003, Manila, Philippines.

[10] Wang, Qing-Guo, Xue-Ping Yang, Min Liu, Zhen Ye and Xiang Lu, 'Stable Model Reduction for Time Delay Systems', Journal of Chemical Engineering of Japan, 40(2), 2007, 139-144.